GENERAL DYNAMICS

GA-1738
Reactor Technology
TID-4500 (16th ed.)

MARITIME GAS-COOLED REACTOR PROGRAM

QUARTERLY PROGRESS REPORT

FOR THE PERIOD ENDING SEPTEMBER 30, 1960

Contract AT(04-3)-187

U.S. ATOMIC ENERGY COMMISSION

and

MARITIME ADMINISTRATION

GENERAL ATOMIC and

ELECTRIC BOAT DIVISIONS

DISCLAIMER

This report was prepared as an account of work sponsored by an agency of the United States Government. Neither the United States Government nor any agency Thereof, nor any of their employees, makes any warranty, express or implied, or assumes any legal liability or responsibility for the accuracy, completeness, or usefulness of any information, apparatus, product, or process disclosed, or represents that its use would not infringe privately owned rights. Reference herein to any specific commercial product, process, or service by trade name, trademark, manufacturer, or otherwise does not necessarily constitute or imply its endorsement, recommendation, or favoring by the United States Government or any agency thereof. The views and opinions of authors expressed herein do not necessarily state or reflect those of the United States Government or any agency thereof.

DISCLAIMER

Portions of this document may be illegible in electronic image products. Images are produced from the best available original document.

MGCR QUARTERLY REPORT SERIES

GA-744--October, November, December, 1958

GA-1030--January, February, March, 1959

GA-1099--April, May, June, 1959

GA-1183--July, August, September, 1959

GA-1195--October, November, December, 1959

GA-1259--January, February, March, 1960

GA-1532--April, May, June, 1960

CONTENTS

PREFACE i

SUMMARY iii

TENTATIVE MGCR DESIGN DATA vii

I. REACTOR DEVELOPMENT 1
- Reactor Design 1
- Mechanical Design 10
- Fuel Handling 22
- Reactor Controls and Instrumentation 23
- MGCR Prototype Thermal Design Analysis 23
- Hanford Loop 24
- Control Rod Drive Mechanism Development 28

II. FLUID SYSTEMS AND PLANT ARRANGEMENT 33
- Develop Reference Design of Primary Loop Components . . . 33
- Mechanical Devices 33
- Development of Plant Control System 35
- Develop Reference Design for Power Plant Arrangement and Structure 40

III. ROTATING MACHINERY 43
- Develop Reference Design of Rotating Machinery 43
- Lubrication and Sealing System Development 43

IV. REACTOR PHYSICS 45
- Beryllium Oxide Reactor Experiment (BORE) Nuclear Conceptual Design 45
- BORE Preliminary Hazards Evaluation 69
- MGCR Critical Facility 70
- Methods Evaluation 73
- Nuclear Data 78

V. MATERIALS DEVELOPMENT 83
- Develop Materials for the Propulsion Plant 83
- Reactor Materials Irradiations 87
- Develop Nonfuel Materials for the Reactor 89
- Electric Boat Division Materials Investigation and Tests . 91
- Westinghouse Metallurgical Program 99
- Stress-Rupture Tests 99

VI. SITE DEVELOPMENT 101
- Prototype Site Development 101

PREFACE

The Maritime Gas-Cooled Reactor (MGCR) Program was initiated on February 17, 1958, under Contract AT(04-3)-187 between the U. S. Atomic Energy Commission-Maritime Administration and General Dynamics Corporation. The over-all project responsibility is assigned to the General Atomic Division of General Dynamics, and the project is carried out by a staff of technical personnel assigned from the Corporation's General Atomic and Electric Boat Divisions. Westinghouse Electric Corporation is subcontractor to General Dynamics for the development of turbomachinery for the project and has participated in the project work since August 20, 1958.

A principal goal of the MGCR Program is the development of a nuclear powered marine propulsion system utilizing a high-temperature, gas-cooled nuclear reactor, closed-cycle gas-turbine power plant.

Design objectives for the power plant are high thermodynamic efficiency, simplicity of design, with attendant ease of operation, low maintenance costs, and maximum efficiency of operation over a wide range of power settings.

SUMMARY

During the period covered by this report, the MGCR Project was directed to study the feasibility and prepare a cost estimate of an experimental reactor to determine the operating characteristics of beryllia-moderated, gas-cooled systems within a power limit of 10 Mw(t). The heat energy produced by the experimental reactor is to be dissipated in a heat dump. No machinery for production of power was to be provided. Other requirements were that the reactor should be capable of testing core types different from the current MGCR design, and the system should permit use of gases other than helium. It was further directed that the reactor should be designated BORE for Beryllium-Oxide Reactor Experiment.

The principal engineering effort of the project during the months of July, August, and September was spent in preparing a preliminary design of the BORE and arriving at a cost estimate. Some of the technical results, as distinguished from cost information, are of sufficient general interest to be summarized in this report. In reviewing the work described in this report, it should be kept in mind that the system described does not represent a complete mechanical design or even a final concept. Instead, it represents the project consensus of the most valuable information which can be obtained from a 10 Mw(t) reactor experiment and one possible design of a system that can provide this information and serve as the basis for a cost estimate.

The interposition of the BORE in the MGCR Project will result in a shift of emphasis from research and development to engineering; however, the time is opportune for such a move. Research and development programs, which were initiated earlier, are now nearing completion and most of the required results will be available by the time designs have to be frozen. Additional research and development which was planned will not be initiated. The BORE will not be as advanced as the MGCR prototype which was planned with an additional years' development, but sufficient information is available to design a reactor if requirements in temperature and fuel cycle economics are relaxed.

Reactor Development

Reactor development work was mainly in connection with the BORE

preliminary design. It was established that the most important information which could be provided by a 10 Mw(t) reactor experiment would be on performance of fuel elements and moderator bodies. This required that the experiment duplicate the power density in the fuel and moderator that would exist in the full size reactor and made it advisable to use full length fuel elements. This resulted in an unconventionally shaped core which is roughly cylindrical with the length more than twice its mean diameter.

Studies continued on performance of fuel elements, and methods were developed for calculation of thermal stress in BeO-moderated modules. These studies are equally applicable to the MGCR prototype and BORE. A thermal analysis of the MGCR pressure vessel and thermal shields was performed and means of externally cooling the vessel were studied.

Some of the components of the experimental control rod drive mechanism were received. Endurance tests of a ball-nut lead screw in hot helium continued.

Fluid Systems and Plant Arrangement

Heat exchanger tests were resumed after an interruption due to leaks in the tube to tube-sheet joints in the test unit. Plant control studies were continued with analyses of the system dynamics with a turbomachinery configuration in which the high pressure turbine provides the output power. This arrangement was found to be more sensitive than the low-pressure drive system.

Rotating Machinery

Turbomachinery component tests at Westinghouse are providing stage performance data. The seal and bearing test rig was completed and tests were begun.

Reactor Physics

The Reactor Physics effort was directed toward physics calculations for the BORE design. The BORE concept will not provide physics information which is directly applicable to larger cores. The requirement of high power density in a small core results in a more epithermal spectrum than would exist in the MGCR prototype.

Basic physics information on Fermi age and neutron thermalization in

BeO was provided during the quarter by experiments in the General Atomic Linear Accelerator.

Materials Development

Materials work continued with further investigations of the effect of additives on properties of UO_2-BeO diluted fuel bodies. Hot cell examination of the MTR-31-3 fuel capsule has indicated no significant dimensional changes after burnups from 30,000 to 45,000 Mwd/T. A second capsule was discharged from MTR in September, and will be examined during the next quarter.

An experiment to determine irradiation effects on BeO was inserted in GETR during September. Work was started on development of high density BeO bodies.

Structural materials research continued with completion of a second series of self-welding tests of different metal pairs in high temperature helium. A series of galling tests were completed by Crane Company under subcontract and a series of creep rupture tests of weld specimens in SA302-B steel were completed.

Site Development

Work on site development has included establishing requirements of the BORE for buildings, auxiliary facilities, and utilities.

TENTATIVE MGCR DESIGN DATA[+]

BeO-Moderated Concept[*]	Prototype	Shipboard Powerplant[1] (Mark I)
Power		
Power at LPT shaft	32,000 shp	32,000 shp
Electric power generation	1,000 hp	1,000 hp
Reactor (thermal)	74.4 Mw	62.7 Mw
Net shaft efficiency	32.1%	34.4%
Cycle efficiency	33.1%	37.0%
Cycle Conditions		
Coolant	Helium	Helium
Coolant pressure		
HPC discharge	1150 psia	1150 psia
LPC suction	442.3 psia	442.3 psia
Coolant temperature		
Reactor inlet	744.1 °F	866 °F
Reactor outlet	1300 °F	1500 °F
Coolant flow (full power)	104.1 lb/sec	78.3 lb/sec
Reactor Vessel		
Inside diameter	114 in.	114 in.
Inside height	17.7 ft.	19.3 ft. max.
Reactor Internals		
Moderator and reflector	BeO	BeO
Core (active lattice)		
Diameter	6.33 ft.	6.37 ft.
Height	6.33 ft.	6.37 ft.
Reflector thickness	7 in.	7 in.
Fuel		
U^{235} loading	160 kg	200 kg
Enrichment	8.53%	10.5%

	Prototype	Shipboard Powerplant[1] (Mark I)
Fuel cont.		
U-238 loading	1652 kg	1700 kg
Fuel loading	1812 kg	1900 kg
Core life (at full power)	2.71 yrs	4.6 yrs
Heat Exchangers		
Regenerator		
Number	2	1
Tube length	49.2 ft	46.0 ft
Number of tubes	2686	4096
Tube material	Cr-Mo	Cr-Mo
Precooler		
Number	1	1
Tube length	22.6 ft	24.5 ft
Number of tubes	2746	1649
Tube material	Cu-Ni	Cu-Ni
Intercooler		
Number	1	1
Tube length	23.4 ft	25.7 ft
Number of tubes	2007	1160
Tube material	Cu-Ni	Cu-Ni
Fuel Elements		
Fuel-body material	UO_2-BeO	UO_2-BeO
Fuel-body cladding material	Hastelloy X, Inconel, or Type 316L stainless steel	Hastelloy X, Inconel, or Type 316L stainless steel
Maximum cladding temperature (with hot channel factors)	1500°F	1700°F
Number of fuel assemblies	308	308

	Prototype	Shipboard Powerplant[1] (Mark I)
Control Rods		
Number	16	16
Material	Rare earth - stainless steel	Rare earth - stainless steel
Turbomachinery		
Over-all length	Approx. 30 ft.	27 ft., 6.25 in.
Maximum diameter	8 ft.	5 ft., 8 in.
Speed		
LPC	12,200 rpm	12,200 rpm
HPC	12,200 rpm	12,200 rpm
HPT	12,200 rpm	12,200 rpm
LPT	7,600 rpm	7,600 rpm
Pressure ratio (at 1300°F)		
LPC	1.7	1.7
HPC	1.54	1.54
HPT	1.64	1.58
LPT	1.45	1.49

+A similar data sheet for the 10 MW(t) Beryllium Oxide Reactor Experiment will be included in future quarterly progress reports as firm design criteria are set.

*Further considerations concerning the BeO-moderated concept are presently under study, and data generated will be inserted into design specifications of subsequent reports.

[1]Report GA-1500-Nuclear Powered Tanker Design and Economic Analysis based on the MGCR, prepared by the MGCR Project Staff and George C. Sharp, Inc., June 30, 1960.

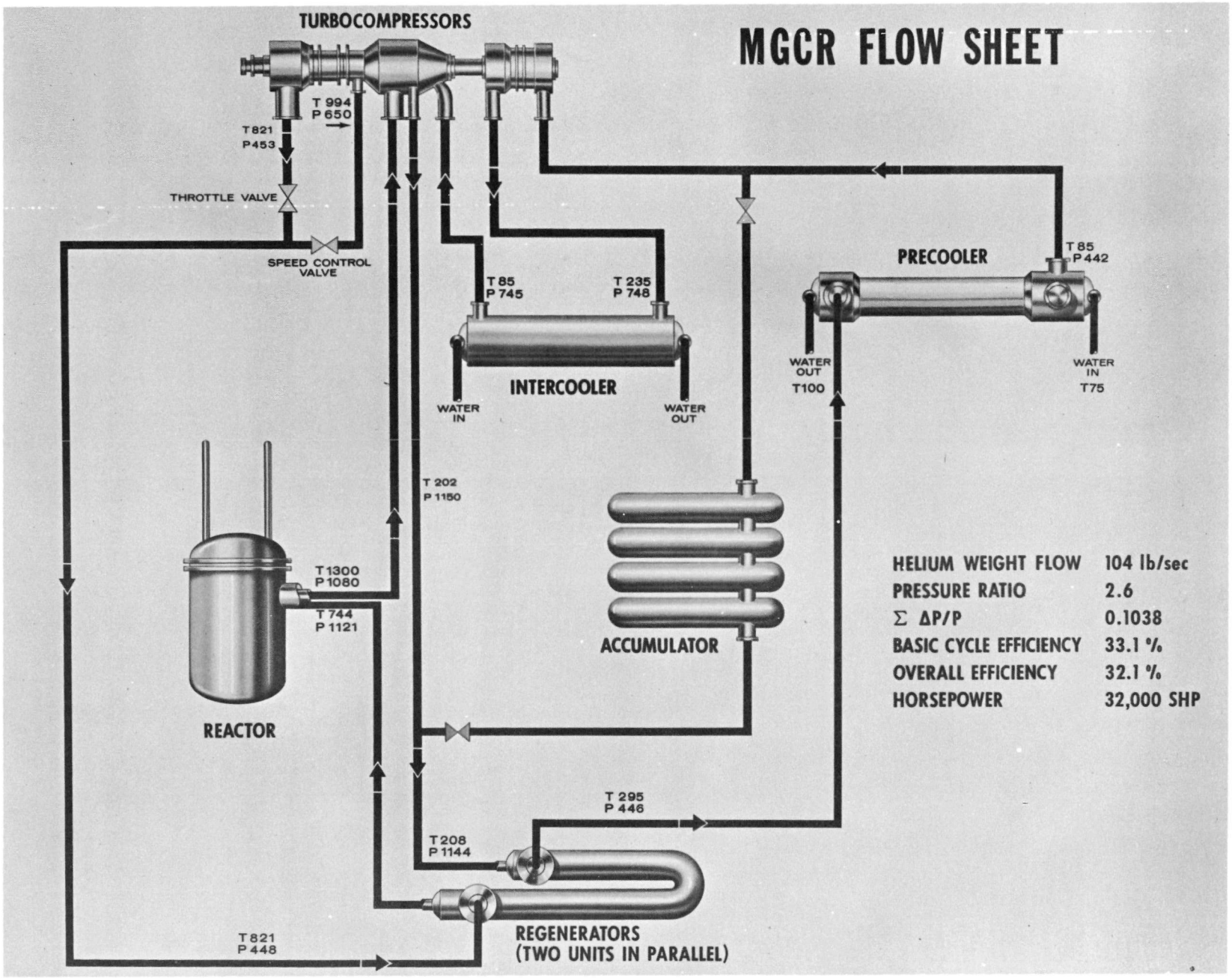

MGCR Flow Sheet

I. REACTOR DEVELOPMENT

REACTOR DESIGN (TASK 8) (K. A. Trickett)

Reactor Thermal Design (J. T. Rogers, R. Katz, G. J. Malek)

Beryllium Oxide Reactor Experiment (BORE)

A preliminary thermal design for the Beryllium Oxide Reactor Experiment core has been developed.[1] This design is based on obtaining an outlet gas temperature of 1300°F, with an inlet temperature of 745°F, using the MGCR prototype fuel element configuration of a cluster of 19 fuel pins in a circular array with a pin diameter of 0.375-in.

Design gas temperatures (1300°F) will be required in only a few of the fuel channels and the remaining fuel elements in the core will, therefore, be run at a significantly lower outlet gas temperature (1148°F). To establish a design basis, it was assumed that a maximum of 12 test channels would run at 1300°F with 24 channels running at 1148°F outlet gas temperature, producing a mixed mean core outlet temperature of 1190°F at 17.14 lbs/sec helium flow rate.

The blower capacity provides a maximum flow rate of 24 lbs/sec at a pressure drop of 45 psi. Of the total flow, 5 lbs/sec will be used for vessel cooling and 19 lbs/sec for the core. The allowance of a 19 lb/sec flow rate, which is 1.86 lbs/sec over the expected operating rate, will permit testing the fuel elements, under full core power, during the initial test phase. Maximum cladding temperature will be 1500°F in the hottest fuel channel.

By adjusting the coolant flow rate and by proper orificing, one to a maximum of twelve test channels can be operated at 1500°F. This capability meets the design requirement for future operation at 1500°F for 1,000 hrs. in addition to the design point operation at 1300°F for 10,000 hrs.

Table 1.1 shows the thermal design characteristics of the Beryllium Oxide Reactor Experiment core.

Because of the importance of structural reliability in the core of a test reactor, approximate calculations have been made for the temperature-time history of the hottest fuel element in the driver section of the core following a loss-of-coolant accident. The analysis has been simplified by

Table 1.1

PRELIMINARY DESIGN THERMAL CHARACTERISTICS*

	Test Elements	Driver Elements	Total Core
Number of elements	12	24	36
Thermal power, Mw	3.50	6.50	10.0
Mass flow rate, lb/sec	4.81	12.33	17.14
Inlet temperature, ^{o}F	745	745	745
Outlet temperature, ^{o}F	1300	1148	1190
Maximum clad temperature, ^{o}F	1520	1330	
Inlet pressure, psia	1120	1120	1120
Pressure drop, psi	32.8**	45	45
Maximum heat flux, Btu/ft^2-hr	200,000	184,000	200,000
Average heat flux, Btu/ft^2-hr	89,100	82,400	84,700
Maximum to average power generation ratio			
Radial within element	1.15	1.15	1.15
Radial over core			1.129
Total over core***			2.055
Heat transfer area, ft^2	134	269	403
Rod clearance-to-diameter ratio	0.10	0.10	0.10
Equivalent hydraulic diameter, ft	0.0114	0.0114	0.0114
Hottest channel average heat			
transfer coefficient, Btu/ft^2-hr-^{o}F	994	1190	
transfer coefficient Reynolds number	29,400	36,320	
transfer coefficient maximum velocity, ft/sec	236	377	

* Start-of-life conditions and with moderator bypass flow neglected

** Design point Δp

*** For the correct axial distribution

assuming that the axial heat conduction and the heat capacity of the fuel rods can be neglected; this implies that all the after-heat is transferred to the moderator.

Allowing for the moderator heat capacity, a mean moderator temperature was calculated as a function of time. The thermal resistance between the moderator mean temperature and the fuel-channel surface temperature was found and this, combined with the thermal resistance of the stagnant helium gap and shroud, permitted the calculation of the shroud temperature as a function of time. The fuel-cladding temperature was then obtained by an IBM 650 code which gave the radiant heat transfer between the fuel rods and the shroud.[2]

Assuming that the moderator normally is cooled by the proposed bypass flow arrangement, the initial mean moderator temperature at the point of maximum power generation in the hottest driver element was calculated to be 1160°F. An overall shroud conductance equivalent to that of a 0.012-in. to 0.016-in. thick stagnant helium gap was assumed in the calculations. The total emissivity of the fuel element cladding and of the shroud was taken as 0.7 which is a reasonable value for the materials being considered in the temperature ranges and service conditions of the Beryllium Oxide Reactor Experiment.

The results of this investigation for the hottest cladding are given in Fig. 1.1. The equilibrium cooling curve corresponds to the cladding temperature, ignoring the fuel-element heat capacity and assuming energy transfer to the moderator. The adiabatic curve corresponds to the cladding temperature neglecting heat radiation from the rods.

The actual temperature curve will lie below these two values, approaching the equilibrium cooling curve asymptotically in the period of 30 to 60 min. after shutdown. The probable temperature curve represents an estimate of the actual temperature-time history of the hottest spot on the cladding. It can be seen that the estimated cladding temperature reaches 1900°F in approximately 35 min., 2000°F in approximately 44 min., and 2100°F in approximately 54 min. after a loss-of-coolant accident.

It is interesting to note that the shroud temperature at any time is not very much greater than the average moderator temperature, the difference

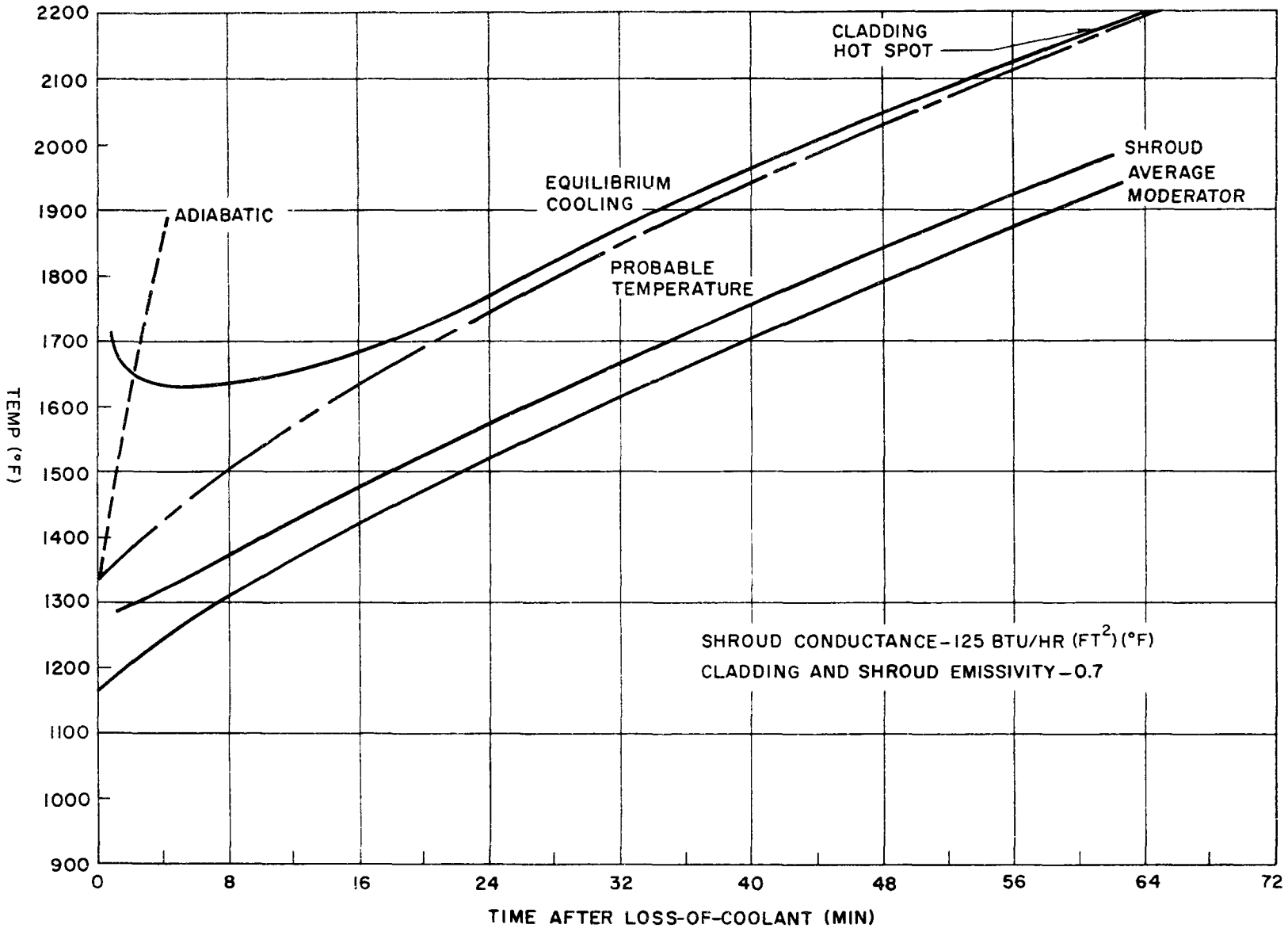

Fig. 1.1--Temperature History Following Loss-of-Coolant Accident - BORE Driver Elements

being less than 60°F for times of approximately 15 min. and longer. This indicates that the cladding temperature is not affected greatly by the presence of the thermal resistance of the shroud during the loss-of-coolant accident and that the limitation of an equivalent thermal resistance of 0.012-in. to 0.016-in. of stagnant helium may be relaxed somewhat after further analytical investigation. The advantage of bypass cooling of the moderator in lowering the initial heat sink temperature to which the fuel rods radiate their after-heat is apparent. Without bypass cooling, the initial sink temperature would be about 250°F higher, which would result in correspondingly higher moderator and cladding temperatures at all later times. Thus, a cladding temperature of 2000°F would be reached in approximately 23 min. rather than 44 min.

The major influence in the rapid increase of the fuel-element cladding temperature following a loss-of-coolant accident is the heat-capacity of the moderator sink. By increasing the moderator-to-fuel volume ratio, the heat capacity can be increased. An increase of only 10 per cent in the fuel-element pitch should lower the fuel-element cladding temperature approximately 100°F to 150°F at times of about one hour after shutdown.

Because of the importance of the loss-of-coolant accident in the design of the fuel-elements, analytical work is planned which will more accurately investigate the time-temperature history of the cladding and take into consideration the fuel-element heat capacity. The effect of cladding emissivities, shroud thermal conductances and moderator-to-fuel volume ratios will also be studied. Experimental work is also planned to determine cladding and shroud material emissivities and over-all shroud thermal conductances under Beryllium Oxide Reactor Experiment temperature and service conditions.

Since the BORE design does not require the high thermodynamic efficiency of the MGCR design, a number of different cooling configurations for the pressure vessel have been considered. They include:

(a) Internal cooling with low-temperature gas (less than the 745°F primary reactor gas inlet temperature).

(b) Internal cooling with system gas (745°F to 870°F).

(c) External cooling with a heat transfer oil or an equivalent coolant, and internal insulation.

Cooling the pressure vessel thermal shields and core support structure with low-temperature gas appears to offer the best means of making the main supporting and pressure-retaining structures least sensitive to the gas conditions in the core. To preclude the development of large pressure differences across the core support shell and head sections, the auxiliary gas flow cooling the vessel and the core inlet gas would have the same pressure source. By varying the temperature rise of the two gas streams between the blower and the reactor, the systems are to a large degree independent of temperature. The two gas streams merge inside the reactor and thus further reduce the mean temperature of the gas leaving the reactor. The general arrangement of this system is shown in Fig. 1.2.

The pressure vessel structure is normally cooled by a bypass flow of helium primary coolant passing between the shell and head sections of the core support, the thermal shields, and the pressure vessel. The temperature of the bypass coolant entering the vessel is independently controlled to limit the structural temperature to a maximum of 650°F during all normal operating conditions. A study has been made to investigate the effects of two arbitrary accidents in order to obtain preliminary data on design-limiting cases for the pressure vessel.[3] The two accident cases analyzed were:

(a) Loss of auxiliary cooling flow

(b) Accidental flooding of the reactor vault

The specific structural areas of interest were the shell section of the core support, thermal shields, shell section of the pressure vessel, and the vessel flange region. The scope of the investigation was limited to evaluating the effects on temperature level, temperature gradient and thermal stresses.

The conclusions reached from this study indicated that although neither accident creates an immediate hazard, the vessel should be externally insulated and regularly inspected to reduce the stresses developed in the vessel flanges in case of the accidental flooding accident.

Subsequent to the preliminary design of the BORE, an evaluation to determine the degree of flexibility in the test reactor was carried out.[4]

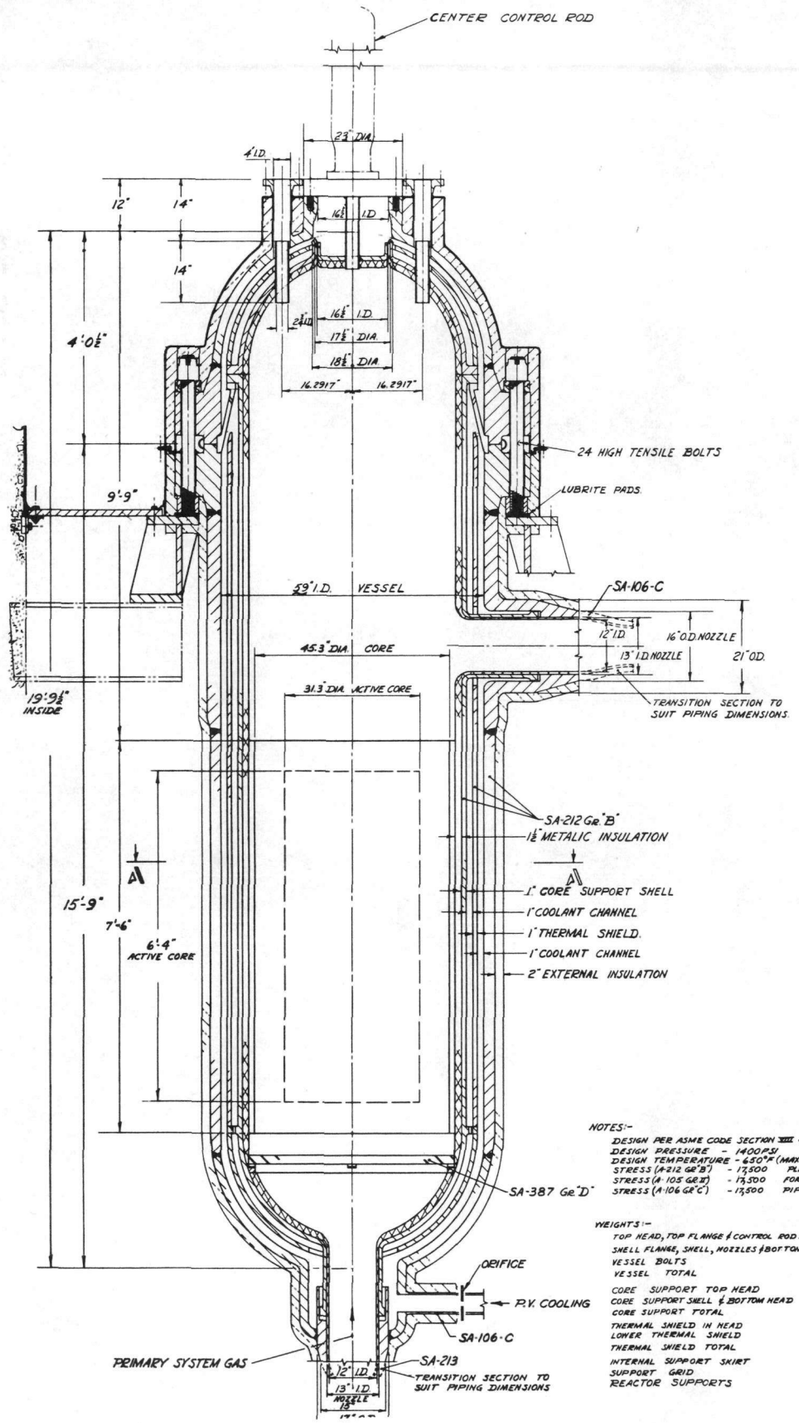

NOTES:-

DESIGN PER ASME CODE SECTION VIII & CODE CASES.
DESIGN PRESSURE - 1400 PSI
DESIGN TEMPERATURE - 650°F (MAX.)
STRESS (A-212 Gr. "B") - 17,500 PLATE
STRESS (A-105 Gr. II) - 17,500 FORGING
STRESS (A-106 Gr. "C") - 17,500 PIPE

WEIGHTS:-

TOP HEAD, TOP FLANGE & CONTROL ROD NOZZLES	- 13,800	LBS.
SHELL FLANGE, SHELL, NOZZLES & BOTTOM HEAD	- 31,300	LBS.
VESSEL BOLTS	- 2,000	LBS.
VESSEL TOTAL	- 47,100	LBS.
CORE SUPPORT TOP HEAD	- 1,500	LBS.
CORE SUPPORT SHELL & BOTTOM HEAD	- 9,100	LBS.
CORE SUPPORT TOTAL	- 10,600	LBS.
THERMAL SHIELD IN HEAD	- 1,500	LBS.
LOWER THERMAL SHIELD	- 10,100	LBS.
THERMAL SHIELD TOTAL	- 11,600	LBS.
INTERNAL SUPPORT SKIRT	- 900	LBS.
SUPPORT GRID	- 1,600	LBS.
REACTOR SUPPORTS	- 4,400	"

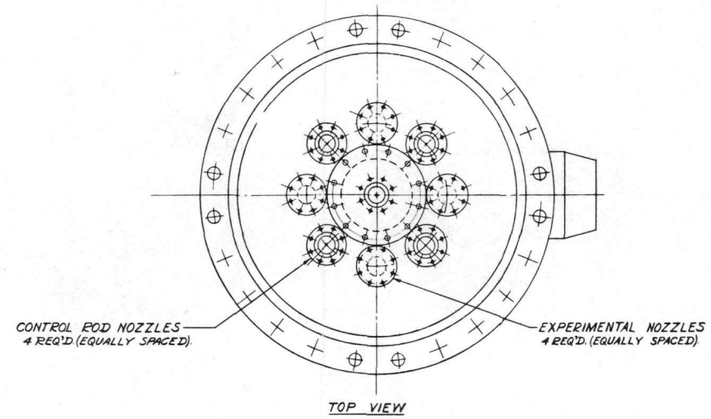

TOP VIEW

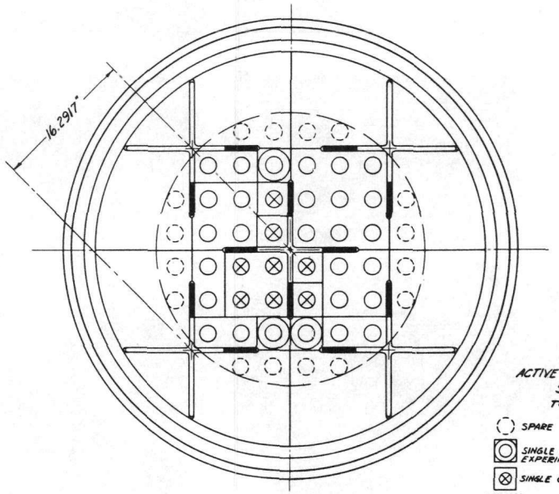

SECTION A-A
SCALE 2" = 10"

ACTIVE FUEL CHANNELS - 36
SPARE CHANNELS - 16
TOTAL CHANNELS - 52

SPARE CHANNELS
SINGLE CHANNEL BeO THERMAL STRESS EXPERIMENT.
SINGLE CHANNEL FUEL ELEMENT EXPERIMENT.
FOUR (4) CHANNEL BeO THERMAL STRESS EXPERIMENT.
FOUR (4) CHANNEL MODULE & FUEL ELEMENTS COMBINED EXPERIMENT.
NINE (9) CHANNEL MODULE & FUEL ELEMENT COMBINED EXPERIMENT.

Fig. 1.2--BORE Reactor Vessel
Preliminary Reference Design

The use of several alternate coolants and fuel-element configurations was examined. The coolants studied were helium, carbon dioxide, nitrogen, and hydrogen.

This study evaluated the thermal design from two major points of view: (1) variation of the hot-spot temperatures while maintaining a constant fuel-element clearance-to-diameter ratio (Table 1.2), and (2) variation of the fuel-element clearance-to-diameter ratio while maintaining constant hot-spot temperatures (Table 1.3).

Using the Beryllium Oxide Reactor Experiment drive elements as a model, an estimate was made of the required change in the fuel-element clearance-to-diameter ratio needed to maintain the same fuel cladding hot-spot temperature. The resulting core pressure drops and pumping powers were also calculated (Table 1.3).

Examination of these data shows that the required fuel-element clearance-to-diameter ratio is reduced significantly from the preliminary reference design value of 0.10 for CO_2 and N_2 coolants. Low c/d ratios of about 0.040 to 0.050 are undesirable from the standpoints of mechanical design and thermal performance.

These investigations also showed that it would not be advisable to adjust the fuel-rod clearance-to-diameter ratio to maintain constant cladding hot-spot temperatures in the driver section. Although the use of hydrogen would solve the problem of flexibility, its use would require a new set of driver fuel-elements. It is recommended, therefore, that the BORE core be designed for helium coolants, and the cladding hot-spot temperatures be permitted to vary.

Thermal conditions which could be obtained with other fuel-element concepts have also been examined. The concepts studied were:

(a) A 7-rod bundle ceramic clad fuel-element with rods 0.80 in. O.D. and with a 3-in. channel diameter,

(b) A cross-flow element with lenticular-shaped fuel rods with a channel diameter of 2 in.,

(c) A cross-flow element with lenticular-shaped fuel rods with a channel diameter of 6 in.

Table 1.2

HEAT TRANSPORT PERFORMANCE OF THE BORE LOOP ON DIFFERENT GASES

Maximum reactor power, Mw	10
Maximum circulator power, hp	1030
Maximum pressure, psia	1120

Gas properties (1000°F)	Helium	CO_2	N_2	H_2
Molecular weight, M	4	44	28	2.02
Thermal conductivity, k Btu/ft-hr-°F	0.17	0.037	0.0337	0.237
Heat capacity, c_p, Btu/lb-°F	1.25	0.288	0.263	3.53
Visosity, μ, lb/ft-hr	0.096	0.084	0.089	0.042
Prandtl number, Pr	0.706	0.65	0.69	0.625
$k^{1/5}/Pr^{2/5}$	0.807	0.614	0.588	0.905
Mc_p^2	6.25	3.65	1.94	25.2
$M^2c_p^3$	31.2	46.4	14.2	179
Reactor power level, Mw	10	10	7.74	10
Reactor temperature,				
Inlet to core, °F	745	745	745	745
Outlet from core, °F	1150	1150	1150	1150
Mixed inlet (incl. vessel coolant), °F	694	694	694	694
Mixed outlet (incl. vessel coolant), °F	1012	1012	1012	1012
Average film drop, central fuel-element, δt, °F	97	127	127	87
Maximum hot-spot temperature, °F	1330	1403	1396	1315
Gas pumping				
Massflow rate, lb/sec	24	104	88	8.5
Volume flow rate, cfs	40	16	21	28
Loop pressure drop, psi	22	37	42	5.5
Core pressure drop, psi	45	77	87	11.2

Table 1.2 cont.

HEAT TRANSPORT PERFORMANCE OF THE BORE LOOP ON DIFFERENT GASES

Maximum reactor power, Mw	10
Maximum circulator power, hp	1030
Maximum pressure, psia	1120

Gas properties (1000°F)	He	CO_2	N_2	H_2
Maximum test fuel-element pressure drop (W/Q = .02), psi	34	85	50	48
Total circulator pressure rise,* psi	67	122	129	53.5
Circulator power	1030	749	1030	578
Regenerator, maximum outlet temperature, °F	1075	880	870	1240

*Loop pressure drop plus core pressure drop or maximum test element pressure drop, whichever is greater.

Table 1.3

CORE THERMAL PERFORMANCE FOR DIFFERENT GASES

Coolant	Helium	CO_2	N_2	H_2
Core power, Mw	10	10	10	10
Core inlet temperature, °F	745	745	745	745
Driver section outlet temperature, °F	1148	1148	1148	1148
Cladding hot-spot temperature, °F	1330	1330	1330	1330
Core inlet pressure, psia	1120	1120	1120	1120
Core design mass flow, lbs/sec	17.14	74.7	79.5	6.06
Core maximum allowable mass flow, lb/sec	19.0	83.0	88.0	6.72
Maximum core plus auxiliary flow, lb/sec	24.0	105.0	111.3	8.5

Table 1.3 cont.

CORE THERMAL PERFORMANCE FOR DIFFERENT GASES

Coolant	Helium	CO_2	N_2	H_2
Rod clearance-to-diameter ratio	0.100	0.049	0.042	0.114
Core pressure drop, psi	45	132	255	110.0
System pressure drop, psi	67	160	300	158
Core design pumping power	511	755	1330	81
Total system pumping power	1030	1192	2080	178

The coolant was assumed to be CO_2 for each case, with the core inlet temperature, driver section outlet temperature and inlet pressure maintained constant at design values. The required outlet gas temperatures studied were 1150°F for concept (a), and 1700°F for concepts (b) and (c).

The selection of these concepts was arbitrary and was made mainly to review the flexibility of test fuel-element designs.

It is not possible in a general study of this nature to determine whether test conditions would be optimum for each concept considered as this would require design point data for each particular element. However, the results do show that other fuel-element concepts could be conveniently tested in the Beryllium Oxide Reactor Experiment.

MECHANICAL DESIGN (TASK 7) (R. W. Bean, K. A. Trickett, C. O. Peinado, T. J. Larson, D. R. Buttemer)

Studies have been completed on a preliminary mechanical design for the BORE.[1] The primary objective in the conceptual design of the core has been to provide the maximum degree of flexibility consistent with safe operation of the reactor. To achieve this, the core has been designed to:

(a) Permit the testing of a number of fuel-element concepts and geometries with a minimum change in the moderator structure.

(b) Provide for testing a number of moderator shapes, sizes, and structural arrangements.

(c) Vary the coolant flow distribution through the various core components with minimum effort.

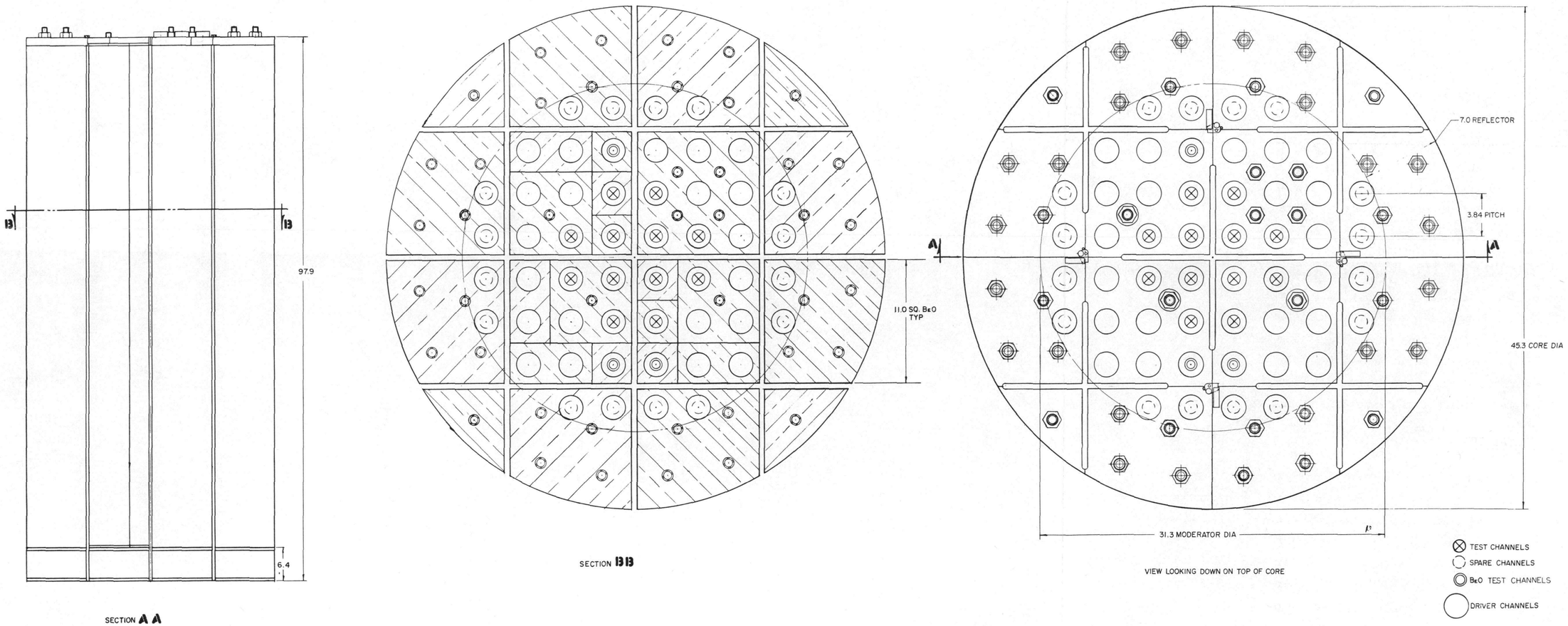

Fig. 1.3 -- BORE Reactor Core Layout

(d) Provide for easy and frequent removal of sections of the moderator and reflector structure for inspection and replacement.

(e) Provide the flexibility to give maximum future utilization for advancement in materials technology.

The resulting core arrangement is shown in Fig. 1.3 and pertinent data for the core are given in Table 1.4.

Table 1.4

MECHANICAL DESIGN CRITERIA FOR THE BERYLLIUM OXIDE REACTOR EXPERIMENT CORE

Over-all diameter, in.	45.3
Over-all height of core (excluding structure), in.	90.0
Average reflector thickness, side, in.	7.0
Average reflector thickness, end, in.	7.0
Moderator material	BeO
Reflector material	BeO
Number of fuel channels, test	12
Number of fuel channels, driver	24
Number of fuel channels, spare	16
Number of control rods	5

The fuel elements for the driver section of the core consist of five major sub-assemblies. These are the fuel pin, fuel pin spacer grid, shroud, latch mechanism, and seal as shown in Figs. 1.4 and 1.5.

Each of the eighteen rods around the center pin consists of a stack of UO_2-BeO fuel pellets in a metallic tube which provides for the retention of fission products. The center rod is unfuelled and contains plain BeO pellets. A void region is provided in each fuel rod in order to limit the end-of-life fission gas pressure.

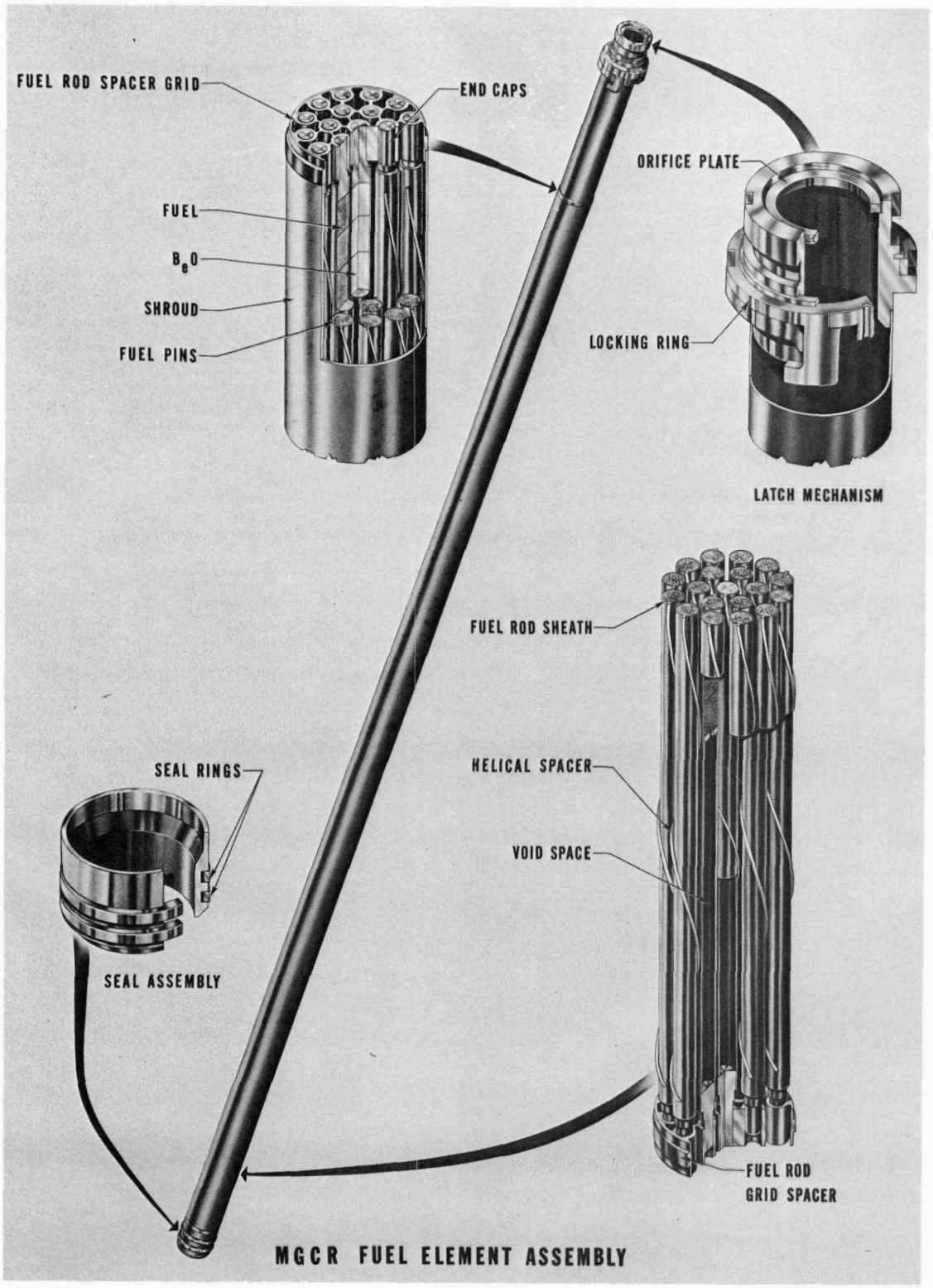

Fig. 1.4--MGCR Fuel Element Assembly (Over-all height 94.25-in.)

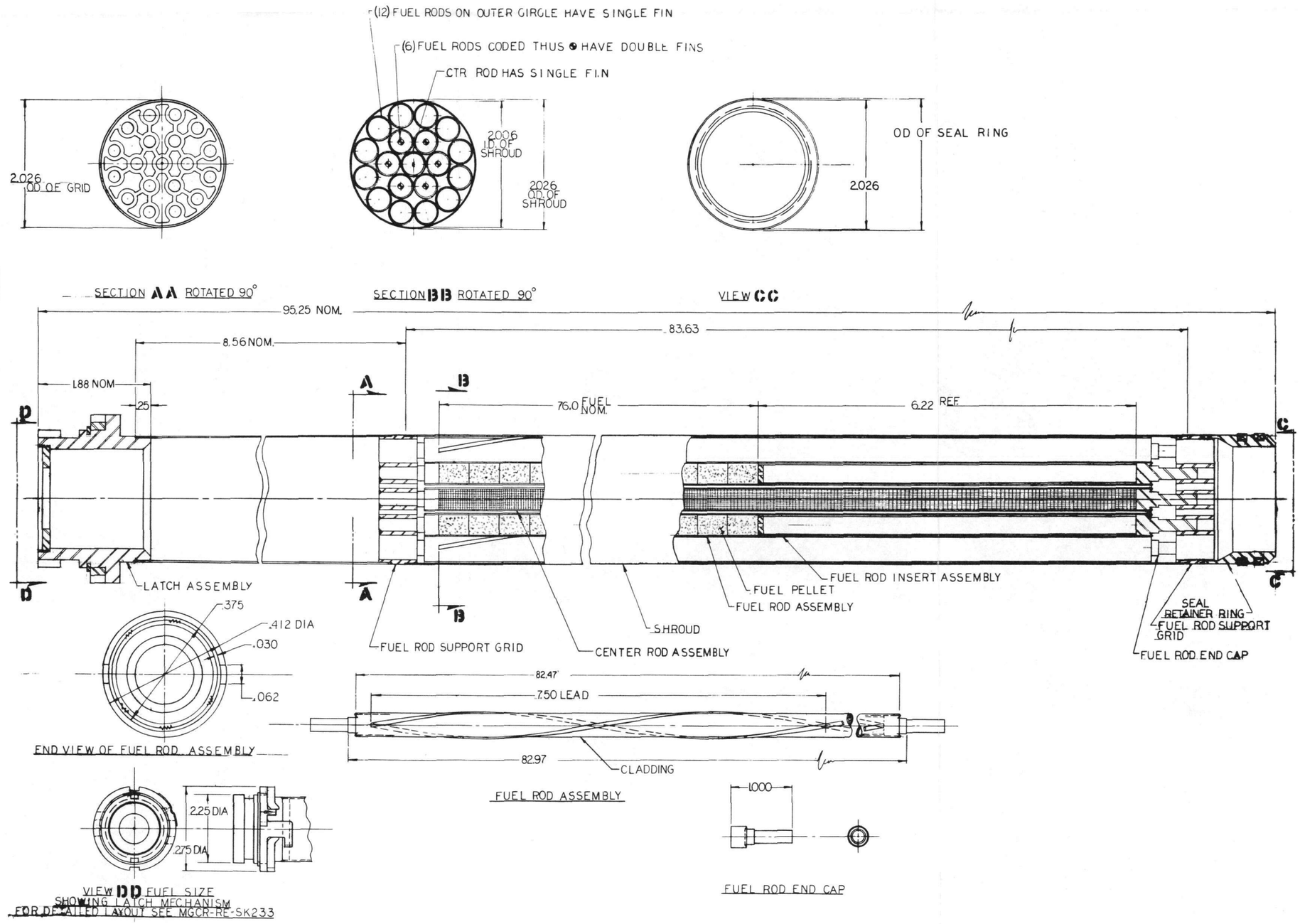

Fig. 1.5--BORE Driver Fuel Element Assembly

Table 1.5

BORE DESIGN POINT DATA FOR EACH FUEL ASSEMBLY

Type	19-rod cluster
Geometry	Circular array
Fuel pin OD, in.	0.375
Clearance between pins (min.), in.	0.038
Clearance between pins and shroud which defines the flow duct, in.	0.019
Outside diameter of shroud, in.	2.026
Fuel pin spacer configuration	Helically wound
Maximum sheath temperature, ^{o}F	1330
Maximum central fuel temperature, ^{o}F	1750
Heat flux, average in hottest channel, Btu/hr-ft^2-^{o}F	88,000
Heat flux, maximum, Btu/hr-ft^2-^{o}F	184,000
Average power density, hot channel, Btu/hr-ft^3	16×16^6
Lifetime at full power, hrs.	10,000
Number of rods	19
Number of fuelled rods	18
Rod OD, in.	0.375
Cladding thickness, in.	0.030
Pitch of helical spacers, in.	7.50
Sectional dimensions of spiral spacers, in.	.062 wide x .019 high
Distribution of spiral spacers	1 on center rod, 2 on each rod of inner ring of 6, 1 on each rod of outer ring of 12
Shroud, ID, in.	2.006
Shroud wall thickness, in.	0.010
Structural material	Hastelloy X
Fuelled length, in.	76.0
Over-all length of assembly, in.	95.25
Estimated weight, lbs.	60

In the proposed design the moderator is stacked into a column of flat plates held together by tension tubes. The 9-channel cell is shown in Fig. 1.6. The stacked height of the beryllia is 90-in. It is anticipated that a ceramic bonding material will be employed between the BeO plates. This material will serve three functions:

(a) It will compensate for plate tolerances during assembly of the column.

(b) It will act as a helium leakage barrier.

(c) It will act to maintain alignment of the BeO plates during operation.

The full-size mock-up of the nine-channel module, using gypsum castings in place of the beryllia, are shown in Figs. 1.7 and 1.8.

Significant data for the core and reflector modules are given in Table 1.6.

Table 1.6

BERYLLIUM OXIDE REACTOR EXPERIMENT CORE MODULE AND REFLECTOR DESIGN DATA

Module height, over-all in.	98
Module height beryllia, in.	90
Cross-section dimensions,	
one-channel, in.	3.7 X 3.7
two-channel, in.	3.7 X 7.4
four-channel, in.	7.4 X 7.4
nine-channel, in.	11.0 X 11.0
reflector, in.	non-uniform
Fuel channel pitch, in.	3.84
Fuel channel diameter, in.	2.28
Estimated weight per module,	
one-channel, lbs.	110
two-channel, lbs.	220
four-channel, lbs.	440
nine-channel, lbs.	1150
reflector, lbs.	950

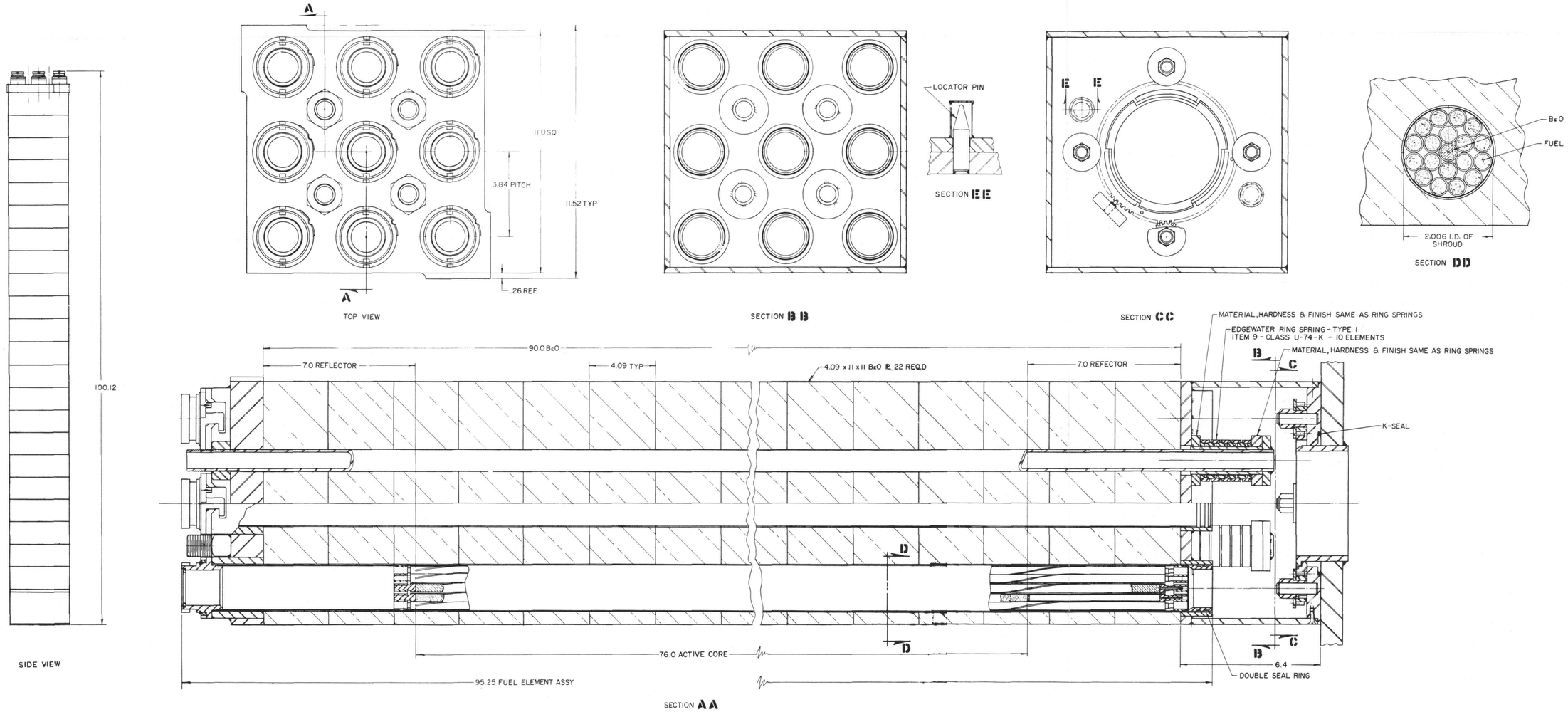

Fig. 1.6--BORE Nine-Channel Core Module

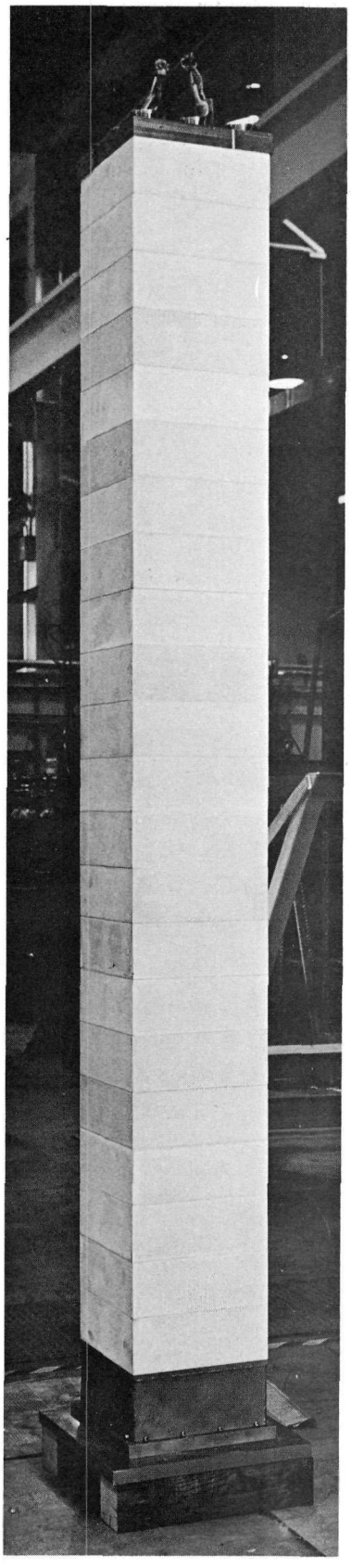

Fig. 1.7--BORE 9-channel Core Module Mock-up (Over-all height 100.15-in.)

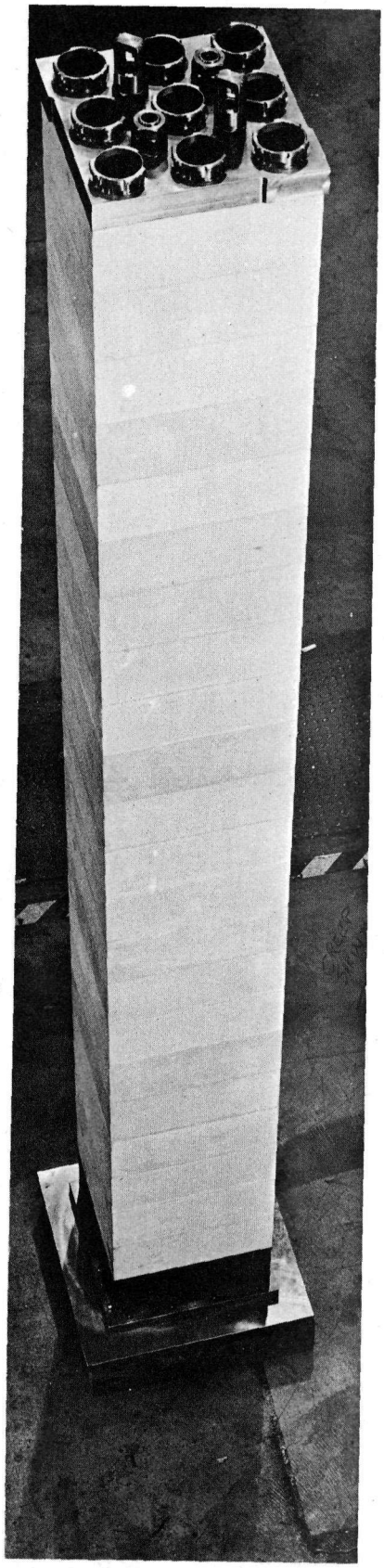

Fig. 1.8--Top View of BORE 9-channel Core Module Mock-up (Over-all height 100.15-in.)

Some preliminary calculations have been made of the thermal stresses developed in the BeO plates of the core module shown on Fig. 1.9. The magnitude of the maximum tensile thermal stresses induced in the BeO plates by internal heat generation has been determined to be 50,800 psi. This was calculated using an equivalent circular annulus model with an inner radius equal to the inside radius of the fuel channel, and the outer radius determined so as to give the same area as that associated with each fuel channel. The outer surface was assumed to be adiabatic and the inner surface cooled. The validity of this model as an approximation has been established for a hexagonal fuel element with seven holes on a triangular pitch.[5] It is expected that a similar study would establish its validity as an approximation for a core module with holes on a square pitch with the same hole spacing to diameter ratio.

The maximum tensile stress equation has been established for a hollow cylinder with these thermal conditions.[6] It can be written in the form:

$$= \frac{E\,\alpha}{1 - \mu} \qquad \frac{Q\,r_i^{\,2}}{K}$$

E = Modulus of elasticity, = 39×10^6 psi(*)

α = Coefficient of thermal expansion, = 6.1×10^{-6} in/in-°F(*)

μ = Poisson's ratio, = 0.34(*)

K = Thermal conductivity, = 10 Btu/hr-ft-°F(*)

r_i = Inside radius, = 1.075 in.

r_o = $\frac{s}{\pi}$ = Equivalent outside radius, = 2.165 in.

s = Hole spacing, = 3.84 in.

= A function that depends on the cooling conditions and the ratio $\frac{r_o}{r_i}$, = 0.489 for $\frac{r_o}{r_i} = \frac{2.165}{1.075} = 2.01$

Q = Volumetric heat generation rate. This was based on the following:

(a) Reactor power = 10 Mw
(b) Moderator to total power ratio = 0.086
(c) Maximum to average power ratio = 2.055
(d) Active core volume = $\frac{\pi \times \overline{26}^{\,2}}{4} \times 76 = 4.03 \times 10^4$ in^3
(e) Moderator volume ratio = 0.7185

(*) BeO properties were based on an average temperature of 1300°F and were obtained from AECU-3647 Reactor Handbook.

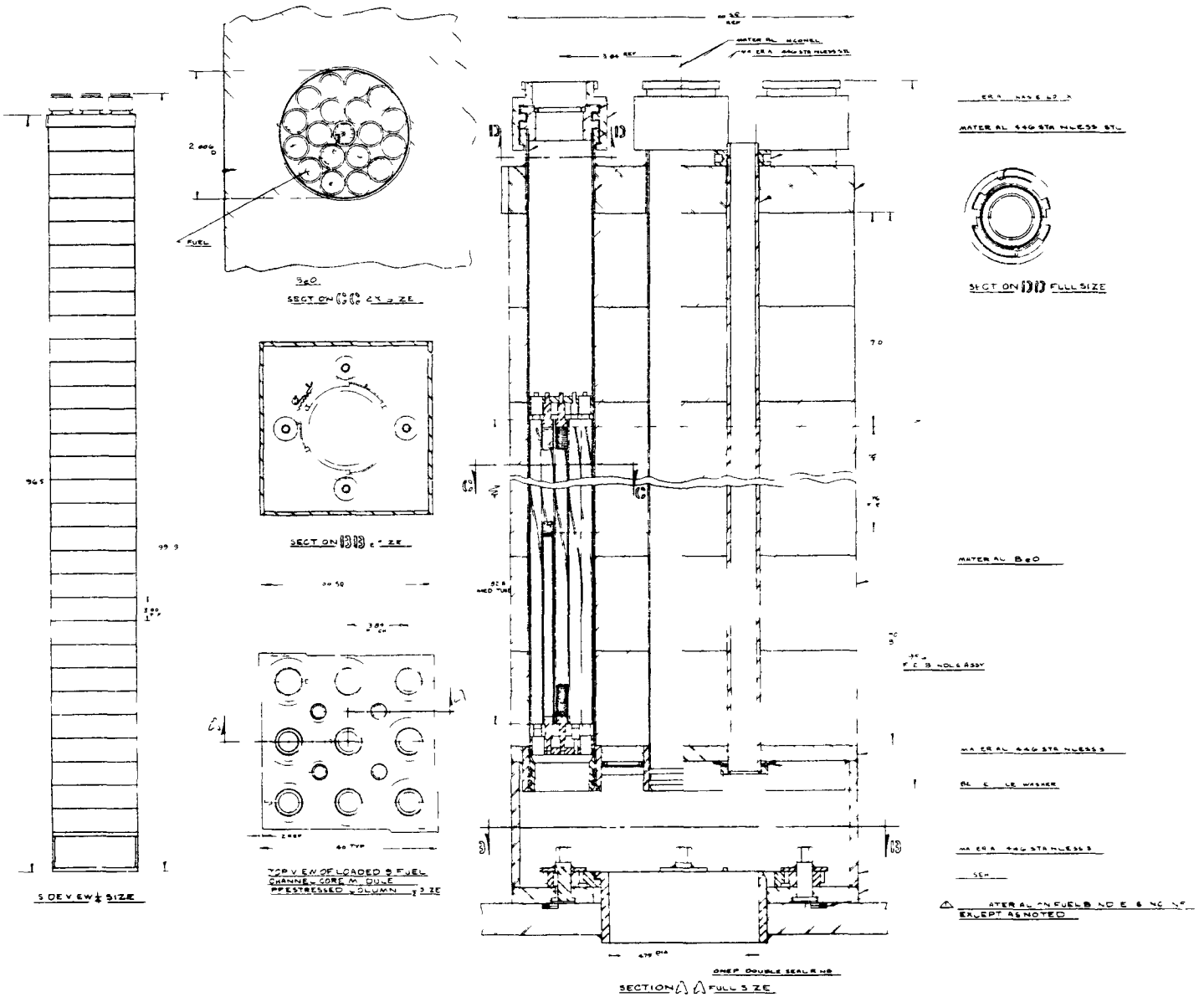

Fig. 1.9--BORE 9-channel Core Module, Prestressed Column, Ceramic Plates

therefore:

$$Q = \frac{0.086 \times 10^7 \times 2.055}{0.7185 \times 4.03 \times 10^4} = 61 \ \frac{\text{watts}}{\text{in}^3} = 208 \text{ Btu/hr-in}^3$$

The maximum tensile stress is, therefore:

$$\sigma = \left(\frac{39 \times 10^6 \times 6.1 \times 10^{-6}}{1 - 0.34}\right) \frac{208 \times \overline{1.075}^2}{10/12} (0.489) = 50{,}800 \text{ psi}$$

(7)

This compares with a reported modulus of rupture strength for BeO of 13,500 psi at 1470°F. As the thermal stress resistance of ceramics is dependent on volumetric stress distribution as well as on the fabrication process, it is not possible at this time to establish an allowable stress. It does, however, appear that this calculated stress would be too high.

A core module design that results in a lower maximum tensile thermal stress (2,540 psi) induced by internal heat generation, than the present design (50,800 psi) has also been evaluated. This proposed design would consist of a prestressed column of BeO plates with holes of larger diameter than the present design and in which are located the BeO annular sleeves that define the fuel-element channels.

The basic principle employed in reducing the maximum tensile thermal stress was to reduce the magnitude of the deviation of the surface temperature from the average temperature; this can be accomplished by reducing the maximum distance that the internally generated heat is required to flow.

A first approximation of the magnitude by which the thermal stress is reduced can be determined by examining the dependence of the maximum stress on the flow distance in a geometry. It can be shown that this stress is given by

$$\sigma = \frac{E\,\alpha}{1 - \mu} \frac{Q\,L^2}{3\,K}$$

where

E = Modulus of elasticity

α = Coefficient of thermal expansion

μ = Poisson's ratio

K = Thermal conductivity

Q = Volumetric heat generation rate

L = Distance from the cooled to the adiabatic surfaces

It is seen that maximum tensile stress is dependent on the square of the maximum distance the heat is required to flow. The proposed design reduces this distance by approximately four, thereby achieving a reduction of approximately 16 in the maximum tensile stress. A slightly larger reduction is obtained by considering the effect of the circular geometry.

For optimum design conditions, the maximum tensile stress in the sleeve and plate should be kept to a minimum and equal in magnitude. For minimum stress in the sleeve, the inner and outer surface should be cooled to give equal surface temperatures. For minimum stress in the plate, the surfaces at the fuel channel and tension-tube holes should be cooled to give the same stress at both surfaces. Thermal stress calculations were based on these cooling conditions.

In the mathematical model used for the plate, the plate was divided into equivalent annular cylinders with a cylinder for each of the areas associated with a fuel channel and a tension-tube hole. These cylinders were assumed to have adiabatic outer surfaces and cooled inner surfaces (Fig. 1.10).

The dimensions of the design were optimized to give approximately the same maximum tension stress at all surfaces. These are also shown in Fig. 1.10. A reduction by a factor of 20 of the maximum tensile stress of 50,800 psi for the design without the annular sleeves was achieved. Use was made of the thermal stress equations established for hollow cylinders with uniform internal heat generation. The maximum tensile stress can be written in the form

$$\sigma = \frac{E\,\alpha}{1 - \mu} \quad \frac{Q\,r_i^{\,2}}{K} \qquad *$$

where in addition

r_i = The inside radius

r_o = The outside radius

$*$ = A function that depends on the cooling conditions and the ratio $\frac{r_o}{r_i}$.

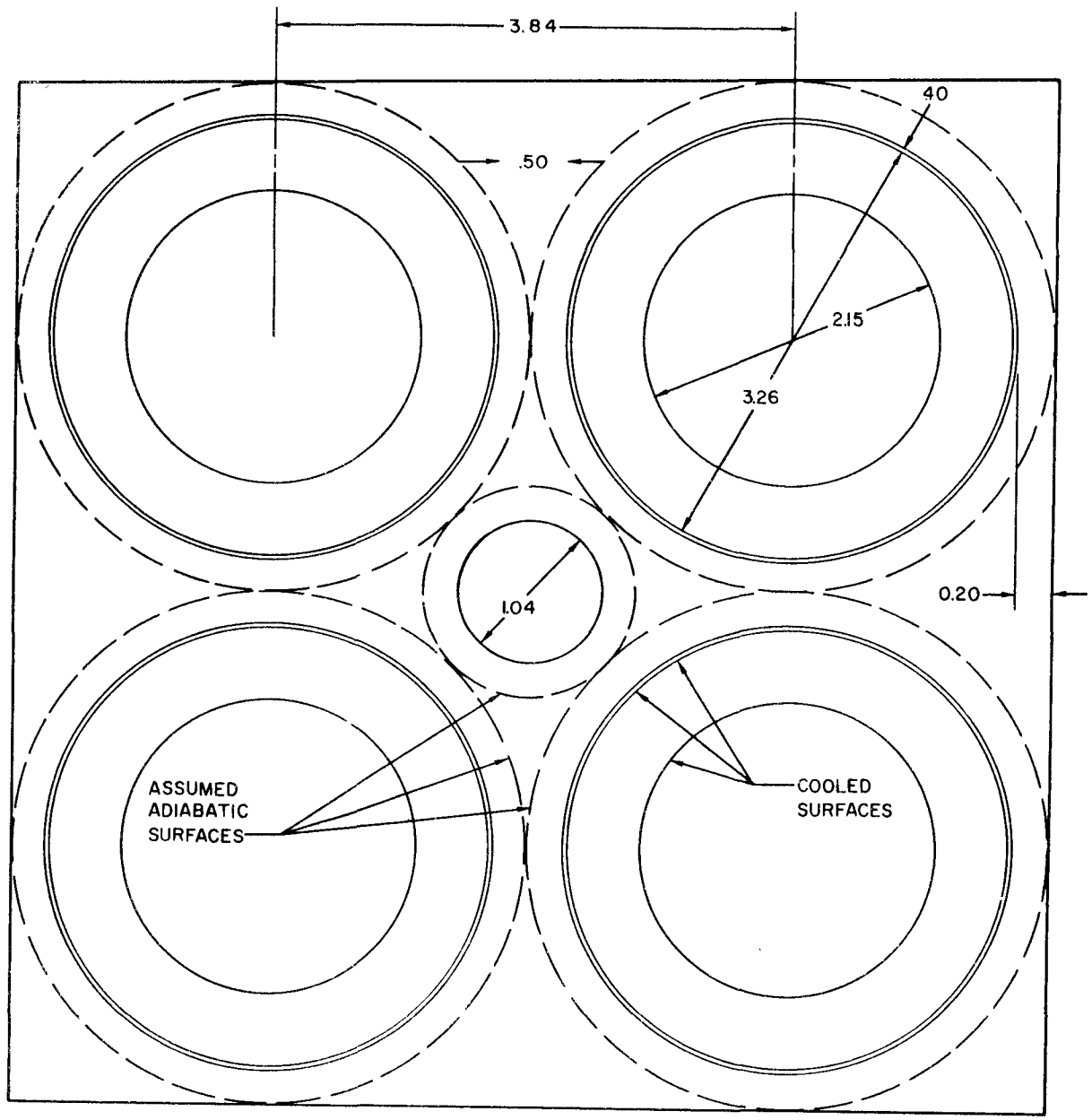

Fig. 1.10--BORE 4-channel Core Module

The approach, while approximate, represents a second approximation to the stress induced in the BeO plate, the first being the use of a slab geometry. More exact methods will be developed and used to establish the final design.

Pressure Vessel and Associated Components

A review of the engineering requirements for the pressure vessel, core support and thermal shields has been made for the BORE. The requirements have been compiled into a tentative specification of engineering requirements to be used by General Atomic. The essential parts of the specification are as follows:

> The design of the pressure vessel, as a minimum requirement , shall comply with the latest edition (including revisions, addenda, and applicable cases) of Section VIII of the ASME Boiler Code (Unfired Pressure Vessels), the State of Idaho Pressure Vessel Code and AEC regulations.
>
> In addition, a detailed stress analysis shall be performed for the pressure vessel and associated components in accordance with the Bureau of Ships' "Tentative Structural Design Basis for Reactor Pressure Vessels and Directly Associated Components", issued December 1, 1958, with addendum February 27, 1959. This analysis is divided into two phases.
>
> Phase I will determine the basic dimensions founded on primary stresses developed by equilibrium loadings and the basic geometry at all structural discontinuities by consideration of secondary stresses resulting from self constraint of the structure or the constraint of adjacent parts.
>
> Phase II will examine the operational requirements and accident cases by evaluating combinations of steady state and transient conditions on a fatigue strength basis for operational cases and on a rupture strength basis for the accident cases.

FUEL HANDLING (TASK 11) (B. C. Hawke)

A "wet" fuel-handling system is proposed for the Beryllium Oxide Reactor Experiment. Shielded fuel transfer casks would be required only during the time when spent or failed fuel or core module assemblies are to

be shipped. Refuelling would be accomplished by handling and moving of fuel and module assemblies under water in a pool system. A telescoping tube-type hoist, which can be positioned and adjusted above the core by optical sighting, is a component of a movable carriage. Tools attached to the lower end of the hoist tube are used to provide simple twist and lift motions to unlock a fuel element and to lift and transport fuel elements and core modules to storage pits.

REACTOR CONTROLS AND INSTRUMENTATION[1] (TASK 14) (W. Lones)

A conceptual design of the operating instrumentation and controls and of the test instrumentation for the evaluation of fuel element performance has been developed for the 10 MW(t) Beryllium Oxide Reactor Experiment. This design incorporates the instrumentation necessary to operate the reactor and gas loop safely and with a minimum amount of shutdown time due to instrumentation component failures or momentary power outages.

The test instrumentation provides for the continuous measurement of the average power generated by each test element and the continuous indication of thermal neutron flux at thirteen equally spaced locations along the length of and in the vicinity of selected test fuel elements.

The feasibility of detecting a fuel element rupture in a fast recycle reactor with a limited number of channels was also considered.

On the basis of this preliminary study it appears that the prevailing signal-to-background ratios obtained in the detection of krypton and xenon, or the detection of the solid daughters of krypton and xenon, would make the detection of individual fuel-channel ruptures possible.

MGCR PROTOTYPE THERMAL DESIGN ANALYSIS[8, 9, 10] (R. Katz)

A thermal design analysis has been made for the MGCR pressure vessel and thermal shields.[9] Two pressure vessel configurations were analyzed:

(a) An internally insulated and externally cooled vessel.

(b) An externally insulated vessel internally cooled with reactor inlet gas.

The results of the analysis show that an internally insulated vessel is inherently safer and more reliable for MGCR requirements and was, therefore, selected as the tentative design configuration. An economic comparison of the configurations has as yet not been made.

A preliminary analysis was made of several external coolants for the pressure vessel. The coolants studied included air, helium, water, and several organic heat transfer fluids. The organic heat transfer fluids were found to be superior to the other coolants considered.[6] It was recommended that a more exhaustive analysis be made to select the best coolant and design arrangement.

A thermal design analysis of the MGCR reactor core support shell section has also been completed.[10]

The core support shell section, referred to in the report[10] as the core barrel, was deemed to be the most critical part of the core support structure from the standpoint of thermal conditions. The initial work on the thermal analysis of the core support structure, therefore, concentrated on this part.

It was found that one inch of metallic insulation is required to protect the core support shell section when it is cooled by one-half of the total coolant flow at the inlet temperature of 745°F passing through a 1-5/8-in. annular gap. This resulted in maximum design temperatures for the core barrel of 815°F and 944°F at core outlet temperatures of 1300°F and 1500°F, respectively.

Some type of internal header will be necessary to provide a reasonably uniform flow distribution around the core barrel although a flow distribution with a ± 25 per cent maximum velocity variation could probably be tolerated from a thermal stress standpoint. Analysis has shown that local thermal stresses in areas which are poorly cooled due to obstructions, non-symmetric flows, or other causes, will probably not be excessive; therefore, great care and complexity will not be required to ensure perfectly uniform local cooling.

HANFORD LOOP (TASK 20) (H. C. Hopkins)

Heterogeneous Fuel Element

The testing of a 5/3-scale fuel element model to obtain pressure drop and heat transfer data has been completed. The heat transfer tests have shown that the pressure drop is slightly higher than originally estimated, and the surface temperature has been slightly underestimated for this heterogeneous fuel element mock-up.

Semi-homogeneous Fuel Element

The irradiation of the second semi-homogeneous fuel element, MGCR-HDR-2, is continuing in the Hanford DR-1 Gas Loop. Over 1000 hrs and a total of six thermal cycles have been logged at design conditions of 1500°F maximum graphite temperature.

The activity measured by comparably placed monitors indicates that the present amount of activity is considerably lower, perhaps as much as two orders of magnitude, for this element than for the first semi-homogeneous fuel element, MGCR-HDR-1. Since the loop activity again increased with increasing element temperature and decreased with decreasing element temperature, a multichannel gamma spectrum analyzer was used to examine a gas sample in an attempt to determine if fission products were present. The following xenon* isomers were identified by energy level and half-life measurements:

Table 1.7

XENON ISOMERS FOUND IN DR-1 GAS-LOOP SAMPLE

Isomer	Half-life	Mev
Xe^{133m}	2.3	0.234
Xe^{133}	5.2	0.081
Xe^{135m}	15	0.252
Xe^{135}	9.13	0.250

Determination of the soundness of the cladding and location of the source of the xenon will be part of the post irradiation examination to be conducted in the General Atomic Hot Cell.

The examination of the first semi-homogeneous fuel element has been completed and the parts of the element will be stored for comparison with MGCR-HDR-2.[11]

* No iodine was found.

Reactor Environmental Test Stand

During the past quarter, consideration was given to the design and construction of a test facility capable of providing an environment which would allow for the evaluation of the thermodynamic performance and structural properties of an MGCR core module under actual reactor operating conditions. A subcontract was, therefore, given to the Marquardt Corporation to carry out a detailed design study for such a facility.

Specifically, the facility would simulate the temperature pressure and high-purity helium environment under which an actual MGCR fuel element and core module would be expected to function. Consequently, a fuel element mock-up with electrical heaters will have to be developed and special pumps will be needed to provide the pressures and flow rates required in that portion of the loop through which high-purity helium will circulate. The facility would operate at the conditions shown in Table 1.8.

Table 1.8

FACILITY OPERATING CHARACTERISTICS

Inlet helium pressure, psia	1120.8
Inlet helium temperature, ^{o}F	745.1
Outlet helium pressure, psia	1080.4
Outlet helium temperature, ^{o}F	1300
Helium flow, lb/sec	0.586
	0-0.60
Maximum helium temperature, ^{o}F	1500
Maximum helium pressure, psia	1215
Maximum input electrical power	426 Kw at 200 v

The proposed environmental facility would consist of a continuously circulating helium loop and its associated service equipment (Fig. 1.11). Connected in series in this loop are the circulating pump unit, helium heater, the test vessel which contains the simulated fuel elements, helium cooler, and associated equipment.

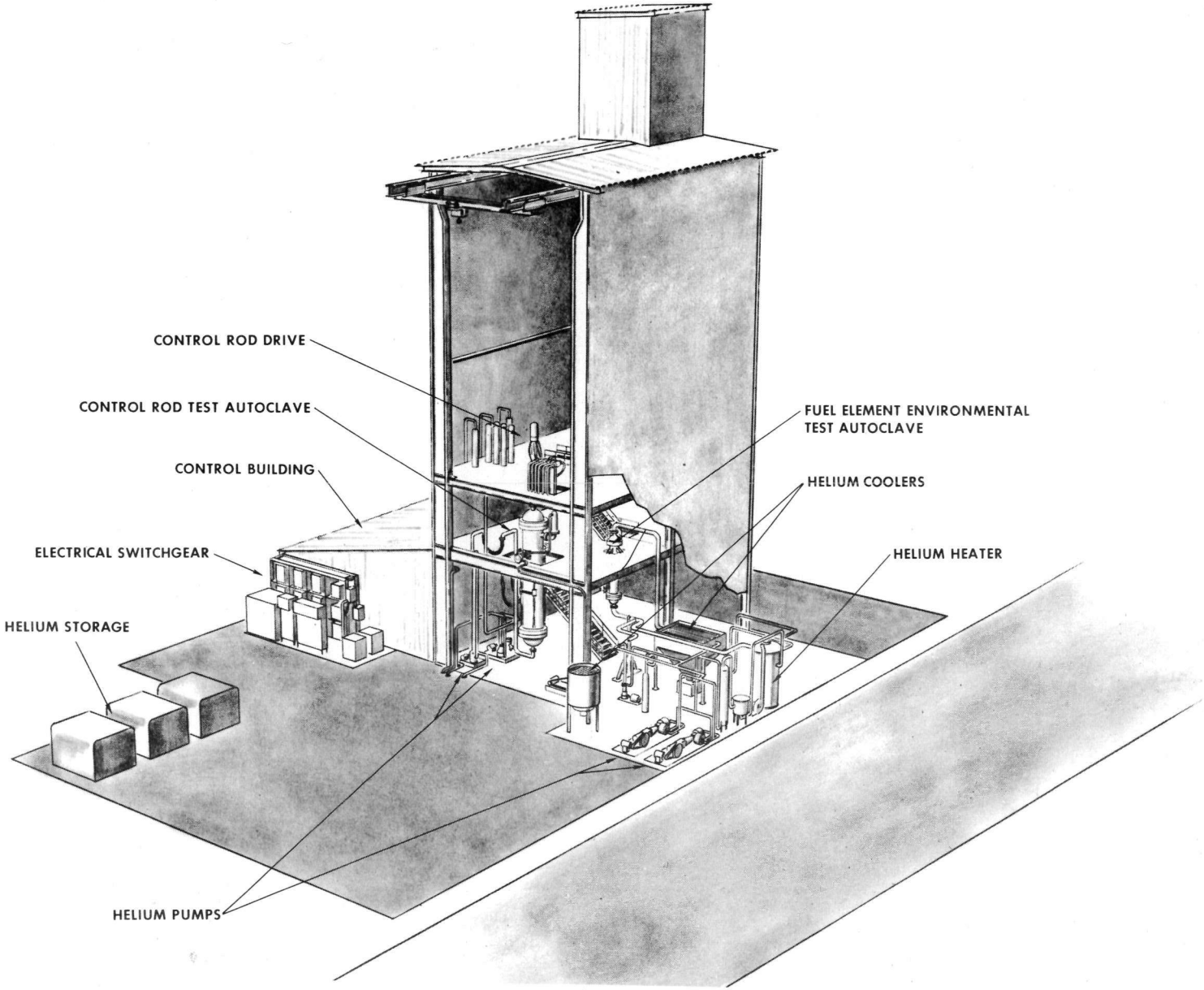

Fig. 1.11--MGCR Reactor Environmental Test Stand

The flow paths during a test run would be as follows:

1. Helium would enter the bottom of the autoclave at 745°F and 1120 psia, flow upward through the fuel element (in the interstices between the rods) and leave the top of the test vessel at 1300°F and 1080 psia; heat from the 426-Kw, the source would be supplied to the fuel element.
2. The helium would then flow through the water-jacketed hot pipe and then through the cooler where its temperature would be reduced to 100°F.
3. From the cooler, it would enter the circulating pump unit at 1060 psia where it would be re-pressurized to 1200 psi and passed through a pulsation damper, particle filter, and flow-measuring unit to the heater.
4. The heater will reheat the helium and deliver it to the autoclave at the inlet condition.
5. A bypass connected purifier is installed up-stream of the heater for use during a pre-run helium purification cycle.

Evaluation of this facility is presently continuing.

CONTROL-ROD DRIVE MECHANISM DEVELOPMENT (TASK 10) (F. J. Liederbach)

The detailed design and stress analysis of the experimental control-rod drive mechanism and thimble is nearing completion. The remaining design analysis is related to the drive-shaft to self-aligning control-rod coupling (Fig. 1.12).

As shown in this figure, the purpose of this coupling is to connect the control-rod stem (A) to its tubular bayonet-type driving element (E) in such a manner as to permit:

(a) Angular and axial misalignment between the two elements

(b) Operation of the coupling by means of a handling tool located within the tubular driving element

The lower end of bayonet (B) is also spherical in order to satisfy these design requirements.

To operate the coupling, a locking sleeve (D) is screwed upwards until the lock balls (F) are free to slip out of their respective detents leaving the rotating sleeve (C) free to rotate.

Rotation of the rotating sleeve (C) to release the bayonet joint (E) completes the uncoupling operation.

The reverse procedure is followed to recouple the two elements.

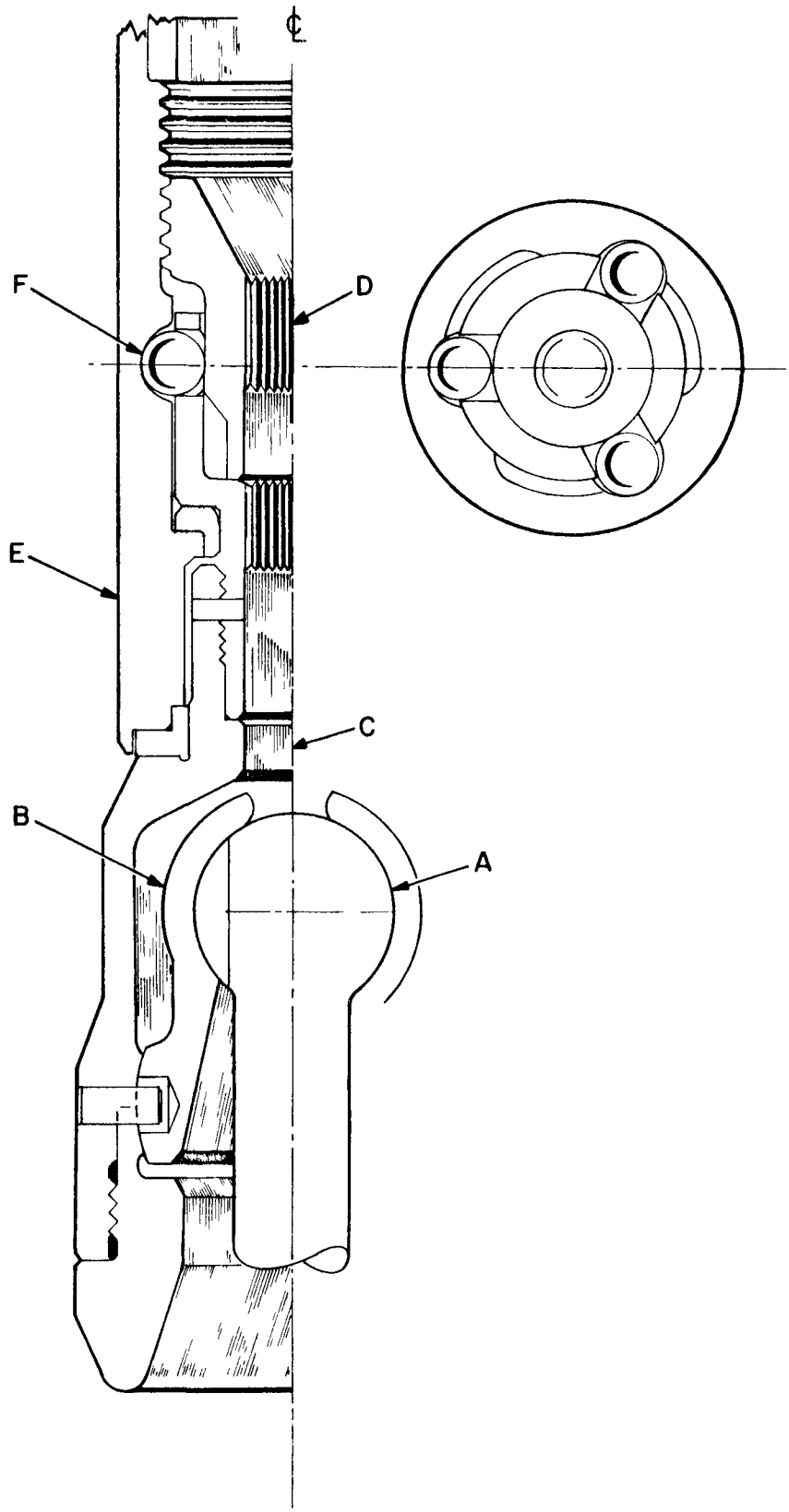

Fig. 1.12--MGCR Self-Aligning Control-Rod Coupling

Control-rod Drive Test Program

Testing of the ball-nut lead screw continued this quarter.[12,13] These tests were performed for over 7500 cycles and at temperatures as high as 500°F with little noticeable wear of the screw or balls.

Future tests will be run at temperatures as high as 750°F using samples of the actual ball screw to be used in the MGCR mechanism.

REFERENCES

1. MGCR Project Staff, Conceptual Design Report for a 10 MW(t) Beryllia Reactor Experiment (BRE), General Atomic Report GAMD-1565, August 5, 1960.

2. W. H. McAdams, Heat Transmission, 3rd edition, McGraw-Hill, 1954.

3. G. J. Malek, J. T. Rogers, The Effects of Loss-of-Vessel Coolant and Accidental Flooding on the BRE Pressure Vessel and Associated Components, General Atomic Report GAMD-1630, August 31, 1960.

4. MGCR Project Staff, BRE Design Report Supplement, General Atomic Report GAMD-1570, August 24, 1960.

5. Battelle Memorial Institute, Numerical Solution of Fuel-Element Thermal-Stress Problems, BMI-1422, February 26, 1960.

6. C. F. Bonilla, Nuclear Engineering, McGraw-Hill, 1957.

7. Reactor Handbook, Technical Progress Report, AECU-3647, January 1958.

8. J. T. Rogers, R. Katz, Thermal Design of the MGCR Core, General Atomic Report GAMD-1542, August 4, 1960.

9. J. T. Rogers, G. J. Malek, Thermal Design of the Pressure Vessel and Thermal Shields of MGCR, General Atomic Report GAMD-1572, August 8, 1960.

10. J. T. Rogers, R. Katz, Thermal Design of the MGCR Core Support Structure, General Atomic Report GAMD-1652, (to be issued).

11. General Atomic Staff and Electric Boat Staff, Maritime Gas-Cooled Reactor Program, Quarterly Progress Report for the Period Ending June 30, 1960, General Atomic Report GAMD-1532.

12. General Atomic Staff and Electric Boat Staff, Maritime Gas-Cooled Reactor Program, Quarterly Progress Report for the Period Ending March 31, 1960, General Atomic Report GAMD-1259.

13. General Atomic Staff and Electric Boat Staff, Maritime Gas-Cooled Reactor Program, Quarterly Progress Report for the Period Ending June 30, 1960, General Atomic Report GAMD-1532.

II. FLUID SYSTEMS AND PLANT ARRANGEMENT

DEVELOP REFERENCE DESIGN OF PRIMARY LOOP COMPONENTS (TASK 6) (D. W. Carreau, W. J. Justusson, B. Lund, H. C. Paulsen)

Heat Exchanger Test Loop

The objective of the Heat Exchanger Test Program is to compile and correlate sufficient experimental data for the aerodynamic and thermal design of the MGCR prototype regenerator. These data will also be used in the design of other power plant heat exchangers of similar configuration.

Early in the quarter, the model heat exchanger was re-tubed to eliminate recurrent steam leaks at the tube-tubesheet welded joint. Tests were then made to assess the fundamental aerodynamic and thermal performance of the new tube bundle. These tests were concluded in September and the data derived are presently being evaluated.

MECHANICAL DEVICES

Duct Design, Development and Test (D. W. Carreau, H. F. Curtis, B. Lund)

The objective of this task is to develop and design ducting to transport the main coolant between the components of the power plant at pressures up to 1150 psi and continuous temperatures up to 1300°F, with capability for 10,000 hr. operation up to 1500°F.

Heat Barrier Tests

Various modifications of the basic heat barrier design configuration described in previous quarterly reports are being considered in order to optimize thermal effectiveness. The heat barriers will be used as internal insulation for the inner wall of the concentric coolant duct. A small test apparatus, (Fig. 2.1) capable of operating at temperatures up to 1500°F, has been designed to make a comparison of the insulating effectiveness of the various heat barrier configurations under consideration.

Flange Tests

Mechanical joints in the ducting will be necessary in order to provide accessibility to the rotating machinery. However, they must provide full tightness under all operating conditions. Modified welding neck flanges are recommended for this application. An apparatus has been designed which is capable of imposing a 100,000 ft-lb. bending moment on a 12-in. flanged piping joint. The apparatus is thus capable of imposing bending stresses

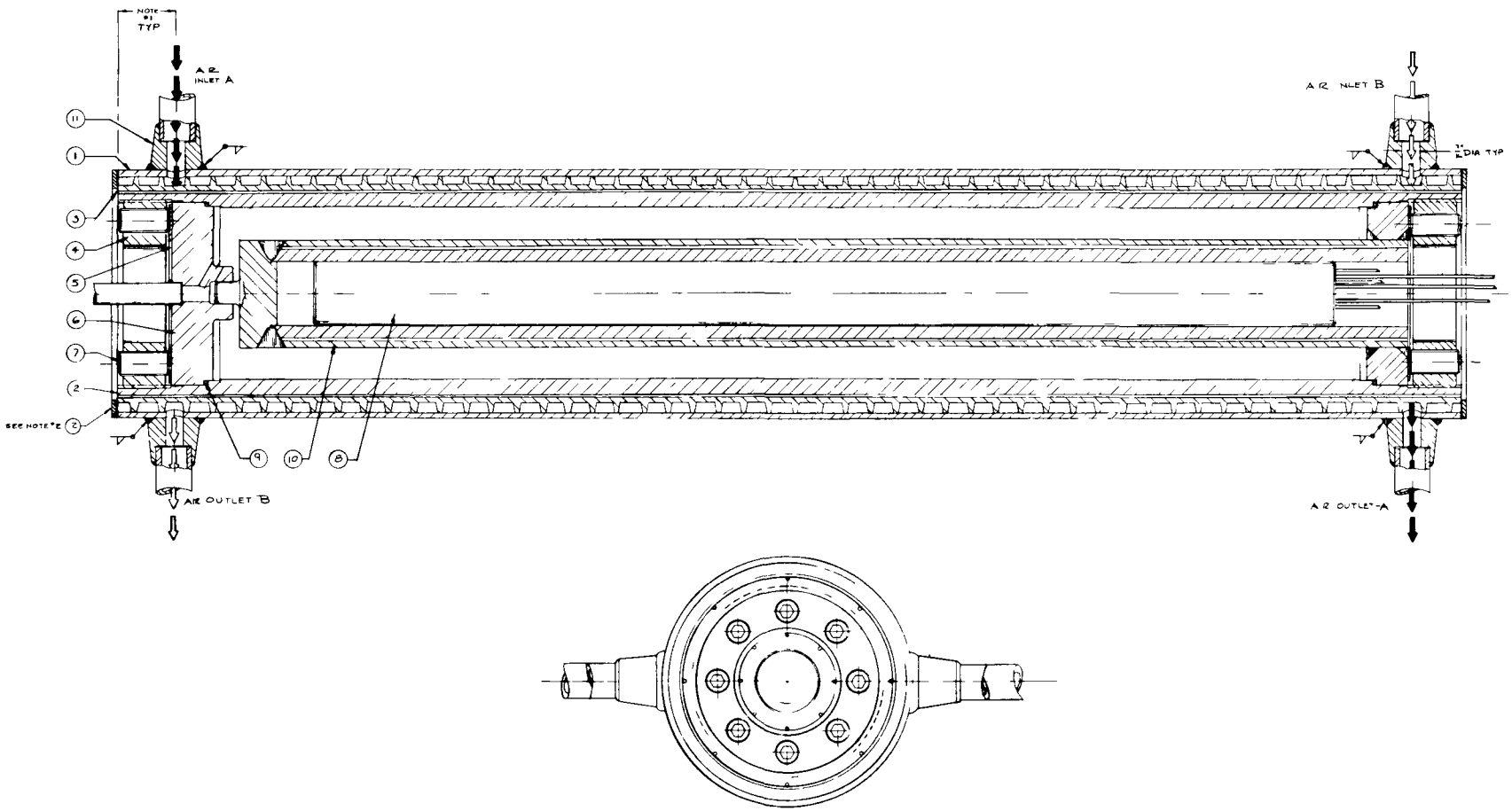

Fig. 2.1--MGCR Heat Barrier High Temperature Test Assembly

on the flanged joint equivalent to the maximum values permitted by the ASA Code for Power Piping. A spiral-wound asbestos-filled gasket with a load ring to prevent deflection will be tested for tightness, in helium, at full plant operating temperature and pressure. Following this test, a groove will be machined in each flange face and ring-type joints will be tested.

DEVELOPMENT OF PLANT CONTROL SYSTEM (TASK 15) (A. E. Holmes, D. Olding, A. McClure)

A computor program designed to study the transient behavior of the high-pressure drive (HPD) plant has indicated that this plant is controllable if certain refinements are made in the control system. The HPD plant however does not seem to have as much inherent stability as the low-pressure drive (LPD) plant.

There is, basically, no difference in the method of controlling the high-pressure drive and low-pressure drive plants. In each case, four items require control: (1) power turbine output, (2) turbo-compressor speed, (3) reactor outlet temperature, and (4) reactor power level. The control elements for these items are, respectively: (1) power turbine throttle valve, (2) power turbine bypass valve, (3) reactor control rods, and (4) accumulator inlet and outlet valves.

The minor refinements required in the control system for the high-pressure drive plant may be traced to the increased sensitivity of this system to bypassing of the power turbine. In the low-pressure drive, by-passing results in a greater pressure ratio for the compressor turbine, providing more power. Bypassing in the high-pressure drive provides the compressor turbine with both increased pressure ratio and increased inlet temperature. The inlet temperature changes rapidly as the bypass valve is opened, so that its rate of opening must be carefully modulated (by means of a proportional control, i.e., rate of valve motion proportional to speed deviation) to maintain turbocompressor speed. For the low-pressure drive, the requirement is less severe and the bypass valve may be actuated by a constant speed motor with on-off control.

The low-pressure turbine in the high-pressure drive plant cannot run for extended periods at the increased inlet temperature which results from bypassing. This imposes the requirement for an interlock which lowers the

set point on reactor outlet temperature as the power turbine throttle valve is closed. Such a device would not be required for the low-pressure drive.

When shut, the bypass valve cannot control against increases in turbo-compressor speed. Compressor bypass is required to prevent such overspeed. Originally, in the low-pressure drive, this was envisioned as a safety device (as opposed to a control element) which, when tripped, would result in plant shutdown. The high-pressure drive, however, has shown a greater tendency to overspeed during ordered (reactor) power reductions when the bypass valve is shut. Under these circumstances, control against overspeed must be provided by means of an additional control valve for compressor by-pass. This additional control valve may possibly be necessary under certain conditions in the low-pressure drive plant. Its use, however, would be less frequent.

The following transients demonstrate the controllability of the high-pressure drive plant:

(a) Maneuvering with Bypass

Figs. 2.2 and 2.3 show the behavior of the high-pressure drive plant during the following transient: with the plant initially operating at full load steady-state condition, the turbine throttle valve was closed in 3 sec. and held closed for 77 sec. In one case, the ordered reactor outlet temperature was dropped to 1115°F; in the other case, it was held constant at 1300°F. The former indicates that about 45 sec. are required for the low-pressure turbine inlet temperature to return to its normal value following closure of the throttle valve.

(b) Ordered Reduction in Reactor Power Level

Fig. 2.4 shows the response of the plant to an ordered reduction in reactor power level from 100% to 61%. This power reduction is accomplished by opening the valve in the line from the high-pressure compressor discharge to the accumulator. This permits inventory to be withdrawn from the system at a rate proportional to the pressure drop across the valve. Initially, the reactor outlet temperature increases, causing the control rods to be inserted. The resulting decrease in power drops this temperature back to its normal level.

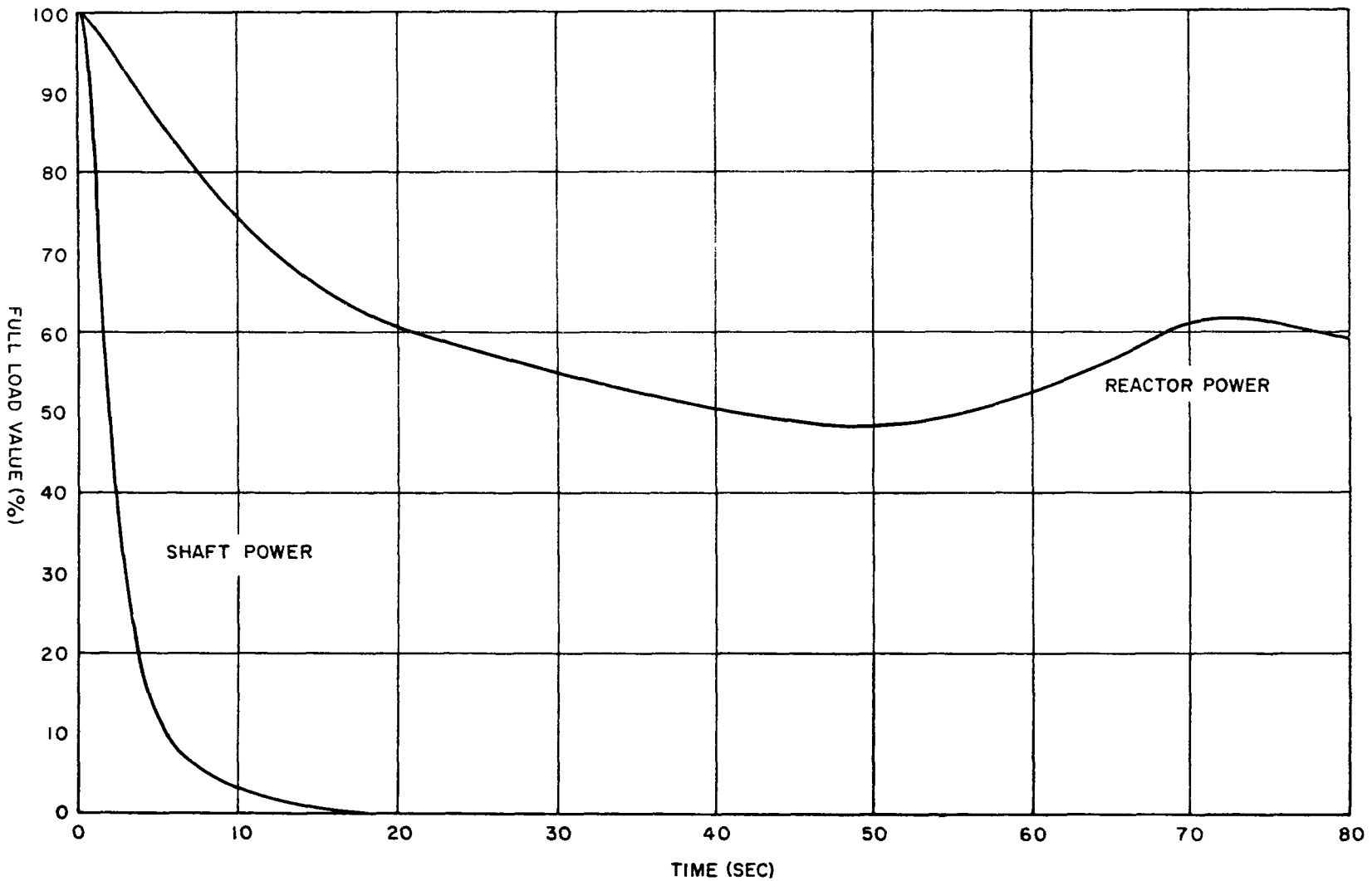

Fig. 2.2--Plant Response to Closing of Turbine Throttle Valve

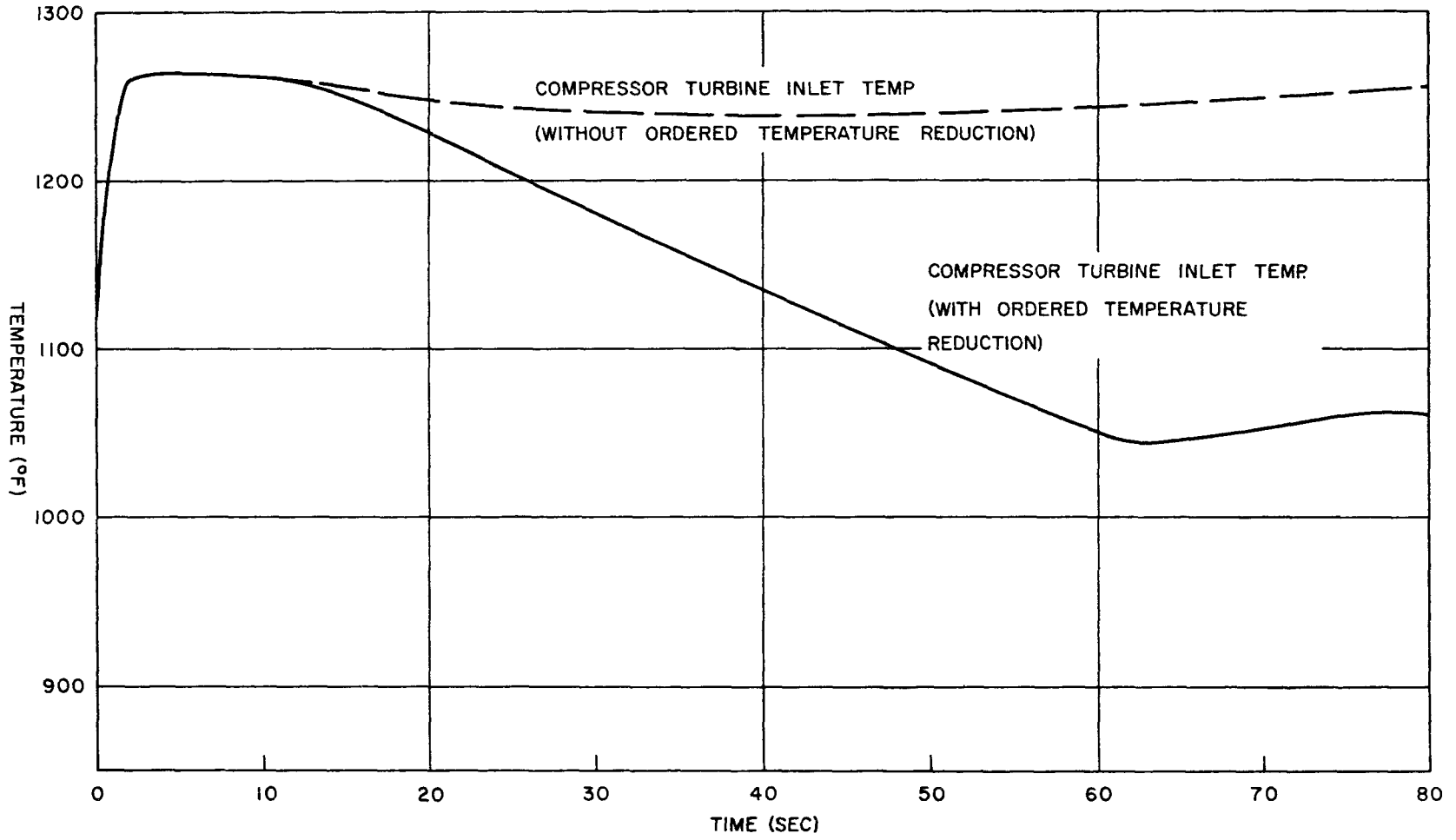

Fig. 2.3--Plant Response to Closing of Turbine Throttle Valve

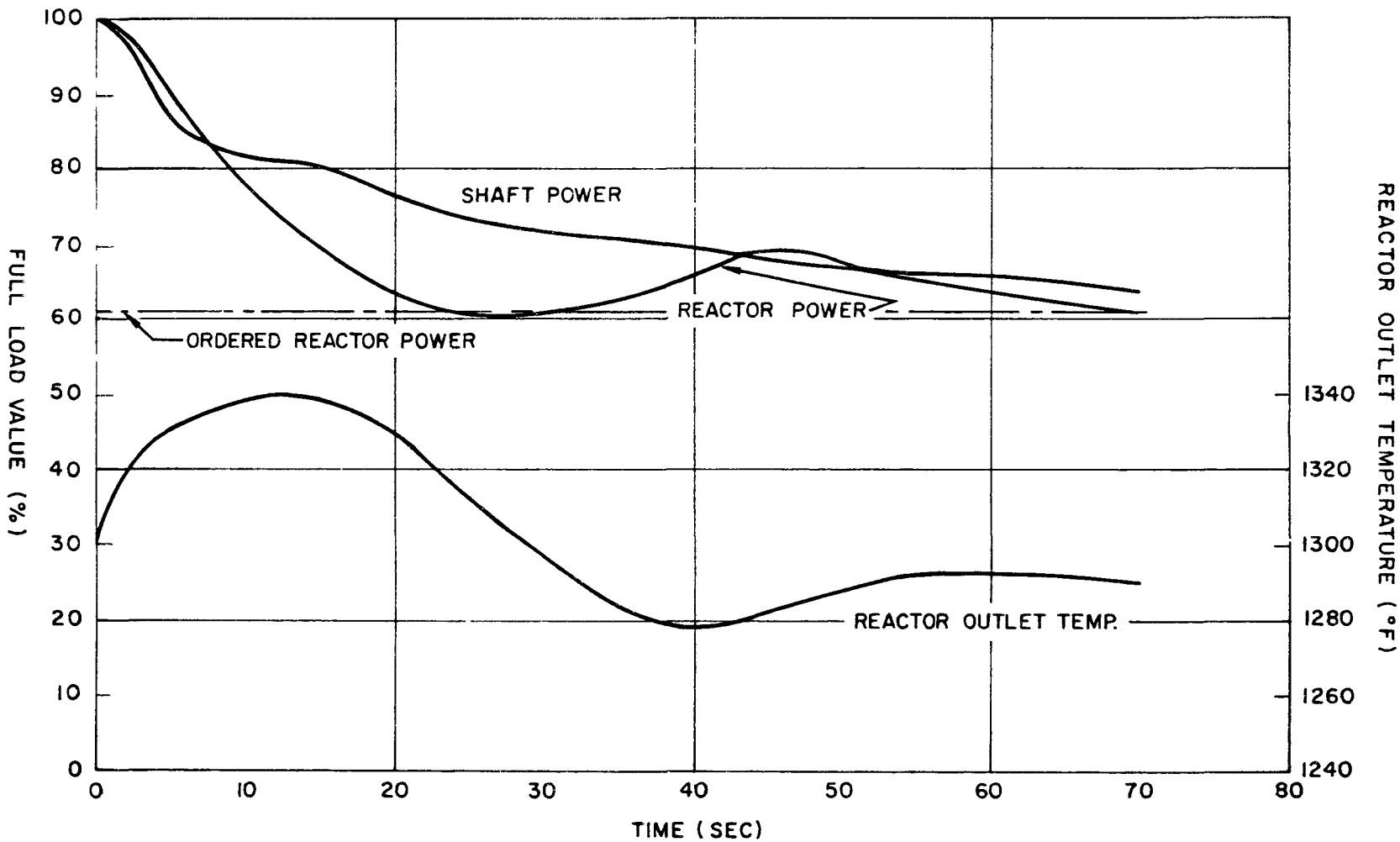

Fig. 2.4--Plant Response to Ordered Reduction in Reactor Power Level

(c) Ordered Reduction in Reactor Outlet Temperature

Fig. 2.5 shows the response of the plant to an ordered reduction in reactor outlet temperature of 50°F. Some overshoot occurs, but the system stabilizes in about 36 sec. Shaft power drops to 90%; reactor power to 95%.

Emergency conditions such as overspeed, loss of cooling water, and reactor scram, should have no more serious consequences in the high-pressure drive plant than in the low-pressure drive plant.

Further transient studies of the high-pressure drive plant will utilize a slightly modified computer program. The modifications and additions which have been made to the program include the following:

(a) Addition of bleed flows to conform with full load program.

(b) Use of compressible flow relationships for the flow through valves.

(c) Addition of bearing friction in equations for shaft acceleration.

(d) Addition of a time delay in the equations describing rod motion as a function of temperature error.

DEVELOP REFERENCE DESIGN FOR POWER PLANT ARRANGEMENT AND STRUCTURE (TASK 17)

(I. Kabler, A. McClure)

Helium Turbine (HT)

A conceptual design study was completed for the HT proposal. This represents a one-quarter power, land-based, fossil-fuel-fired version of the MGCR rotating machinery and auxiliary equipment.

Various locations were considered for the proposed site in the North Yard of the Electric Boat Division.

The HT test facility has been suitably arranged as a land-based prototype. The fossil-fuel-fired heaters obviate all shielding from the plant, permitting unrestricted access to all components. The basic compact shipboard requirements have been relaxed, where possible, without affecting the short piping runs and minimum pressure drop of the shipboard plant.

High-Pressure Drive (HPD)

The high-pressure drive machinery concept results in many changes in the machinery compartment arrangement. The major difference between the high-pressure drive and the low-pressure drive is the location of the four

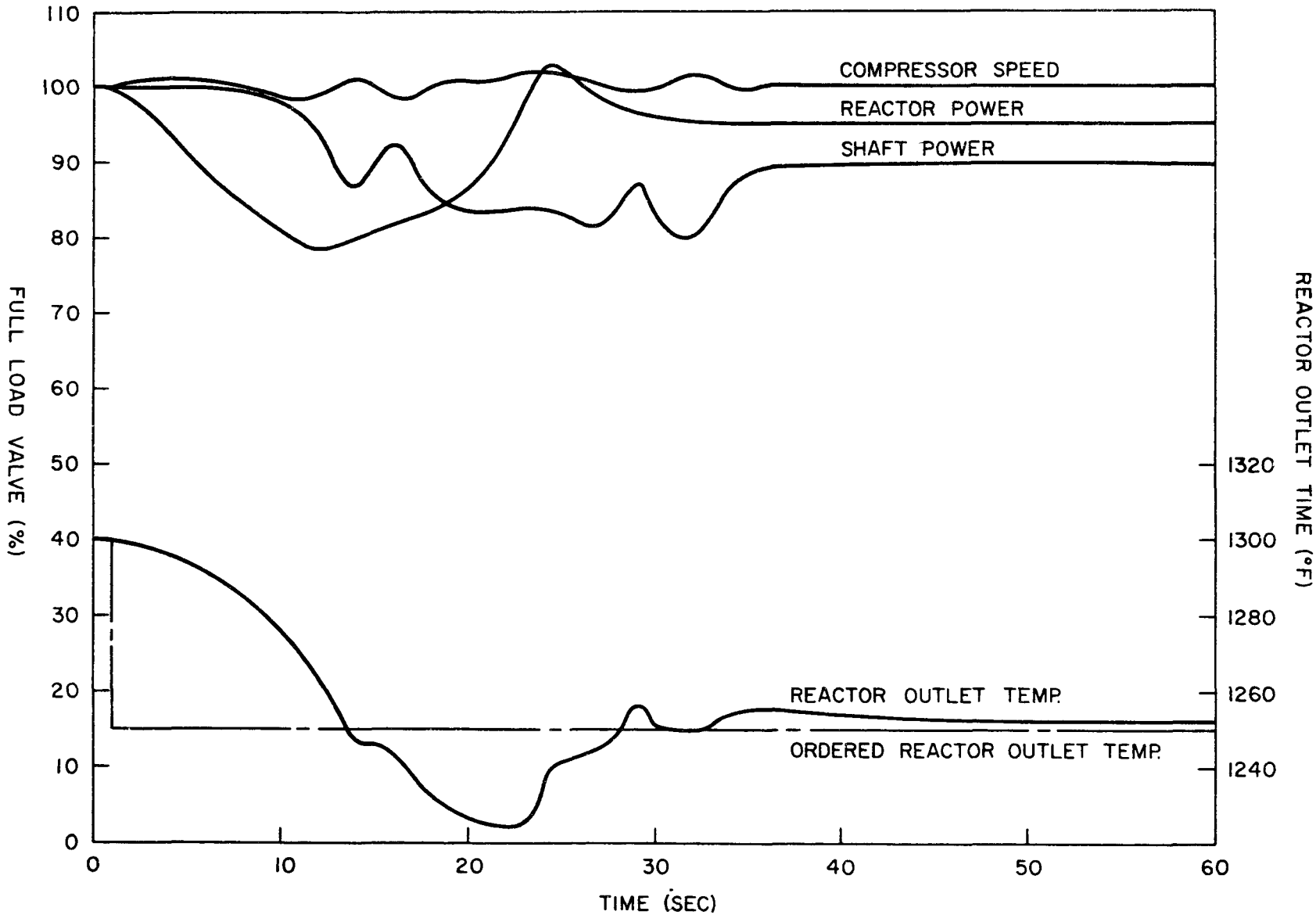

Fig. 2.5--Plant Response to Ordered Reduction in Reactor Outlet Temperature

basic units which comprise the rotating machinery. For the HPD systems, the high-pressure turbine is the power turbine and is directly coupled to the main reduction gear. The turbomachinery remains along the centerline, fore-and-aft at its predetermined 1/2 in/ft rake. The four units arranged from fore-to-aft are the high-pressure compressor, the low-pressure compressor, the low-pressure turbine, and the high-pressure turbine.

The regenerator has been modified to accommodate the new locations of the rotating machinery units. It has also been reversed, in that the closed end of the "U" is now aft with the open end forward. The precooler and intercooler remain unchanged in design and location, but are reversed in orientation to agree with the machinery nozzle locations.

A major problem associated with the HPD system is the increase in piping lengths required. Various alternate schemes are now being worked out to reduce the piping to a minimum.

III. ROTATING MACHINERY

DEVELOP REFERENCE DESIGN OF ROTATING MACHINERY (TASK 5) (F. E. McDonald, A. McClure, D. F. Putnam)

Compressor Tests

The 4-stage compressor model, now running in the variable density tunnel at Westinghouse has provided data which gives the pressure coefficient and efficiency as a function of flow coefficient. Curves of ψ vs ϕ have been experimentally established on each side of the design point with adjustments of the blade setting angle. Maximum efficiency is 0.88 to 0.89.

Where:

$$\psi = \text{pressure coefficient} = \frac{gH}{U^2}$$

$$\phi = \text{flow coefficient} = \frac{Ca}{\mu}$$

It was found that increasing the Reynolds number brought about a decrease in ψ at a given value of ϕ. This is the opposite effect from that predicted from turbomachinery experience. A number of runs were made in which the Reynolds number was changed by changing the speed of rotation instead of loop pressure. The resulting data indicate that the effect is a function of pressure instead of Reynolds number, per se. Attempts are being made to locate the source of this anomaly by checking the instrumentation and the flow distribution entering the model.

Turbine Test Program

Single-stage turbine tests are in progress, and preliminary tests indicate good aerodynamic performance. The turbine test stand has been modified and improved. Among the changes made were: (1) changing water brake and turbocompressor couplings to reduce vibration, (2) use of lighter oil in turbine model and dynamometer bearings to reduce tare correction, and (3) improvement in the accuracy of instrumentation and controls.

LUBRICATION AND SEALING SYSTEM DEVELOPMENT (H. E. Holmes, A. McClure)

Testing at Westinghouse

Installation of piping and components for semi-closed loop operation of the lube and seal system test rig at Westinghouse was completed during the quarter. Testing to evaluate components designated as Configuration I[1]

commenced after the system had been cleaned, leak tested and preliminary shakedown runs had been made.

In the semi-closed mode of operation, the system is pressurized with commercial helium. Helium bottles are connected to the system at all times and, by means of reducing valves, supply a small amount of the make-up helium required to maintain system pressure. Seal gas circulation is provided by a blower installed in the system. Testing on Configuration I will be carried out at system pressure up to approximately 150 psi.

Oil Vapor Contamination Measurement

Oil content of the seal gas being returned to the cycle at the low-pressure compressor inlet from the oil-gas separation and filtering system is limited to 2 ppm by volume (200 ppm by weight). Oil contamination of the seal gas will be measured at several locations in the seal gas return system in the lube and seal system test rig.[1] This will be accomplished through the use of sampling bombs installed in sampling bypass lines and normally isolated from the system by a system of valves. When a sample is to be taken, the bomb and adjacent piping is evacuated and the valves adjusted to divert the main flow through the bomb. The bomb will then be removed and contents analyzed in the laboratory for oil content.

The final system will make use of a hydrocarbon detecting instrument, which utilizes the flame ionization principle, to determine the hydrocarbon and hence oil content of the return seal gas. The seal gas samples will be tapped from the stream by means of a suitable isokinetic probe and led to the instrument for analysis.

(1) MGCR Project Staff, Maritime Gas-Cooled Reactor Program, Quarterly Progress Report for the Period Ending June 30, 1960, General Atomic Report GA-1532.

IV. REACTOR PHYSICS

BERYLLIUM OXIDE REACTOR EXPERIMENT (BORE) NUCLEAR CONCEPTUAL DESIGN (TASK 18)

(J.M. Stein, L.R. Amyot, A.J. Goodjohn, A.D. McWhirter, J.R. Seibold, H.A. Vieweg)

A conceptual design for the BORE was developed during this quarter. In considering several core configurations in which test elements could be subjected to conditions simulating those in MGCR-class power reactor system, the number of fuel element required within the limitation of 10 MW(t) output was found to be such that a maximum reactor diameter of 4 ft would be adequate.

Figure 4.1 shows a schematic representation of a cross section of the 36-element preliminary reference core showing the location of the active control rod blades. For initial performance estimates, the 36 elements were each considered to be of the driver element design, i.e., 30 mils of Hastelloy X cladding on the 0.375-in. fuel rods. Data on the size and composition used in the nuclear calculations are given in Table 4.1.

Reactivity estimates for the reactor have been based on two-dimensional criticality calculations using the PDQ code. The reactivity-lifetime history was obtained by bulk treatment of core life using the OPTIM code.

Because of the large fuel loading required in the BORE, particular attention has been focused on the self-shielding aspects. In order to check the applicability of the analytical models previously employed in nuclear design calculations for the MGCR prototype, calculations of the local heterogeneities were made with the S_8 transport code.

To achieve the BORE design lifetime of 10,000 hrs at 10 Mw reactor output, with a 70 v/o dilution of the fuel body, would require initial loadings of 100 kg of U-235 and 74 kg of U-238 -- an enrichment of 57.5%. Although little additional fabrication and operating expense would be incurred by using a fully enriched fuel body, it is desirable to utilize the maximum U-238 loading possible in order to maintain a reasonable value of the prompt negative temperature coefficient.

Table 4.2 gives nuclear parameters and reactivity estimates for the BORE at operating temperature. The heavy isotope composition of the fuel at the end-of-life is shown in Table 4.3.

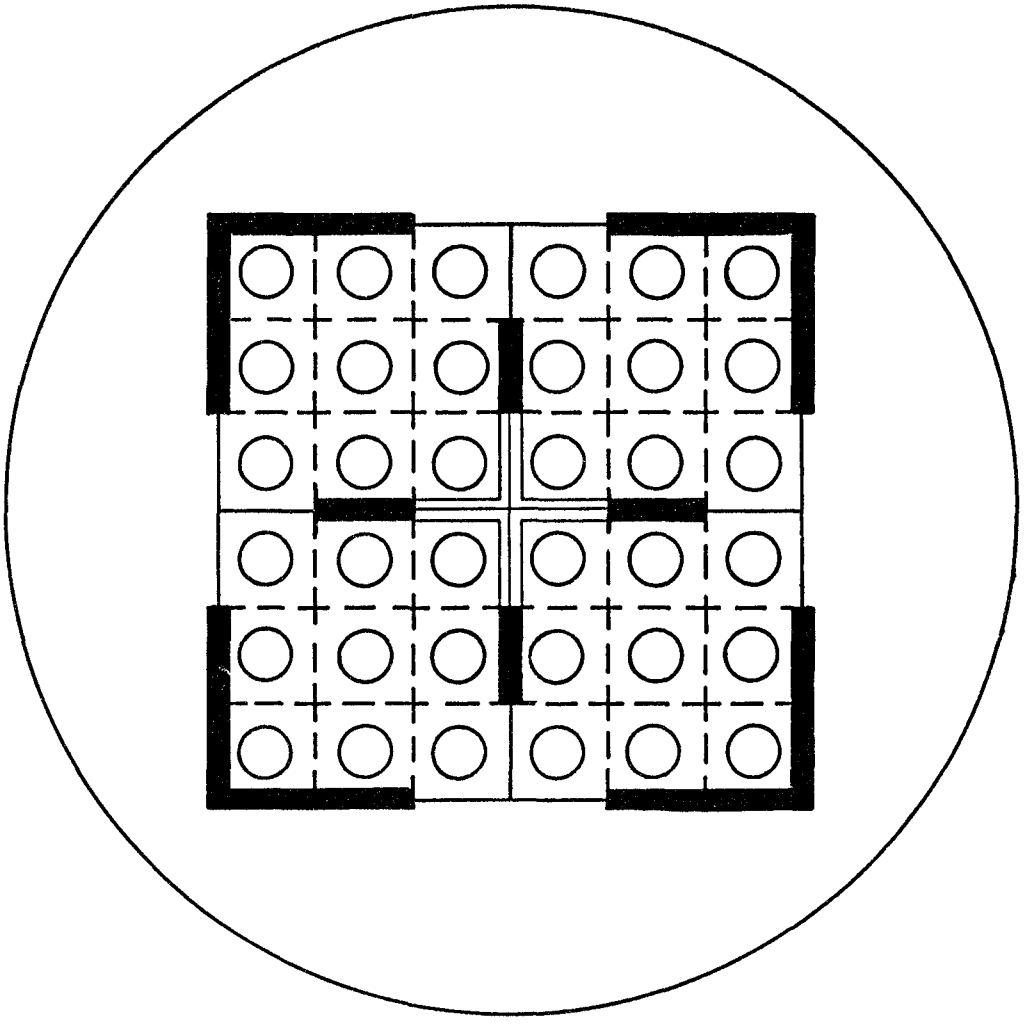

Fig. 4.1--BORE Configuration No. 2, Square Modules-9 Element Type
(Effective Core Diameter 26-in., Reflector Diameter 40-in., 36 Fuel Elements)

Table 4.1

SIZE AND COMPOSITION DATA FOR PRELIMINARY REFERENCE CORE

Number of fuel elements	36
Fuel element type	Shrouded 19-rod bundle, center rod unfuelled
Fuel rod O.D., (in.)	0.375
Clearance between rods, (in.)	0.050
Cladding - Hastelloy X, (in.)	0.030
Inside diameter of shroud, (in.)	2.067
Equivalent shroud thickness - Hastelloy X, (in.)	0.020
Equivalent core diameter, (in.)	26
Active core length, (in.)	76
Diluent in fuel body, v/o	70.1
Composition, v/o	
UO_2	2.85
Diluent	7.20
Cladding and spacers	4.40
Shroud	0.89
Fuel cooling void	8.31
Moderator	71.85
Moderator plus control rod void	4.50
	100.00

Table 4.2

NUCLEAR PARAMETERS AND REACTIVITY ESTIMATES FOR BORE AT OPERATING TEMPERATURES

Initial U-235 loading, kg	100
Initial U-238 loading, kg	74
Effective neutron temperature, ev	0.121
Thermal disadvantage factor for fuel	3.23
Fermi age, cm^2	179.3
Infinite medium resonance escape probability	0.799
Ratio of average epithermal to thermal fluxes	2.67
K_{eff}, hot clean	1.052
K_{eff}, equilibrium poisons	1.032
Lifetime at 10 Mw (uniform burnup assumed), hrs.	12,200

Table 4.3

HEAVY ISOTOPE COMPOSITION OF FUEL AT END-OF-LIFE

Isotope	Weight (kg)
U-235	93.2
U-236	1.8
U-238	72.3
Pu-239	1.1
Pu-240	0.12
Pu-241	0.05

The addition of water to the reactor to fill the voids has a large influence on reactivity because of changes in the fast neutron leakage and resonance escape probability. Table 4.4 shows the reactivity under cold and cold water-flooded conditions.

Table 4.4

REACTIVITY AND SIGNIFICANT NUCLEAR PARAMETERS
FOR BORE REFERENCE REACTOR UNDER COLD CONDITIONS

	Cold Clean	Cold Water-flooded
Effective neutron temperature	0.049	0.040
Thermal disadvantage factor for fuel	4.64	5.52
Fermi Age, cm^2	179.3	92.4
Infinite medium resonance escape probability	0.836	0.904
Ratio of average epithermal to thermal flux	2.82	1.11
K_{eff}	1.088	1.293

The high K_{eff} under cold water-flooded conditions dictates the amount of reactivity which must be controlled to permit water flooding as a means for loading and unloading the reactor. Allowing 2% as a minimum shutdown margin, the total complement of control rods must have a worth of at least 31%.

The worth of the control rods has been obtained from PDQ calculations

in which the rods were assumed to be thermally black. For cold, clean, water-flooded conditions the five rods were found to be worth 32.1%, which is adequate for the minimum shutdown condition.

Table 4.5 gives individual and banked rod worths obtained for hot-clean conditions in the BORE. The worth of the center rod in the presence of the other rods is seen to be nearly 44% higher than the worth of this rod inserted alone. This is the result of a very weak mutual influence between rods, and the smaller effective core to be controlled when the outer rods cut off the thermal neutrons returning from the reflector. The same effects make the outer rods worth twice as much in the presence of the other rods as when inserted alone.

Table 4.5

HOT-CLEAN ROD WORTHS IN BORE

Rods	$\delta k/k$ (%)
All five rods	32.0
Center rod in presence of outer rods	14.8
Center rod inserted alone	10.4
One outer rod in presence of all other rods	5.8
One outer rod inserted alone	2.9

The variation of the total rod bank worth with insertion in the hot-clean reactor is illustrated in Fig. 4.2. The differential rod worth as a function of rod bank position is shown in Fig. 4.3. As control rods are withdrawn from the core, the rate of change of K_{eff} with position of the rod bank is at first relatively small, increasing to a maximum rate after the rods have been withdrawn more than halfway from the core, and then decreasing again as they are fully withdrawn.

The power distributions have been calculated on the basis of the reactor consisting only of driver elements. The value of the average thermal flux and power within every unit cell on a plane normal to the vertical axis for the unrodded portion of the BORE core is given in Fig. 4.4. Similar information for the rodded region of the core is given in Fig. 4.5.

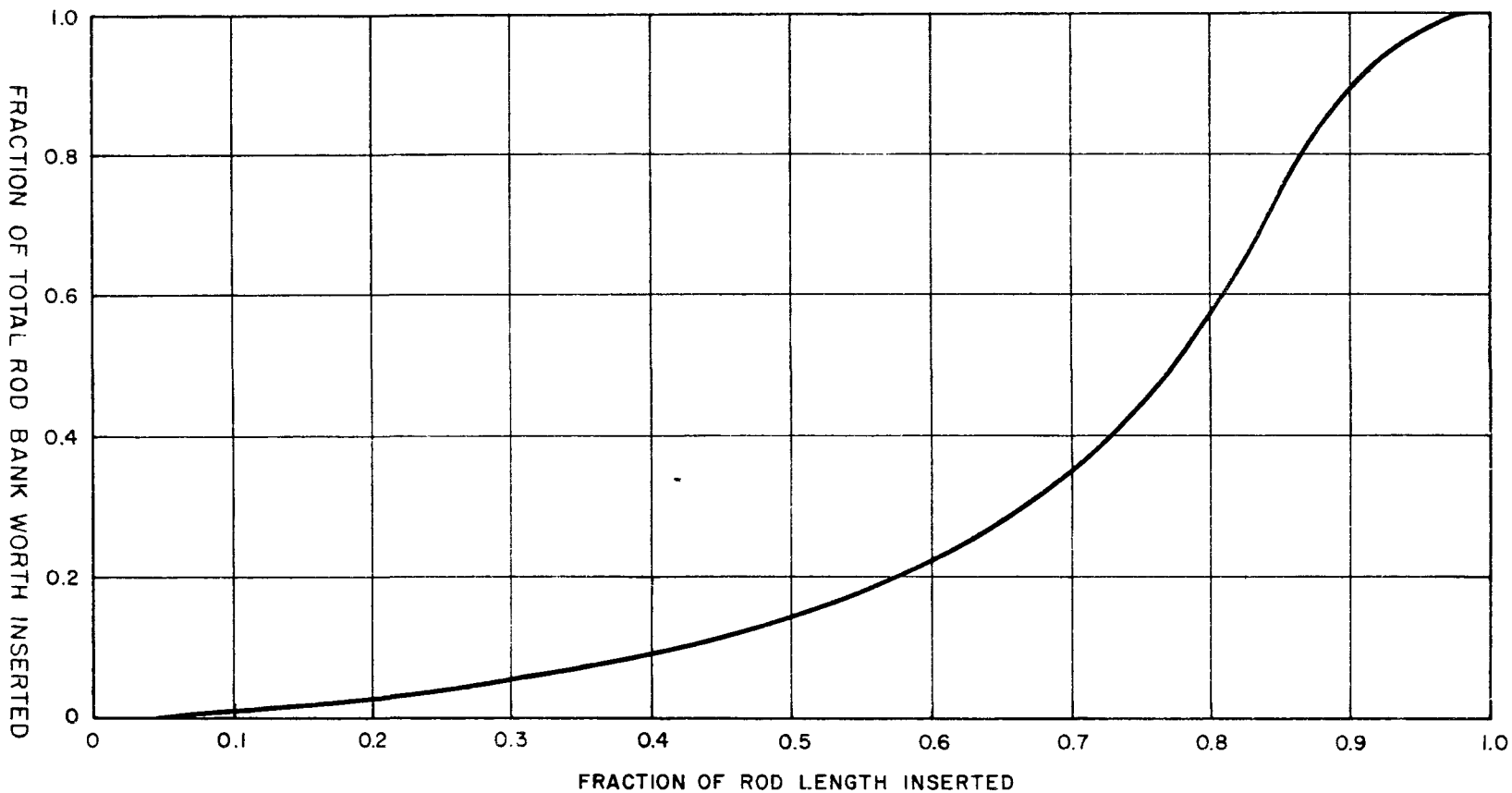

Fig. 4.2--Variation of Total Rod Bank Worth with Insertion in the Hot Clear Reactor

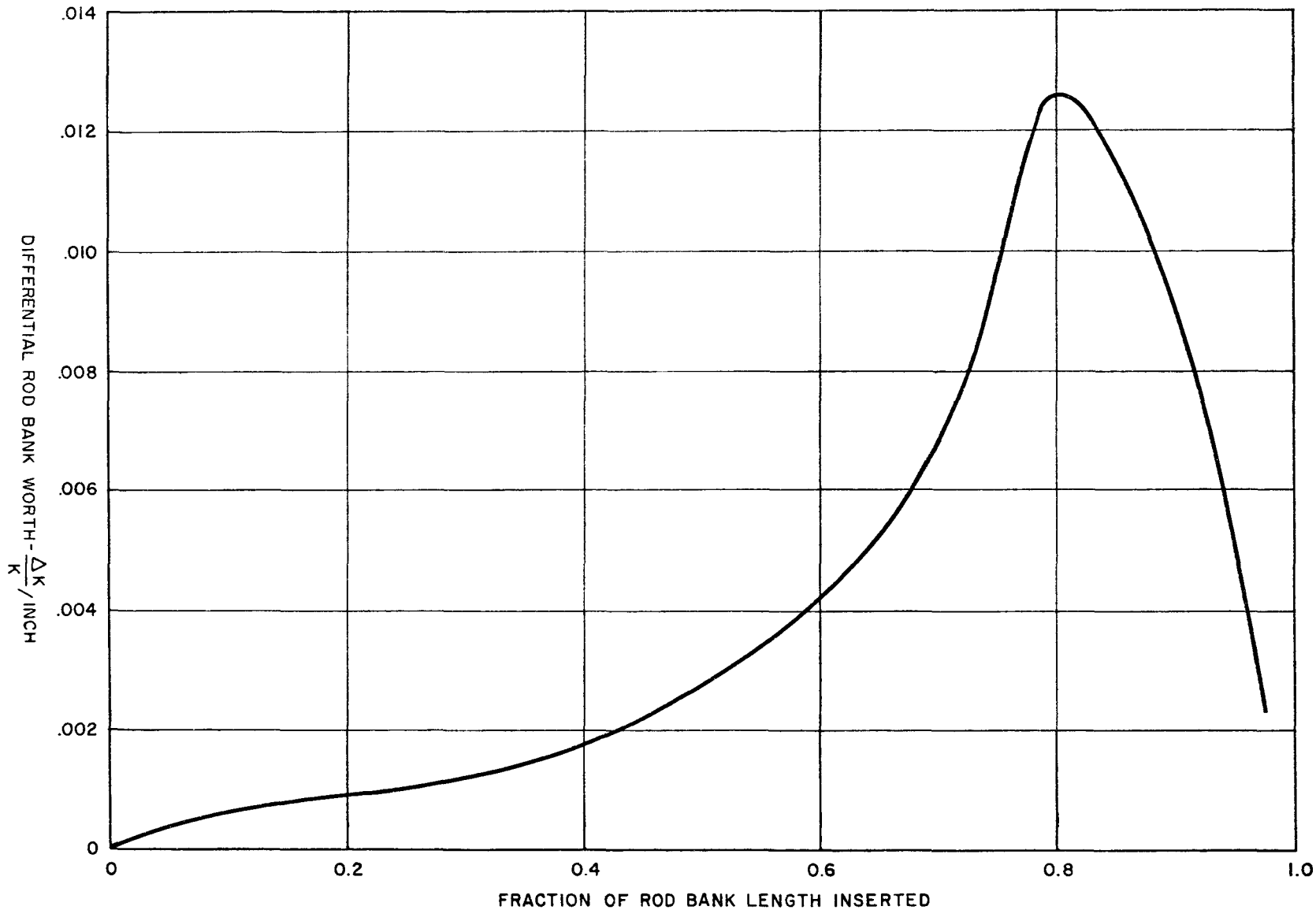

Fig. 4.3--Differential Rod Worth as a Function of Rod Bank Position

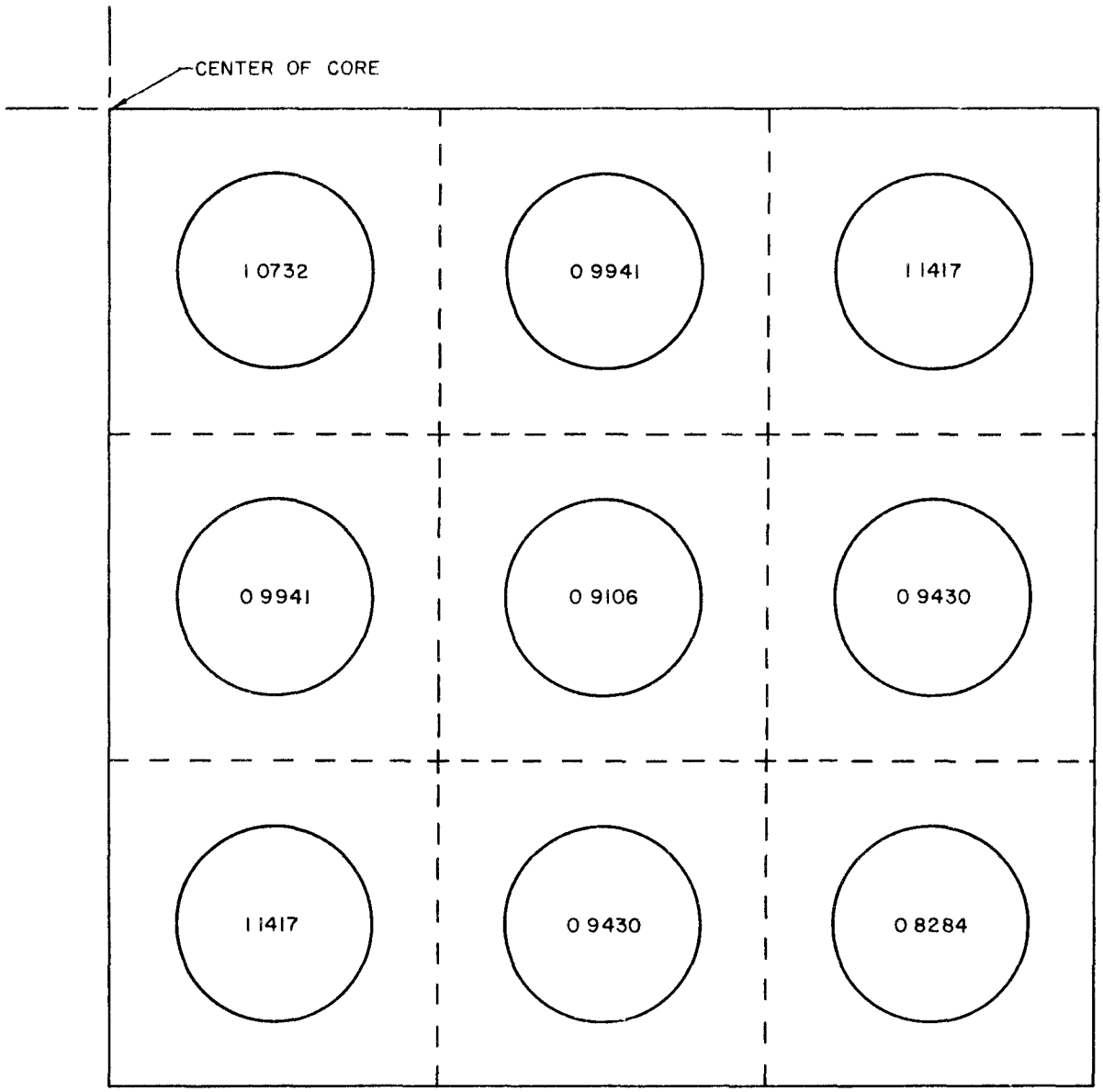

Fig. 4.4--Power Distribution Normalized to Core Average Over x, y Plane-Unrodded Case

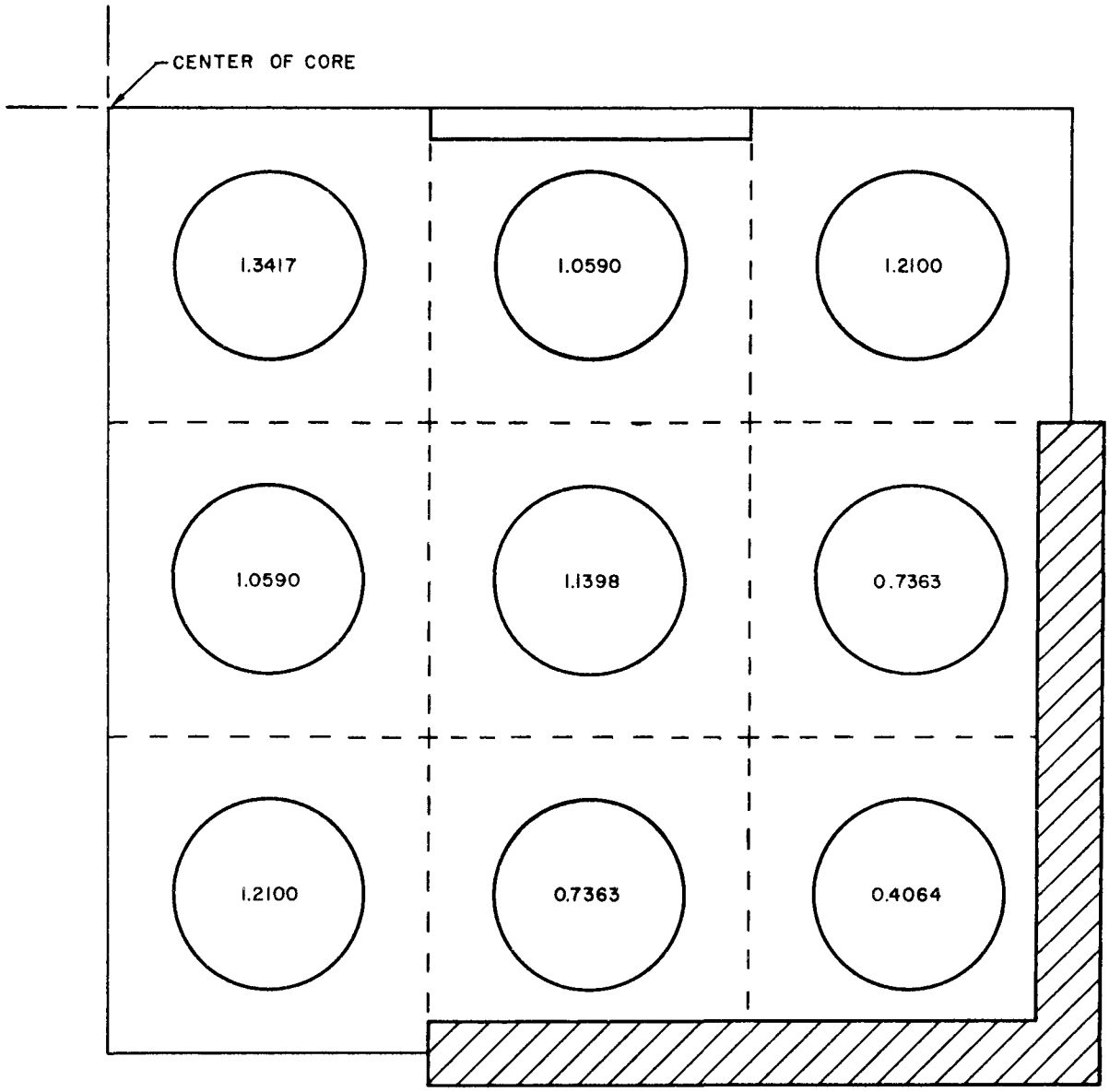

Fig. 4.5--Power Distribution Normalized to Core Average over x, y Plane-Rodded Case

Figure 4.6 shows a contour plot of the thermal flux in the same plane for the rodded core. The gross axial power distribution at criticality at beginning of core life is shown in Fig. 4.7.

From these results it is seen that the maximum-to-average power density factor for the axial power distribution is 2.00 and the radial factor 1.10, giving a value of 2.20 for the over-all maximum-to-average power density ratio in the core.

Because of the high concentration of fuel in the driver elements, the power density is severely depressed within these elements. Calculations were, therefore, made with the S_8 code to assess the distribution within the element. An equivalent cylindrical cell was employed which was divided into five regions: (1) a center circular region representing the center rod with diluent and no fuel, (2) separate annular regions for the inner ring of six fuel rods, (3) an outer ring of twelve fuel rods, (4) an annular shroud region, and (5) the moderator region. Void volume and fuel cladding were proportioned and homogenized with the rods.

Figure 4.8 demonstrates the thermal flux variation in the equivalent cell for two assumed source conditions -- with and without a source contributed by the diluent in the fuelled rods. A more severe depression is estimated when the source from the diluent in the fuelled rods is omitted.

The ratio of average flux in the inner ring of fuel rods to the average flux in the outer ring of rods is 0.652. Thus, each of the fuel rods in the inner ring of six rods would generate about 4.1% of the total power, and each of the outer twelve rods about 6.3% of the total power.

It will probably be desirable to simulate in the test elements in the core the axial power distribution expected in the full-size reactor for which the elements are being tested.

Because of the very high worth of the control rods in the small core, reasonable simulation of a desired axial power distribution will not be possible with the contemplated number of control rods. Even if the center rod and outer rods could be adjusted to obtain criticality with the center rod positioned at the desired insertion distance, the power density peak below the center rod and the percentage of power generated in the rodded upper portion of the test elements would be significantly different from their values in the distribution to be simulated. To match more closely

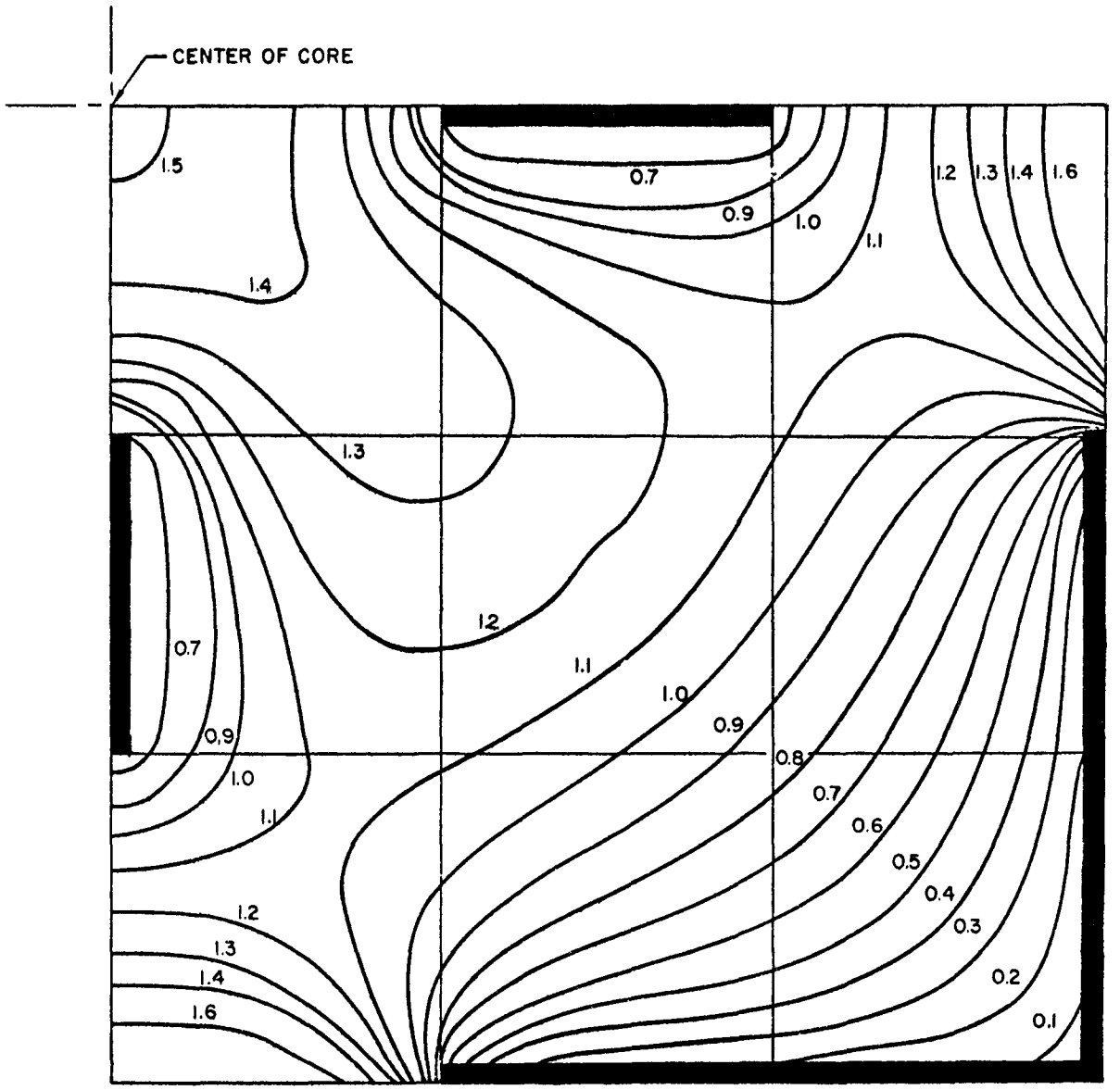

Fig. 4.6 -- Thermal Flux Distribution on One Quadrant of Symmetrical Roddle BORE Core (Normalized to Average Over Plane)

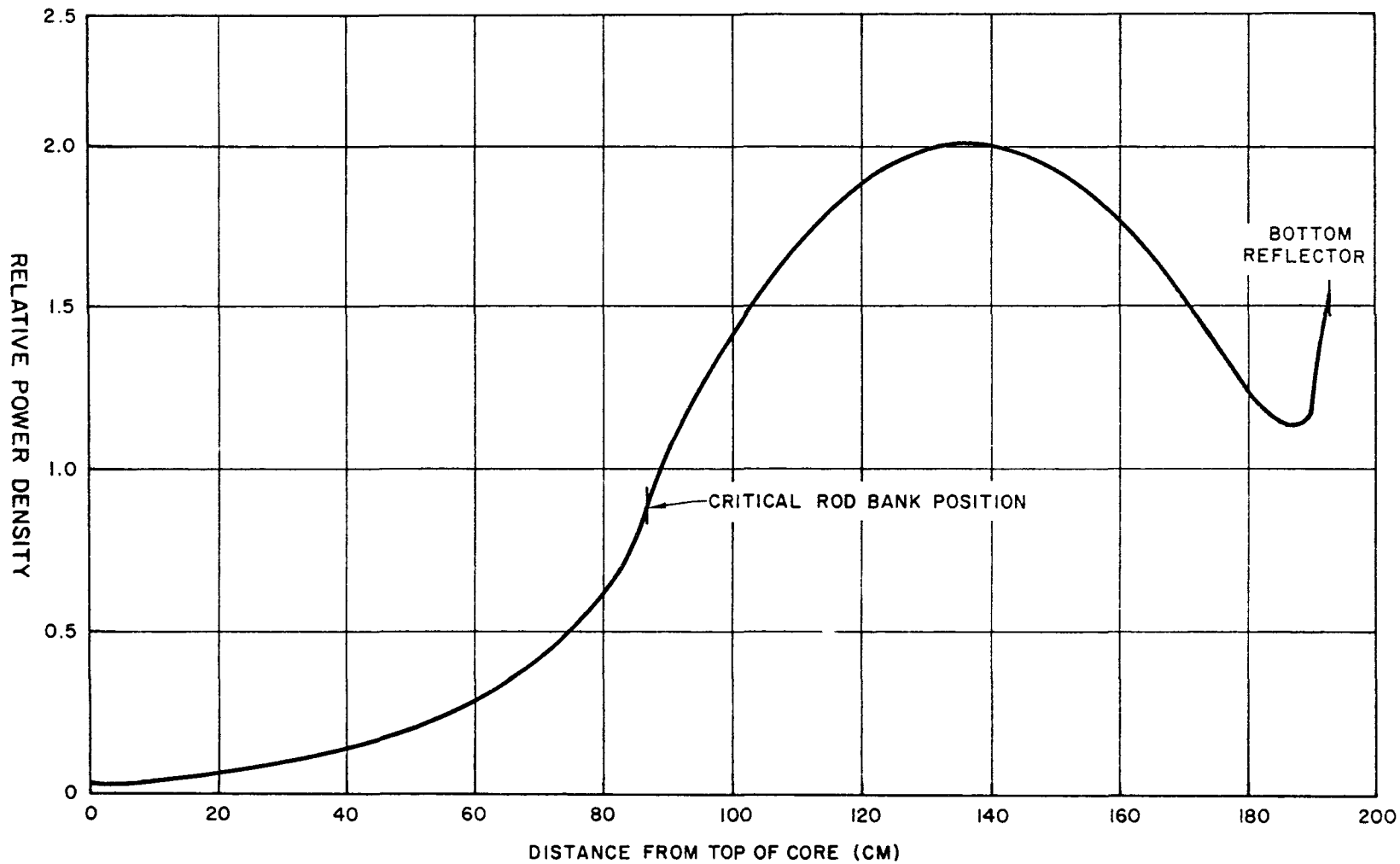

Fig. 4.7--BORE Gross Axial Power Distribution (Normalized to Axial Average)

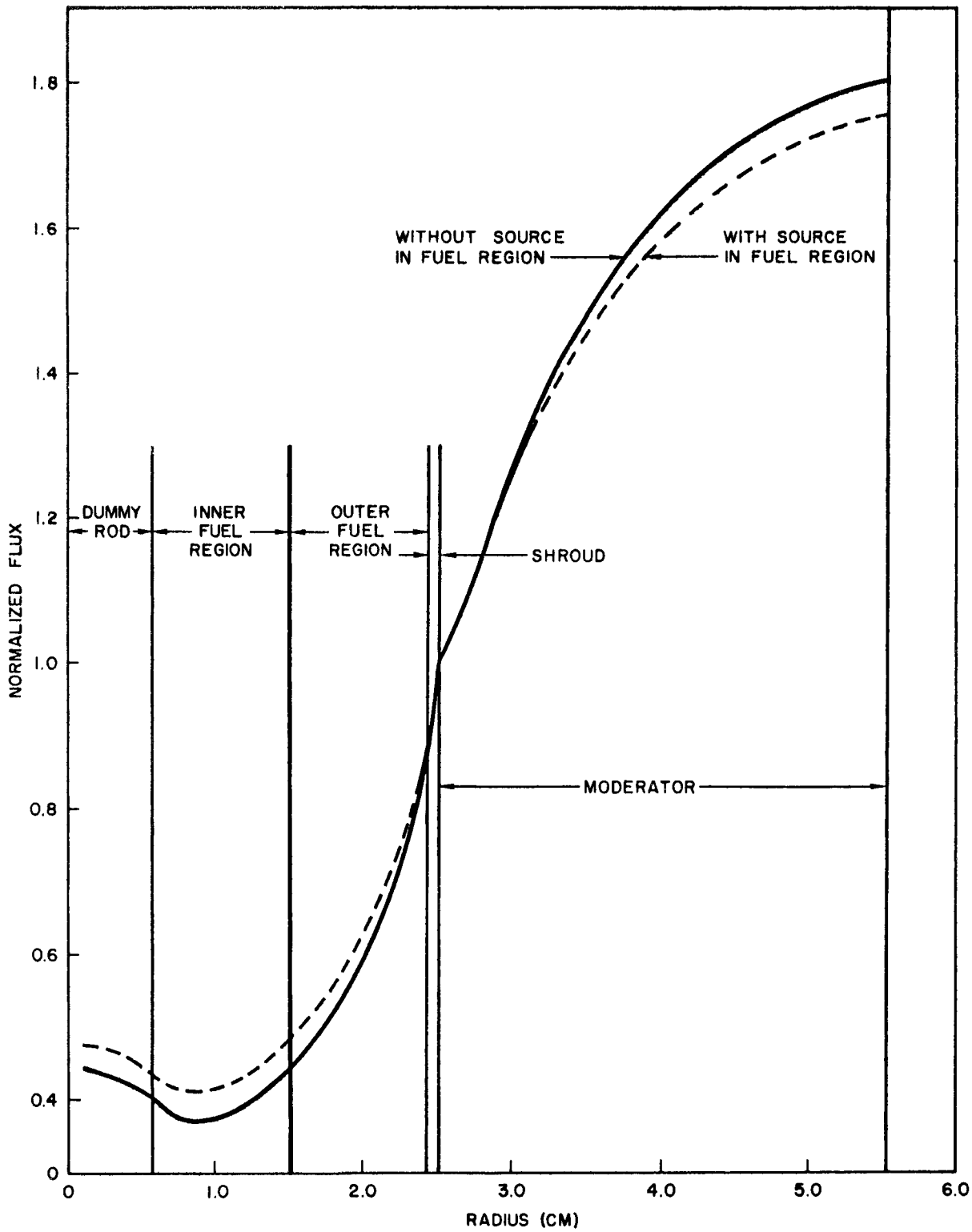

Fig. 4.8--Thermal Flux Distribution Across Unit Cell for the BORE Core (Normalized to Outer Edge of Shroud)

the desired power distribution in elements near the center of the core, it will be necessary to withdraw the center control rod completely into the upper reflector and attach separate control rod absorber sections to the center moderator elements.

These added control rod sections will have a different effectiveness from that of the active blade tips of the center rod. Under these circumstances it would be necessary that they displace moderator in order to permit the center rod to be inserted for shutdown under water-flooded conditions.

As previously mentioned, the high fuel concentration necessary to obtain the proper power level causes a large flux depression within the fuel elements. If the same fuel concentration was used in all the fuelled rods of the test elements, the ratio of power density in the inner ring of fuel pins to that in the outer ring would be considerably lower than desired for nearly any reactor application. Therefore, it may also be desirable to have fuel pellets of high enrichment in the inner ring of fuel pins than in the outer ring to more closely simulate the radial power density variation within the fuel element.

The initial complement of fuel elements used in the BORE consists of 36 driver elements which are clad with 30 mils of Hastelloy X. The performance has been calculated for a core using these elements. In addition to these elements, experimental elements of an advanced design will be constructed for testing. These elements will be developed for use in the MGCR Experimental Prototype, shipboard reactors or other applications. In general, they will differ from their full-scale counterparts only in that they will be loaded more heavily with U-235 in order to produce the proper power level in the lower thermal flux of the BORE.

Reactivity temperature coefficients have been evaluated for beginning-of-life conditions. Prompt coefficients were evaluated from U-238 resonance integral calculations using the Adler-Nordheim-Hinman code. Delayed coefficients were estimated from calculations with the OPTIM-III code at different moderator temperatures, in which the spectrum and self-shielding effects are taken into account. The resulting coefficients are shown in Table 4.6.

Table 4.6

REACTIVITY TEMPERATURE COEFFICIENTS FOR BORE

Coefficients	$\frac{\delta k}{k}/^{o}C \times 10^{4}$ HOT		
	Cold Clean	Clean	Equivalent Poisons
Prompt	- 0.542	- 0.253	- 0.253
Delayed	+ 0.140	- 0.027	+ 0.107
TOTAL	- 0.402	- 0.280	- 0.146

The most important criterion for determining the rapidity of response of the reactor to a change in reactivity is the prompt neutron lifetime. This lifetime consists of three parts which play different roles in defining the transient behavior of the reactor. The slowing down time of a neutron from fission to thermal energy defines a fixed time delay between fast and thermal diffusion, whereas the diffusion time for thermal neutrons defines an exponential period for the variation of thermal flux and power. As a result of the high velocity the fast diffusion time is so small that, for all practical purposes, it may be neglected. However, as a reasonable factor for defining the time scale of transients, the slowing down time and thermal diffusion time may be combined to represent an over-all prompt neutron lifetime. The slowing down time is strongly dependent on the average thermal neutron energy which, in turn, is determined by the moderator temperatures. Values of the slowing down time corresponding to cold and hot conditions have been obtained and are given in Table 4.7.

Table 4.7

SLOWING DOWN TIME FOR PROMPT NEUTRONS

	Moderator Temp. (^{o}F)	Thermal Neutron Energy (ev)	Slowing Down Time (sec)
Cold conditions	68	0.049	0.8×10^{-4}
Hot conditions	1200	0.121	0.5×10^{-4}

The thermal diffusion time varies with the moderator temperature and the total absorption cross section. It is therefore a function of the control rod worth and would have different values for various degrees of insertion of the rod bank. However, the value is of greater interest when the reactor is nearly critical and the values shown in Table 4.8 are for this condition.

Table 4.8

THERMAL DIFFUSION AND PROMPT NEUTRON LIFETIME

	Diffusion Time (sec)	Prompt Neutron Lifetime (sec)
Beginning-of-life		
Cold	0.58×10^{-4}	1.38×10^{-4}
Hot	0.29×10^{-4}	0.80×10^{-4}
End-of-life		
Hot	0.28×10^{-4}	0.78×10^{-4}

The BORE must be safe under water-flooded conditions in view of the unloading and emergency cooling procedure involving water flooding. Because of the undermoderated nature of the assembly, the presence of water in the core will introduce a large variation in the thermal neutron energy which, in turn, will affect both the slowing down and thermal diffusion times. The thermal diffusion time will also be changed by the additional absorption cross section of the water. For the just-critical flooded core the slowing down time is 0.88×10^{-4} sec., and the thermal diffusion time 1.02×10^{-4} sec., resulting in a prompt neutron lifetime of 1.9×10^{-4} sec.

Shielding

The biological shielding of the BORE for power operation will be separated into a primary and secondary shield in the regions of the coolant loop system. The secondary shield will surround both the loop and cooling system and a separately shielded full-flow fission-product trap in order to reduce the radiation level to a permissible level. However, the primary and secondary shields will be joined into a single unit in other areas of the reactor not involved with the loop or its associated components.

In order to provide containment for the release of radioactive materials in a controlled manner through a stack, all areas are separately ventilated and connected through check valves to the stack so that no flow between the compartments can occur.

Energies and intensities of the primary sources of radiation originating in the core are shown in Tables 4.9 and 4.10. Neutron dose rates will be minimized by the addition of borated surfaces on thermal shields and the use of a thick concrete shield. Concrete necessary to shield gamma sources will be more than sufficient to reduce any neutron sources to negligible levels outside the shield.

A preliminary estimate of the gamma source concentrations as they are expected to be found in the secondary compartment were made; the following criteria were used in this evaluation:

(a) Five percent of the gaseous and volatile fission products being produced in 5 fuel pins are released into the coolant stream.

(b) A full-flow trap at the reactor outlet will remove 50% of I, Te, and Mo in addition to H^3, O, H_2O, and N_2.

(c) Fifty percent of volatile fission products which get through the full-flow trap are plated out in the loop.

(d) The remaining volatile fission products are reduced by means of an efficient cleanup system which handles the total loop gas volume every hour.

(e) Secondary compartment size is 33 ft. by 10 ft. by 28.6 ft.

(f) Nominal thickness of containment pipes for the coolant, heat exchangers, etc., is 1 in.

(g) Fuel rod surface temperature is between 1200°F and 1800°F.

(h) System pressure is 800 psi to 1200 psi.

Based on these assumptions and ground rules, the calculated equilibrium source concentration of gamma radiation for various locations in the system is listed in Table 4.11. Since little applicable information concerning fission product traps and purification systems is available, the shielding for the loop system has been designed on a conservative basis, assuming that 100% of the activity is concentrated in the loop and 100% is concentrated in the traps.

Table 4.9

GAMMA SOURCES WITHIN REACTOR

Gamma Energy	1 Mev	2 Mev	3 Mev	5 Mev	8 Mev
Primary fission, γ/cm^3-sec	1.34×10^{12}	0.66×10^{12}	6.3×10^{10}	--	--
Fission product, γ/cm^3-sec	13×10^{10}	0.51×10^{10}	0.843×10^{10}	--	--
Capture moderator, γ/cm^3-sec	--	--	--	1.1×10^{10}	--
Capture fuel, γ/cm^3-sec	--	--	0.88×10^{10}	--	--
Capture SS, γ/cm^3-sec	--	--	--	--	$.136 \times 10^{12}$
Total core source, γ/cm^3-sec	1.44×10^{12}	7.112×10^{10}	8.018×10^{10}	1.1×10^{10}	$.136 \times 10^{12}$

Table 4.10

CAPTURE GAMMA SOURCES OUTSIDE CORE

Gamma Energy	5 Mev	8 Mev
Outer reflector surface, γ/cm^2-sec	4.3×10^8	--
Outer pressure vessel surface, γ/cm^2-sec	--	5.4×10^8
Total source, γ capture, γ/cm^2-sec	4.3×10^8	5.4×10^8

Table 4.11

EQUILIBRIUM SOURCE CONCENTRATION OF GAMMA RADIATION

Element	Production Rate of γ Activity Mev/sec	Eq. Conc. in Primary Coolant Mev/sec	Eq. Conc. in Loop Due to Plate Out Mev/sec	Eq. Conc. in Full Flow Trap Mev/sec	Eq. Conc. in 1 Hr. Clean-up System Mev/sec
Kr	0.329×10^{14}	0.227×10^{14}	--	--	0.103×10^{14}
Xe	0.286×10^{14}	0.074×10^{14}	--	--	0.212×10^{14}
I	1.210×10^{14}	0.092×10^{14}	0.304×10^{14}	0.591×10^{14}	0.223×10^{14}
Cs	0.372×10^{14}	0.052×10^{14}	0.186×10^{14}	--	0.134×10^{14}
Ba	0.574×10^{14}	0.055×10^{14}	0.287×10^{14}	--	0.233×10^{14}
Sr	0.252×10^{14}	0.014×10^{14}	0.126×10^{14}	--	0.112×10^{14}
Mo	0.193×10^{14}	0.013×10^{14}	0.048×10^{14}	0.096×10^{14}	0.035×10^{14}
Te	0.349×10^{14}	0.036×10^{14}	0.087×10^{14}	0.173×10^{14}	0.053×10^{14}
Rb	0.644×10^{14}	0.242×10^{14}	0.322×10^{14}	--	0.079×10^{14}
Total	4.209×10^{14}	0.805×10^{14}	1.359×10^{14}	0.861×10^{14}	1.183×10^{14}

The general design of the primary shield consists of a simple rectangular concrete shell 15 ft. by 15 ft. The reactor is surrounded on three sides by earth and the nominal thickness of concrete in these areas is dictated on the basis of structural requirements only. On the side adjacent to the fuel storage pits, the nominal thickness will be 6 ft. Because of the inability of concrete to resist thermal stress, a series of cooling pipes near the inner surface will be necessary. For reasons of general economy and ease of fabrication, the major portion of concrete will be of the ordinary portland cement type with a waterproofed surface.

The major portion of the primary shield presented no unusual problems. However, serious consideration was given to the method of shielding above the pressure vessel head; access to the reactor and support equipment will be through this top shield.

Because of difficulties with an all-water overhead shield, the overhead shielding design utilizes a simple concrete block arrangement which will be used in conjunction with a wet refuelling system. This permits dry operation of the reactor and complete flooding during shutdown for fuel or core-component handling purposes.

The shield will consist of a number of interlocking concrete blocks which can easily be lifted back and forth over the reactor cavity. The area in the center of the slab will be provided with a plugged port which can be removed for access to the rod drives and small head. The block will be thick enough to provide adequate shielding to allow complete drainage of water above the reactor during operation. Variation of dose rate with concrete thickness for upper concrete blocks at vertical conterline is shown in Fig. 4.9. This eliminates the necessity for any waterproof insulation that would be required to reduce thermal stresses in the vessel head during operation. The lower portions of the concrete block would be lined with 18 in. of Masonite and a boral plate to reduce activation of the vessel head, concrete, and rod drives by neutrons thermalized in the concrete and reflected back toward the reactor. The upper shield block consists of 6.3 ft. of concrete. When access is required into the reactor, the upper primary shield cavity is filled with water and the shield blocks are then lifted off, allowing complete access to the head and drives. The water then provides the streamproof shielding for personnel performing the refuelling or other operations.

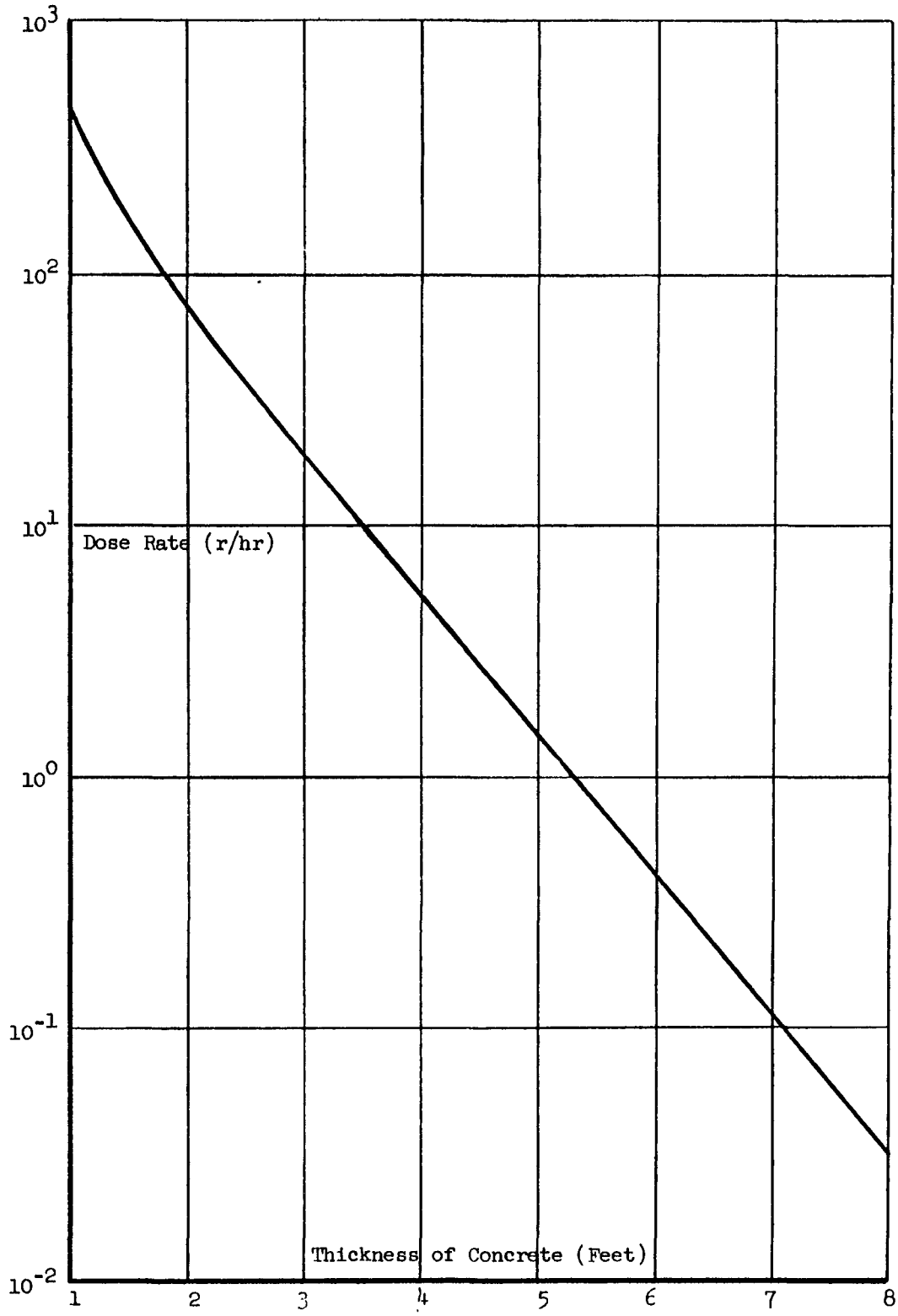

Fig. 4.9--Variation of Dose Rate with Shield Thickness at Vertical Centerline of BORE Upper Concrete Slab

One problem associated with this type of system is activation of air in the upper cavity during operation. However, since an 18-in. or greater clearance between vessel and side walls has been specified, the present ventilation system would be adequate for this area.

The secondary shield will house the primary-loop fission-product trap and associated equipment. An additional concrete shielding thickness of 4-ft. is provided around the fission product trap located inside the secondary compartment. The additional shielding around the trap reduces the contribution of trap radiation in the secondary compartment to a level equal to that set by the loop itself. The reactor is situated below ground level and a minimum of 15-ft. of earth will separate the reactor and secondary compartment; radiation from core sources is therefore considered negligible. The secondary compartment is essentially airtight and vented to an outside stack of sufficient height to permit ample dispersal of radioactive materials.

Thickness of shielding for the secondary compartment is a nominal 3.2 ft. reducing the radiation adjacent to areas continuously occupied by personnel to 1 mr/hr.

In order to reduce plant costs, the top primary shield reduces radiation levels to 7.5 mr/hr in order that no secondary shielding other than that necessary for the loop will be required.

Fuel loading and unloading is to be accomplished under flooded conditions. Transfer of the fuel elements and other reactor components from the reactor to the storage pit makes use of an overhead crane and a water-filled fuel storage pit. The variation of dose rate with water thickness above a vertically withdrawn fuel element has been calculated and is shown in Fig. 4.10. The calculation was based on assuming infinite operation of the fuel element at 10 Mw.

A multigroup problem was run to determine the radial neutron flux distribution in the thermal shields and pressure vessel in order to investigate radiation heating and consequent damage. Preliminary hand calculations on an ultraconservative basis yielded excessive heating rates and indicated the need for more refined machine calculations.

Results of the initial problem using no boron is shown in Fig. 4.11. Several additional calculations incorporating boron layers and various

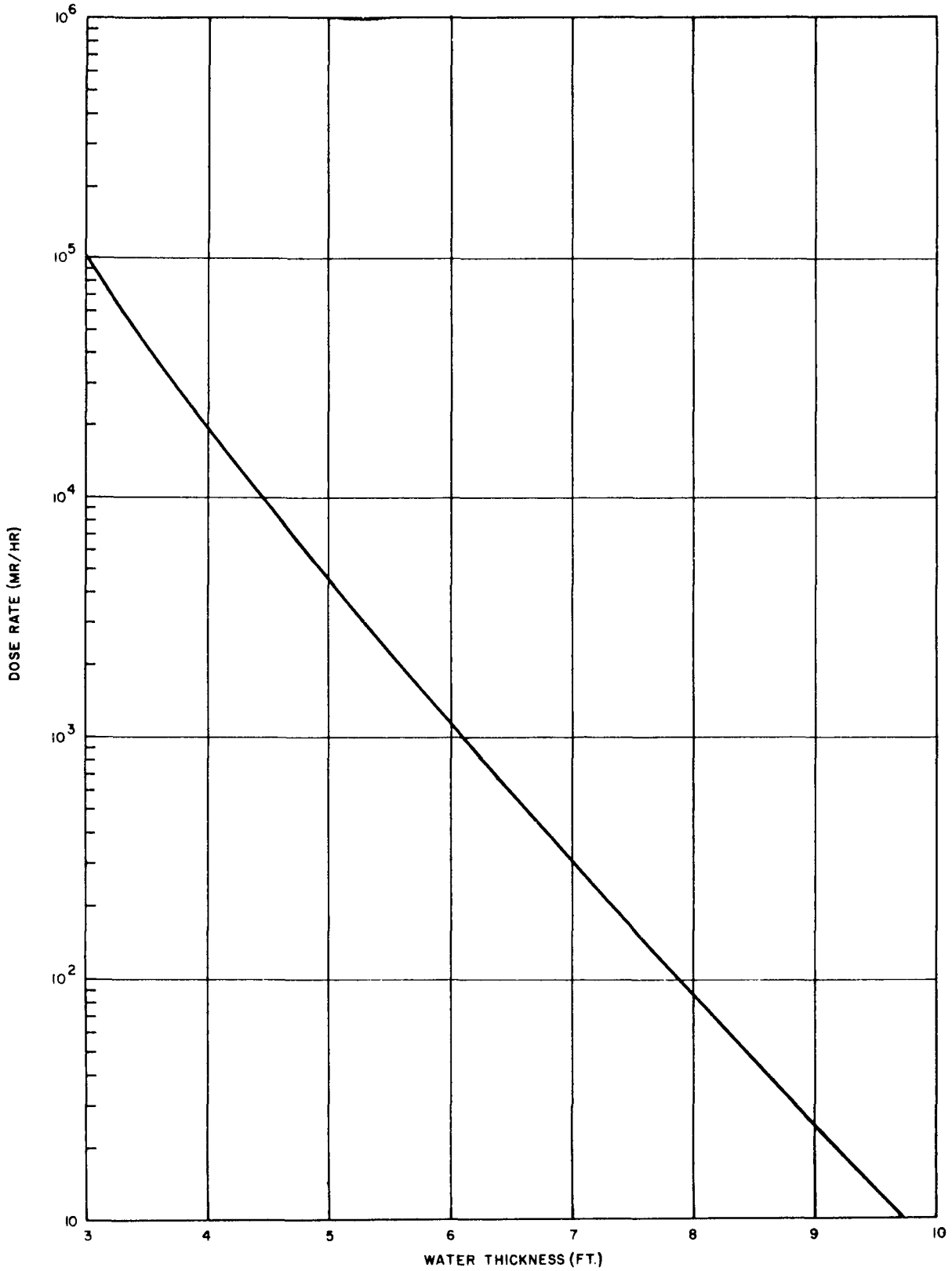

Fig. 4.10--Variation of Dose Rate with Water Thickness above Vertically Withdrawn Fuel Element After Infinite Operation (BORE)

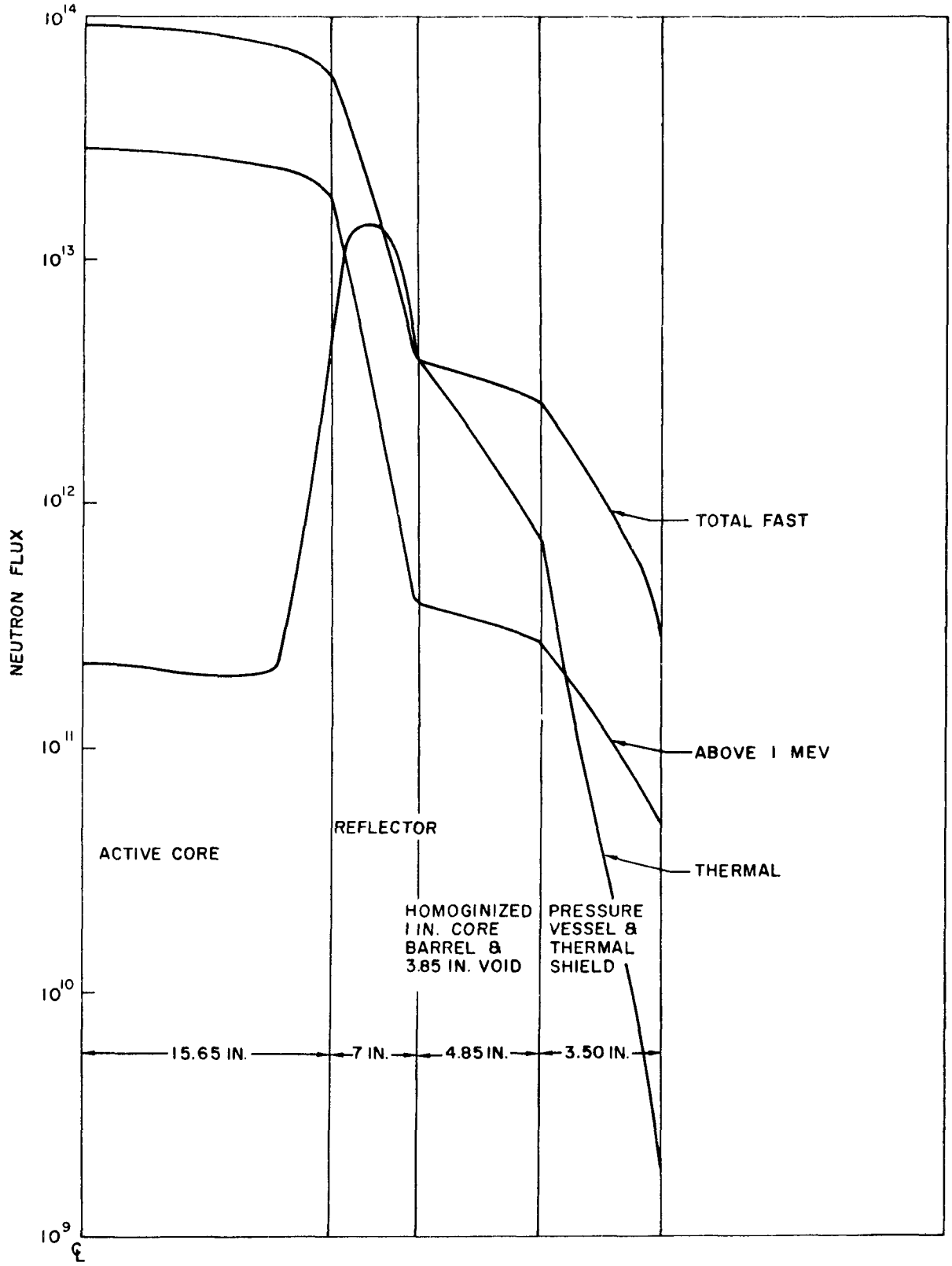

Fig. 4.11--Fast Flux in BORE Pressure Vessel and Thermal Shield--No Boron (Radial)

thicknesses of thermal shields are planned. Absorption data in the various regions will be used as secondary gamma sources outside the active core regions.

BORE PRELIMINARY HAZARDS EVALUATION (J. M. Stein, L. R. Amyot, A. D. McWhirter, J. R. Seibold, H. A. Vieweg)

A preliminary hazards analysis is in preparation. A brief summary of the major investigations made is given below.

Reactivity Accidents

Accidents of particular concern in the design of a nuclear system are those involving large changes in reactivity. The reactivity can be changed quickly and by a large amount as a consequence of control rod withdrawal or water flooding.

Rod withdrawal accidents of serious consequences are generally of two types: (1) those generally referred to as start-up accidents, and (2) those occurring under power operation due to malfunction of the control system. Start-up accidents are avoided by restricting control rod withdrawal rates, providing interlocks and mechanical sequencing, and by proper operational procedures. Rod withdrawal accidents under high power operation require a number of sequential failures or errors; e.g., the shim control system and the safety system must both be inoperative. Under these circumstances, such accidents are not considered credible.

In the BORE core, a third type of rod withdrawal accident is liable to produce serious consequences. During fuel unloading the core will be deliberately water-flooded. It is, therefore, conceivable that through a procedural error an operator could manually withdraw a control rod. with the pressure vessel head open and the fuel not yet completely unloaded. The worst possibility would be that the center rod be pulled from the fully loaded core. The seriousness of such an accident has made it imperative to render it extremely unlikely by proper procedural restrictions and design.

It has been necessary to make the total control rod worth sufficiently large to keep the reactor subcritical when the core is completely filled with water. Therefore, unless the scram system should fail to function, inadvertent water flooding will not endanger the reactor.

Nonreactivity Accident

A complete loss-of-coolant flow could come about by rupture of the loop or through a failure of all power supplies. Thus, an auxiliary and emergency power supply have been provided.

In the event of a temporary loss of all power sources, the radial power distribution across a fuel element would quickly reach equilibrium, after which the rate of temperature rise would be limited to a slow climb by the large heat capacity of the core. If the loss of power persists for a period of no more than one-half hour, the fuel rods are designed to maintain their integrity and not release fission products.

A crack might develop at a welded joint or a defective instrumentation penetration, or a rupture might be produced in the coolant loop, piping or circulator housing. In any case, the integrity of the system would be lost and radioactivity released to the atmosphere.

In the most severe case, that of a loop rupture, it is assumed that all the normal radioactive content of the coolant in the reactor and the tritium accumulated in the moderator is suddenly released to the atmosphere. Because of the finite time required to introduce emergency coolant (air or water) into the loop, the fuel will have heated up and many fission products normally solid in the core will have reached the gaseous state. Due to the severity of this accident, involving loss of system integrity and release of radioactivity to the atmosphere, the rupture of the coolant loop is considered to be the maximum credible accident for the reactor.

MGCR CRITICAL FACILITY (TASK 13) (J.M. Stein, S.H. Levine, H.A. Vieweg, L.R. Amyot)

The construction of the MGCR critical facility was completed during the early part of this quarter and criticality was attained on August 11. Subsequent test runs were made using graphite as the moderator. The various components performed as anticipated and the facility was considered in operating condition for the performance of the critical experiments proposed for the MGCR prototype.

The change in emphasis toward the BORE necessitated the shutdown of the facility. A program was therefore initiated to: (1) modify the facility, (2) re-evaluate the safety aspects in light of the modifications, and (3) draft a new experimental program commensurate with the BORE technical and schedule requirements.

Modification to the Design

Since the BORE is a much smaller reactor than the MGCR prototype, and since it is a specific testing device, the critical facility will be used to make a nuclear mockup of the BORE instead of exploring a range of BeO reactors, as was originally contemplated in connection with the MGCR prototype.

The exact size of the unit cell in the critical assembly is dictated by the size of the aluminum support structure. The presence of the vertical and horizontal partitions, which determine the internal geometry of the filing-cabinet assembly, would necessitate a prohibitively large number of sizes of BeO pieces and fuel foils to approximate very closely the BORE cell spacing of 3.84 in. The unit cell of the critical assembly will therefore be slightly larger -- 4.61-in. horizontally by 4.125-in. vertically.

The large fuel loading of the BORE core and the changes in geometrical configuration required redesign of the fuel channels for the critical assembly. The length of the fuel channels is maintained at 4-1/2 ft. to permit loading from opposite faces. In order to reduce to a minimum the amount of reactivity introduced at each step during fuel loading, four U-shaped, stainless steel fuel channels are used side by side in each cell. Stainless steel is used for mechanical sturdiness within a limited space and at high temperature. In the event of a meltdown accident, the channel must contain the fuel. The two adjacent channels within a given slot in the aluminum structure are contained in a third U-shaped stainless steel channel topped with projections from the sides which act as a support for the moderator located above the fuel region (Fig. 4.12).

As in the MGCR Critical Facility, it is desired to use fuel meltdown as a shutdown mechanism in the event of an accident. To accomplish this, at a few locations to be determined by calculation, a void space will be provided at the bottom of each fuel channel within a cell into which the fuel, upon melting, will flow and assume a more lumped and therefore less reactive configuration. This void space will be maintained by the insertion of a stainless steel bridge punched with holes through which the molten metal will flow.

Additional rod worth would be provided by the addition of a horizontal safety rod. This rod, approximately 5 1/2 in. in width, would be activated

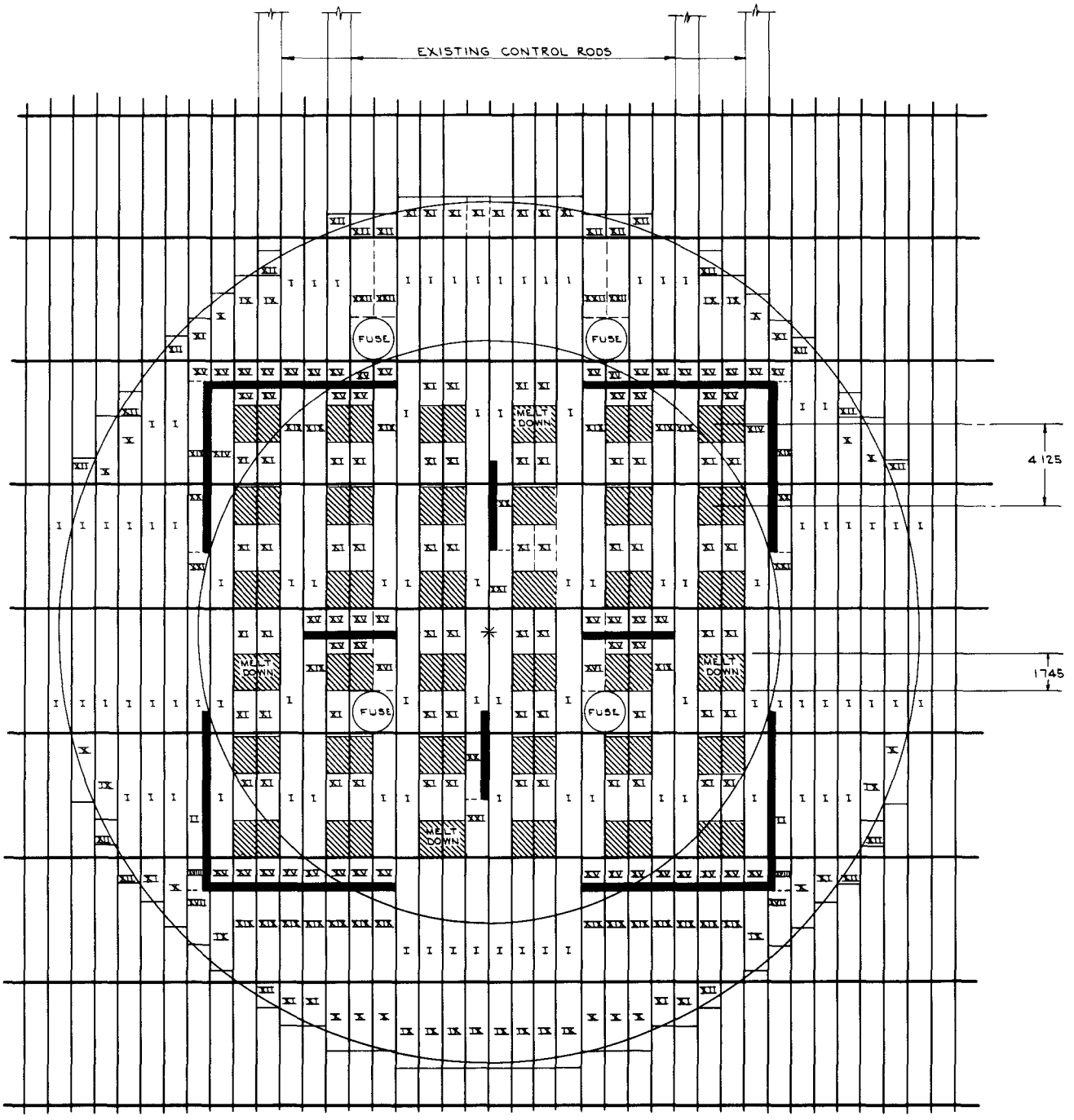

Fig. 4.12--Cross Section of BORE Critical Assembly

by a rack-and-pinion drive which would be placed so as not to interfere with fuel loading.

Hazards Evaluation

The use of the modified facility to study the nuclear performance of BORE requires a re-evaluation of hazards associated with the changes in design of the facility, the change in experimental program, and the basic geometrical differences between the MGCR prototype and the BORE. This re-evaluation will be submitted for approval to the AEC and the General Atomic Safeguards Committee in the form of a supplement to GA-1100.[2]

The re-evaluation has not been completed, but preliminary calculations indicate that the modifications made in fuel channels will provide fuel meltdown protection in the same manner as in the prototype assemblies. The safety fuses in this assembly are worth 5.5% on the basis of preliminary calculations. Using the same type of calculation, the four safety rods are worth 4.3%. A program of more accurate calculations is under way for the final evaluation. These involve the use of the ZOOM code to assess the spectrum aspects of the problem. The 18 groups used in these calculations will be combined to yield 4 groups for use in PDQ calculations to assess the geometrical aspects of the problem.

METHODS EVALUATATION (Task 22) (J. M. Stein, L. R. Amyot, A. J. Goodjohn, G. W. Hinman, A. D. McWhirter, H. A. Vieweg)

Spectrum Calculations

The results of a 15-group ZOOM calculation for the BORE core show that this reactor is decidedly more epithermal than the MGCR Prototype. The radial flux distribution and power distributions for the BORE and for the MGCR Prototype are given in Figs. 4.13 - 4.15. The fluxes in Fig. 4.13 are normalized to the same fast flux at the center of the core for both cases; the differences between the resonance and thermal flux levels show the ratio of the BORE resonance-to-thermal flux to be higher than that for the MGCR Prototype. In addition, the effect of the reflector on the slowing down of neutrons is shown in the thermal flux distributions by the large buildup near the core-reflector interface. This calculation was made using U-235 epithermal cross sections that were probably too large. In the next quarter, a series of calculations will be started using PDQ, ZOOM, and its

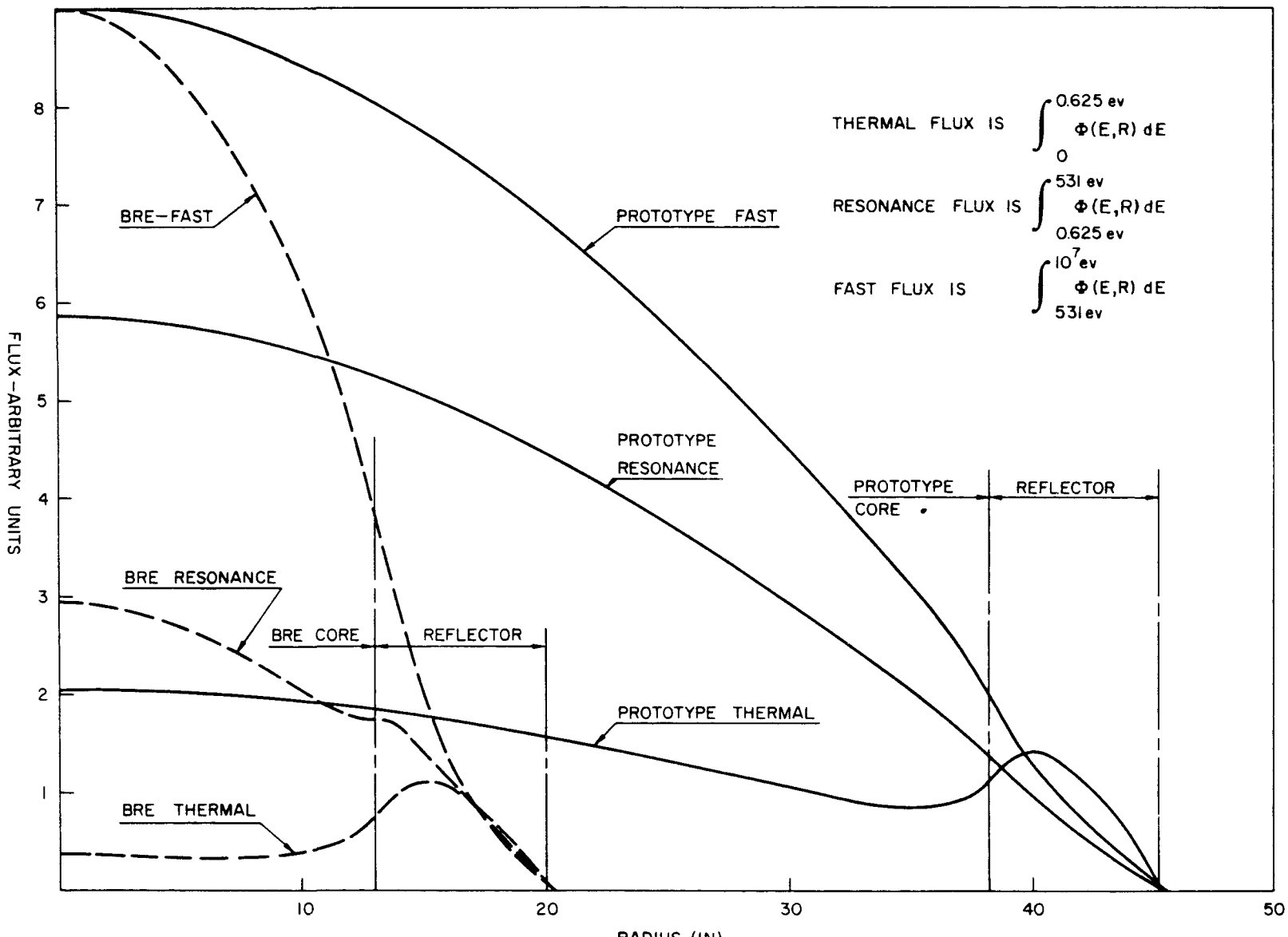

Fig. 4.13--Comparison of MGCR Prototype and BORE Radial Flux Distributions

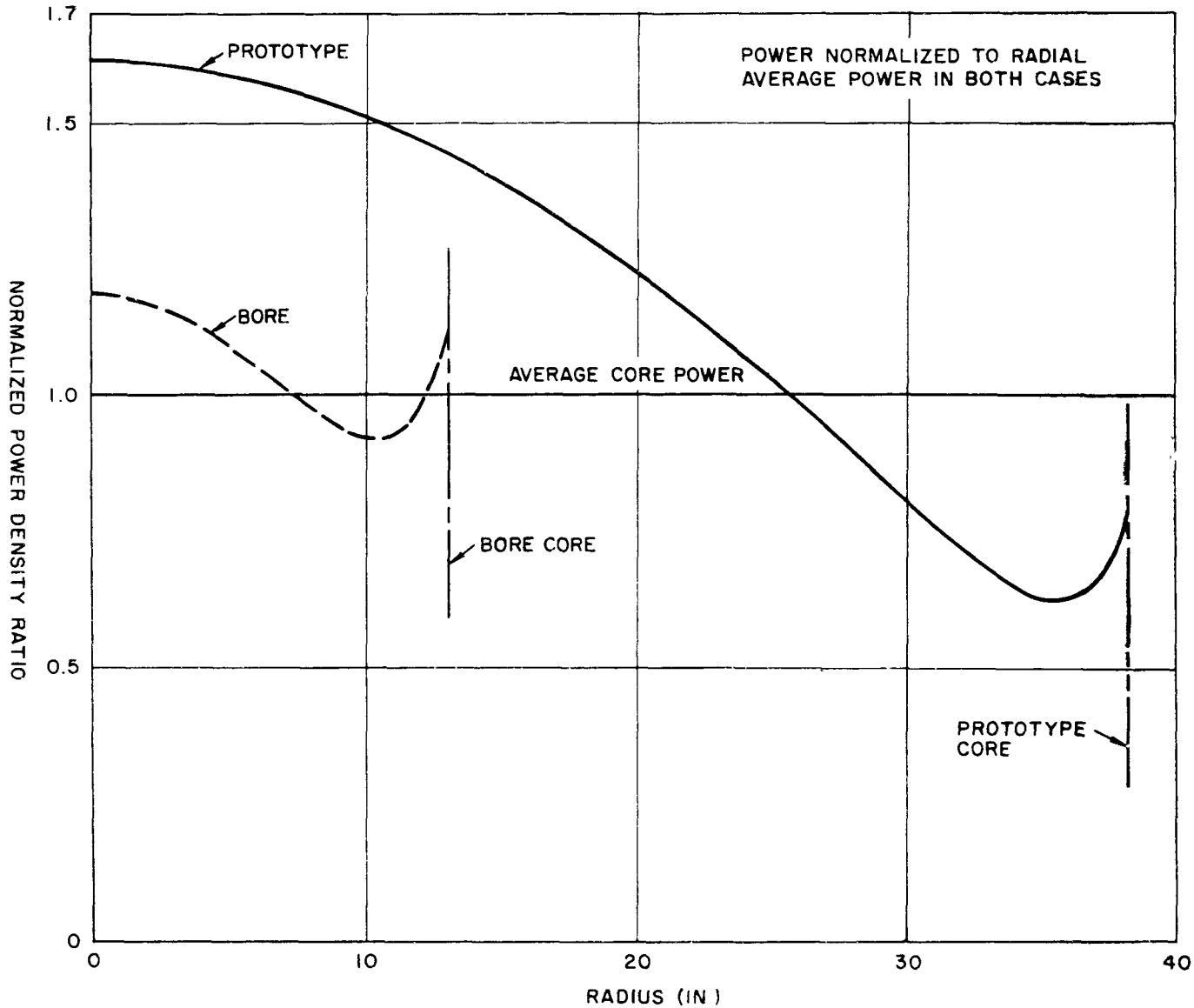

Fig. 4.14--Comparison of MGCR Prototype and BORE Radial Power Distribution

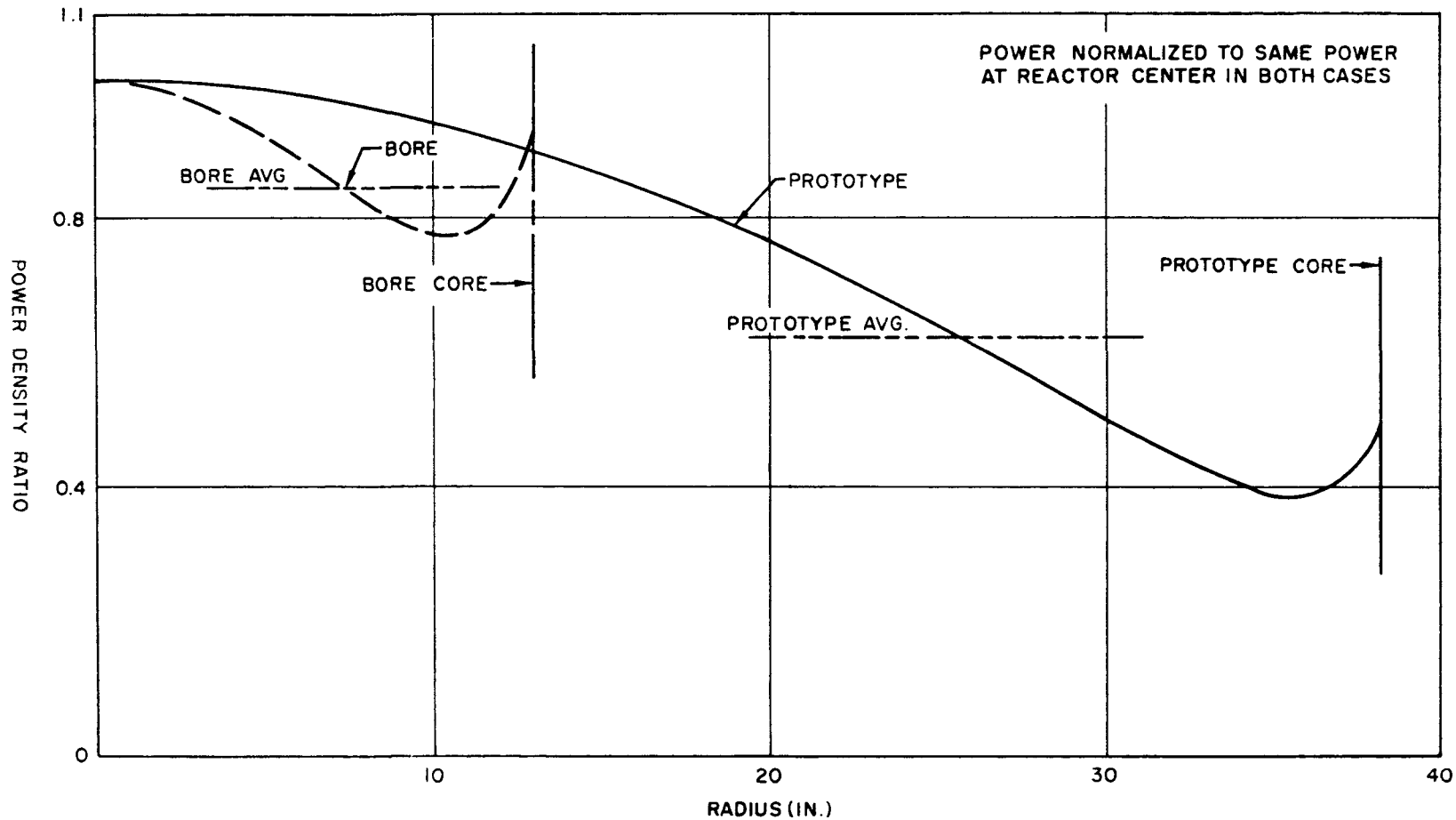

Fig. 4.15--Comparison of MGCR Prototype and BORE Radial Power Distribution

two-dimensional counterpart, ANGIE, on the problems of rod worths and water flooding, and on equivalent experiments to be done with the critical assembly.

Resonance Absorption

The high fuel loading required for BORE results in a high thermal disadvantage factor and enhancement of the contribution of resonance absorption in U-235 to the reactivity of the reactor. Analytical techniques generally applied to determine effective resonance integrals or cross sections are suitable for materials with narrow width, widely spaced resonances such as U-238, but will not properly deal with wide, closely spaced resonances in materials like U-235.

Programming of a new code for treating resonance absorption for a cylindrical cell containing a central fuel-bearing region was initiated this period. The code, called BIG, will generate Doppler-broadened cross sections as a function of energy from resonance parameters, will then self-shield cross sections as a function of energy, and utilize the effective cross sections to establish a spectrum over the energy range in question by the same technique employed in the General Atomic SPECTRUM code. The effective cross sections will then be averaged over the resulting spectrum. Replacement of some of the subroutines will enable the program to deal with slab or spherical cells.

Reactivity

The eigenvalue result from the ZOOM calculation indicates a k_{eff} for the hot-clean core of 1.26, compared to 1.05 as obtained from survey-type calculations. This difference is the result of placing resonance absorption in U-235 in competition with leakage and slowing down in the ZOOM calculation, whereas this absorption has previously been included in an equivalent thermal group cross section. On this basis, more refined calculations to be made of resonance absorption in U-235, when used in criticality calculations in competition with leakage and slowing down, will undoubtedly permit a significant reduction in the U-235 loading for BORE.

Future calculations will rely heavily on the use of the PDQ code for few-group, two-dimensional criticality results. The small diameter of BORE and the ability to represent control materials explicity in PDQ make its use very desirable even at the expense of multigroup calculations. The

BIG code mentioned previously also can be used for thermal neutron cell calculations. Averaged cross sections for thermal and epithermal groups will be obtained and used in ZOOM to obtain detailed information on space-energy relationships. Four-group constants will then be derived from the ZOOM results for a few discrete regions of the reactor and used in PDQ for criticality estimates.

Control Rods

Control rod calculations are being planned in the same manner as the criticality calculations. In PDQ calculations, the rods will be represented explicitly with epithermal absorption taken into account. The transport aspects of these lumped absorbers will be taken into account by deriving equivalent diffusion theory constants which achieve the correct boundary condition at the surface of the absorber in the PDQ problem.

Heterogeneities

A start was made during this quarter on a combined multigroup transport and Monte Carlo calculation for the BORE core. The main purpose of the work was to use the Monte Carlo calculation in the epithermal range, to evaluate the resonance absorptions in U-235, and to use the DSN multigroup one-dimensional transport code to investigate the upscattering and other energy-group-to-energy-group interactions in the thermal range. The highly heterogeneous nature of the core and the core plus reflector, and the higher U-235 loading warrants such calculations. Cell problems will be performed initially, to be followed by boundary source problems and gross core calculations. Results of these inventigations will be available during the next quarter.

NUCLEAR DATA (J. M. Stein, A. J. Goodjohn, G. W. Hinman, J. R. Seibold)

Be^9 (n, 2n) Reaction

Discussions were held during this quarter with staff members of Los Alamos Scientific Laboratory on a proposed experiment using beryllium-loaded nuclear emulsions to measure the (n, 2n) cross section in beryllium. Concern was expressed over the ability to actually see the tracks due to the two low energy alpha particles from the decay of the resulting Be^8 nucleus. Efforts were made through correspondence with nuclear emulsion manufacturers to locate suitable fine grain emulsions for the experiment. Replies indicate that such emulsions are available but loading with beryllium compounds must be made at a separate location.

More recently, an evaluation of some of the latest data on the Be^9 (n,2n) cross section indicates that the main doubt concerns the threshold of the reaction and not the value of the cross section in the higher energy region. The energy range between 1.7 and 2.8 Mev (laboratory system) should be investigated prior to an emulsion experiment designed to measure the (n,2n) cross section in beryllium, in order to establish at least semi-quantitatively the magnitude, if any, of the cross section in this range. Such an experiment has been proposed to be performed at Rice Institute. If a cross section greater than 100 mb appears to exist in this energy range, then further experimental investigation would be warranted.

From a compilation of data, a re-evaluation of ϵ_M, the net fast effect in BeO, was made. The results of this work were reported in GAMD-1619.[3] The calculations indicate that in an infinite homogeneous BeO moderator, the ϵ(n,2n) = 1.073 and the net fast effect ϵ_M = 1.040, with an error no greater than 0.008 if the threshold is at 2.7 Mev rather than 1.7 Mev. The existence of a cross section rising linearily from zero at 1.7 Mev to 125 mb at 2.7 Mev results in an increase of 0.014 in ϵ(n,2n) or a net fast effect of 1.054. Experiments are planned which will resolve the question of whether or not a measurable cross section exists in the region 1.7 to 2.7 Mev.

Fermi Age

The analysis of the experimental results on the Fermi age in BeO was completed during this period. Fig. 4.16 is a plot of the experimentally measured indium resonance flux as a function of axial distance in the rectangular BeO stack. The experimental arrangement is shown in Fig. 4.17. Corrections to the experimentally measured distribution were made at regions close to the fission plate to account for resonance flux depression in the immediate vicinity of the fission plate, and at distances beyond 50 cm from the fission plate in order to subtract contributions due to the (γ,n) reaction in beryllium. Neither correction significantly affects the accuracy of the resulting age calculation. Moments of the distribution in the finite stack were calculated and the Fermi age in BeO for fission neutrons was calculated to be 93.4 $cm^2 \pm 4\%$ to indium resonance energy (1.4 ev). The density of the stack was 2.80 gm/cm^3.

Thermalization

A number of experiments were performed at the General Atomic Linear

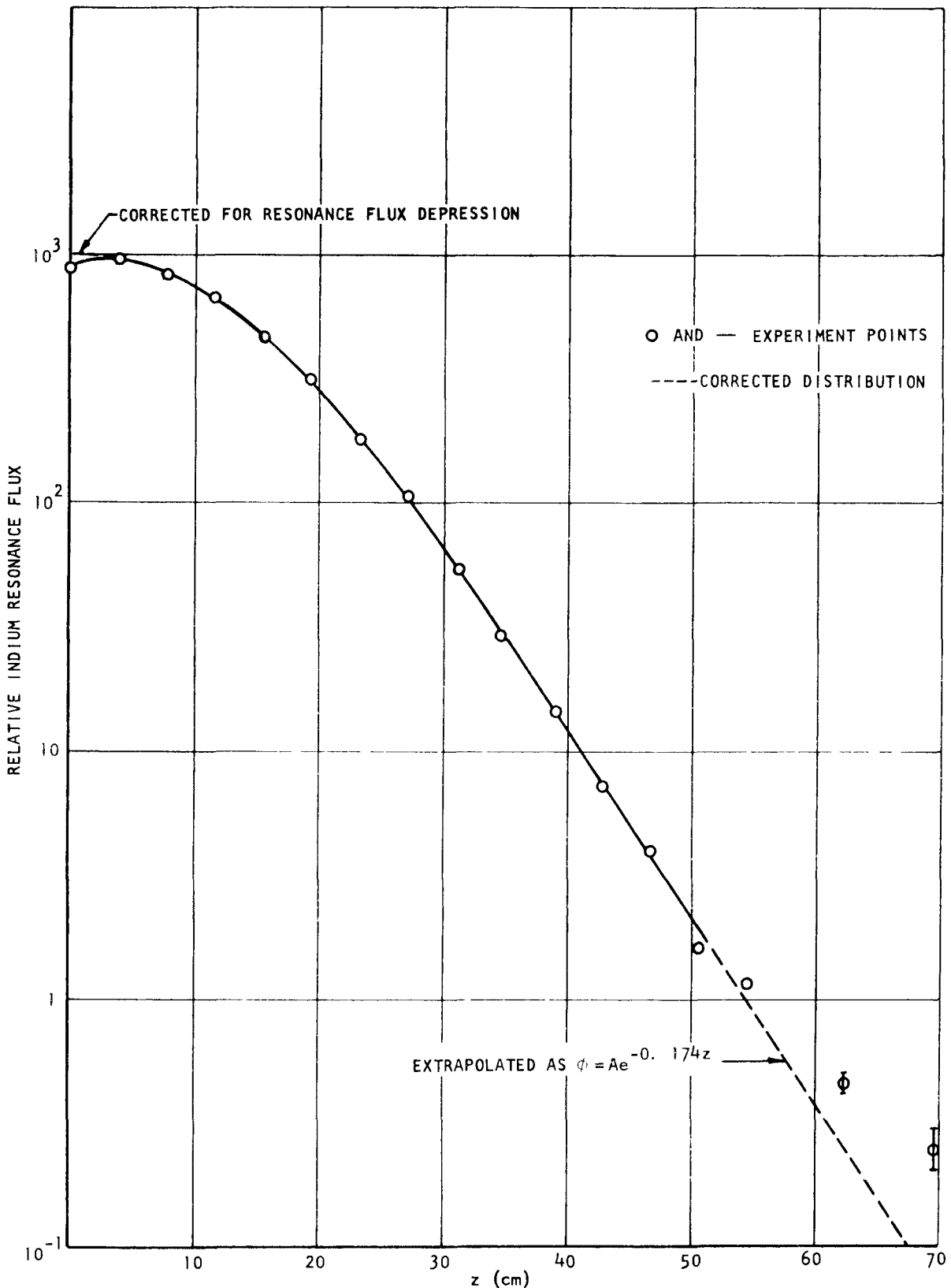

Fig. 4.16--Slowing Down of Fission Neutrons in Beryllium Oxide

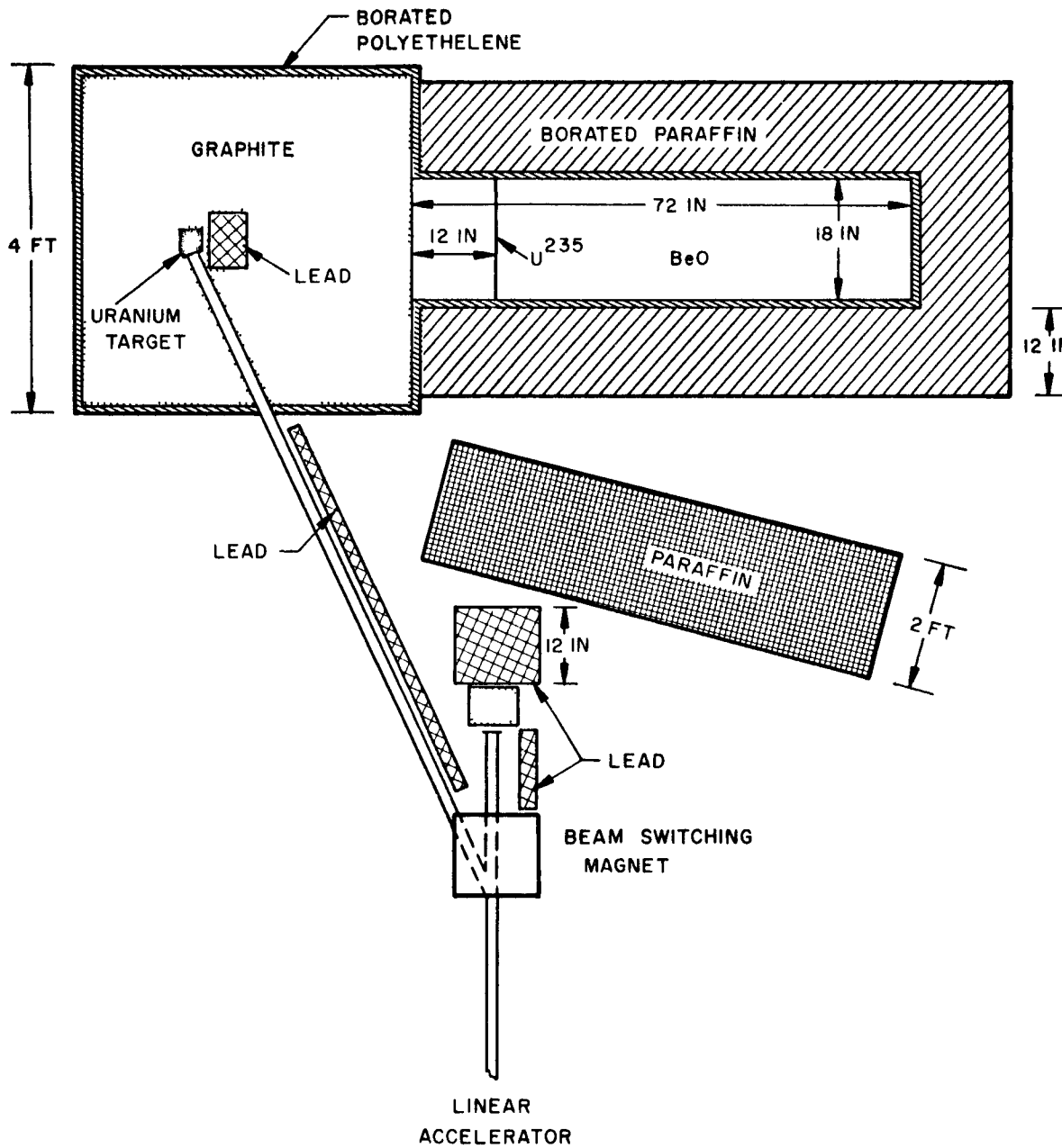

Fig. 4.17--Experimental Arrangement for Fermi Age Experiments in BeO

Accelerator on the total cross section of BeO for cold neutrons. These experiments were adjunctive to the measurements made during the last quarter on the effects of crystalline binding in BeO on the spectrum of thermal neutrons. These experiments measured the total cross section of BeO for neutrons with energies less than 0.004 ev. At these energies, the total cross section consists only of absorption and inelastic scattering. A calculation of the inelastic scattering cross section using the assumed model for the vibrational spectrum of the atoms in the BeO lattice then serves as a comparison. The cross sections were measured for three different temperatures of the BeO moderator. Several experimental difficulties were encountered in separating the required inelastic scattering cross section from background. These difficulties are particularly evident in measurements made at liquid nitrogen ($77^{\circ}K$) temperature, where the inelastic scattering cross section is expected to be of the order of only a few millibarns. Efforts are being made to resolve these difficulties.

Calculations were made of the inelastic scattering cross section for low energy neutrons in BeO. The purpose of the work was to check the experimental results obtained during this period and to compare these results with the assumed model for the spectrum of lattice vibrations in BeO. Table 4.11 gives a comparison of the experimental data with the calculations made, assuming a Debye spectrum of levels with a Debye temperature of $1200^{\circ}K$. More recently, an evaluation of specific heat data indicates that perhaps a Debye temperature of $855^{\circ}K$, together with an optical level of $1170^{\circ}K$, fits the specific heat data, at least up to room temperature values. Preliminary calculations based on such a frequency spectrum give results approximately 50% larger than those quoted in Table 4.12.

Table 4.12

COMPARISON OF CALCULATED AND EXPERIMENTAL CROSS SECTIONS FOR BeO AT 0.0025 EV

Temperature $^{\circ}F$	σ^{*}exp x 10^{24} cm^2	σ^{*}calc. x 10^{24} cm^2
77	0.40	0.035
293	0.65	0.38
575	2.6	2.1

* σ = scattering

V. MATERIALS DEVELOPMENT (W. P. Wallace)

DEVELOP MATERIALS FOR THE PROPULSION PLANT (TASK 24*) (J. Bokros, D. Guggisberg, R. Coburn)

Creep and Stress-rupture of Niobium Alloys

Creep-rupture tests on 85 w/o Nb-15 w/o Ti alloys have been extended to include the evaluation of protective coatings to determine the feasibility of using niobium alloys in the MGCR. Two types of coatings were studied:

Coating No. 1 - Vapor deposited and diffused Cr-Ti

Coating No. 2 - Vapor deposited and diffused Cr-Ti-V-Al

Control and coated samples were tested at 1700°F and 5600 psi in pure helium (99.999%) and in helium containing 5×10^{-3} atmospheres air. Due to a water leak, the environment for the uncoated niobium specimens also contained 1 to 2×10^{-3} atmospheres of H_2O. The data obtained are presented in Figs. 5.1 - 5.3. The results showed that in all cases, the specimens tested in the impure atmosphere had lower creep rates indicating strengthening through contamination. This contamination will ultimately lead to severe embrittlement, especially at lower temperatures. It should be noted, however, that the coatings did afford some protection as evidenced by lesser differences in the creep rates exhibited by duplicate specimens. Both coatings were observed to crack and spall under the high strain rates imposed. It is possible, however, that the coatings will maintain their integrity longer and afford better protection at lower strain rates. The investigations to evaluate the properties of Nb alloys will be continued on a minimum effort basis in order to keep abreast of advancements in the field of Nb alloy development and the development of protective coatings for Nb.

*This work has erroneously been reported under Task 19 in previous quarterly reports.

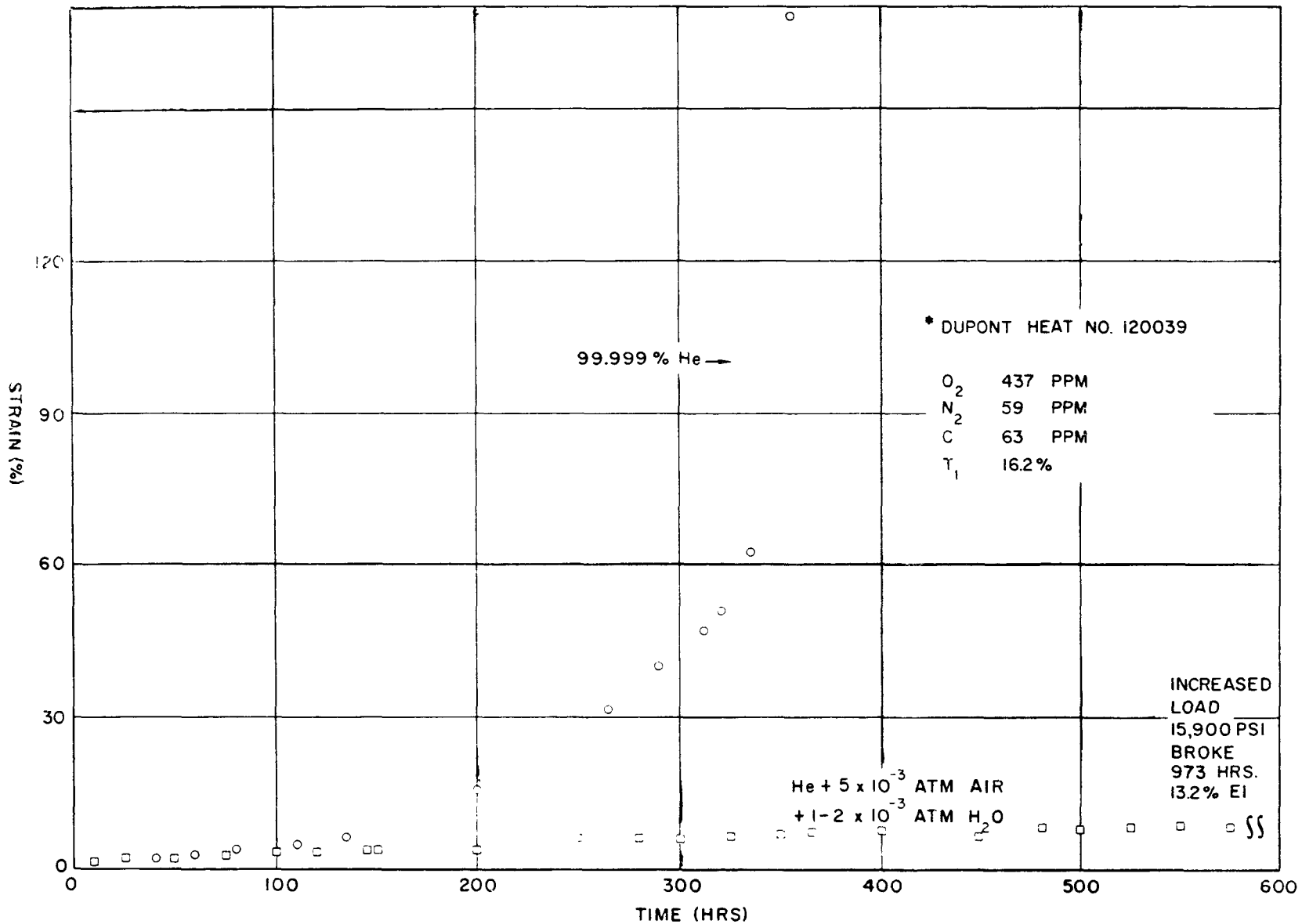

Fig. 5.1--Creep Strain vs Time for Nb + 15% Ti Uncoated at 1700°F and 5300 psi

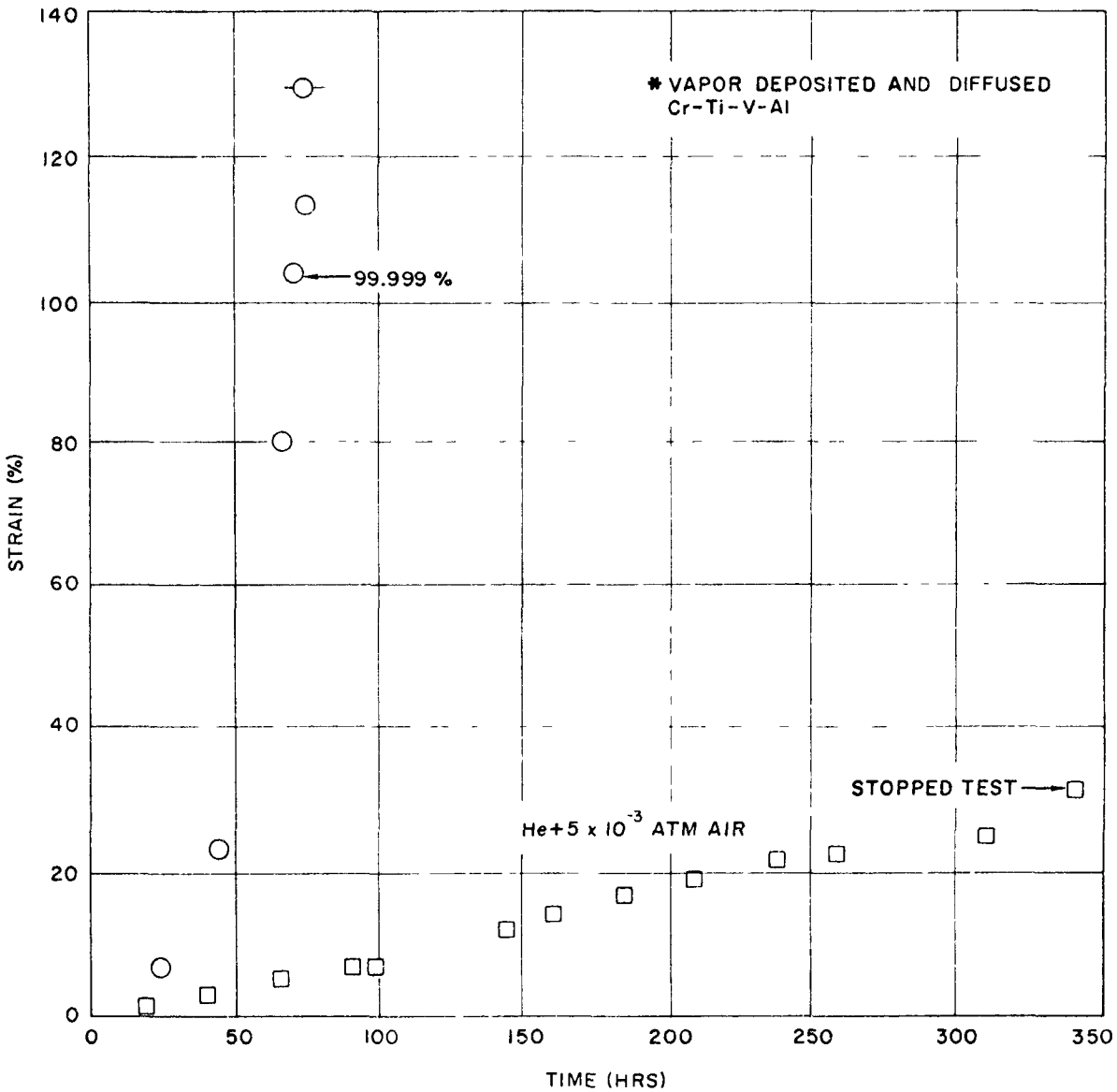

Fig. 5.2--Creep Strain vs Time for Nb + 15% Ti with TRW Coating No. 2 at 1700°F and 5300 psi

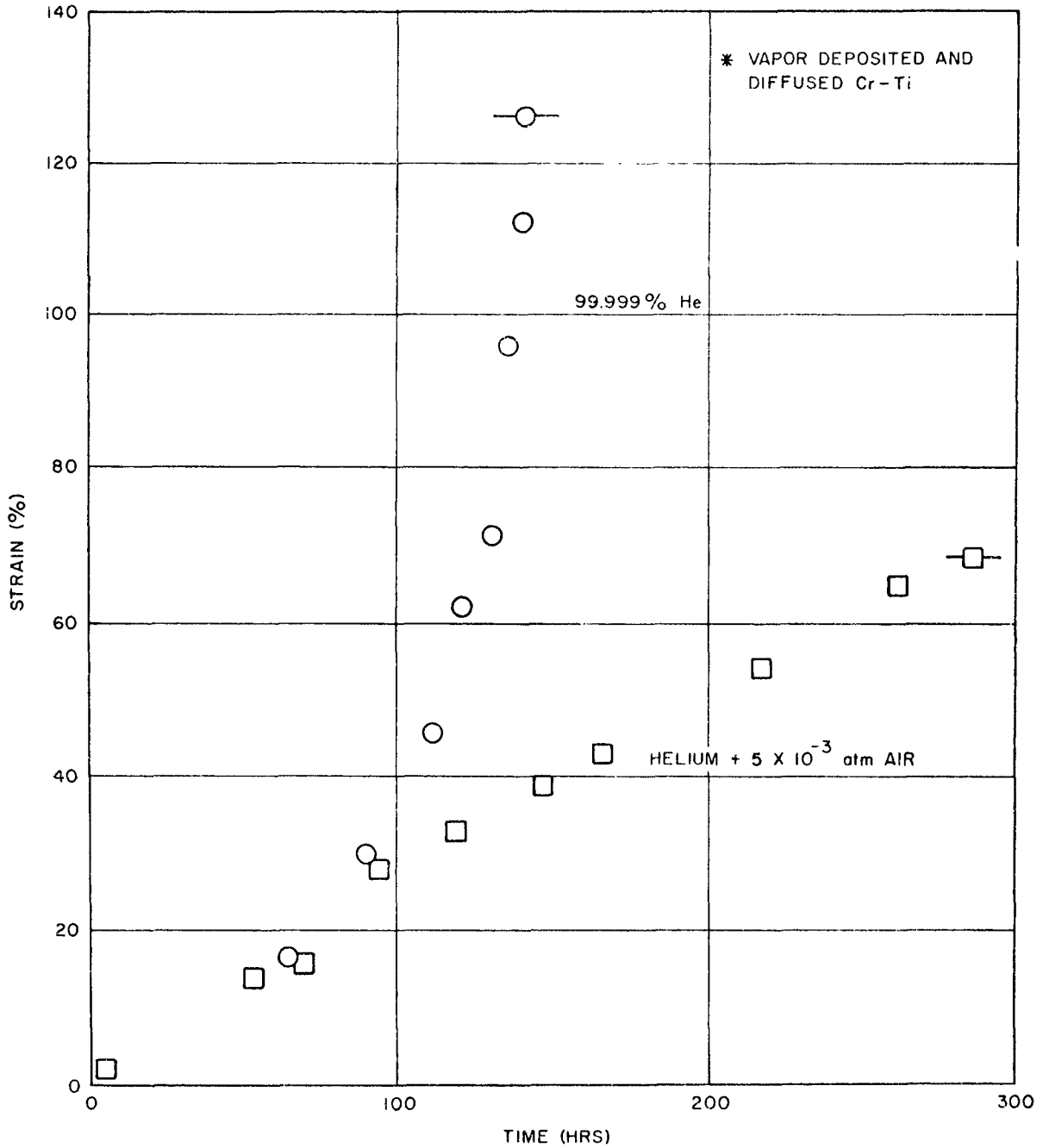

Fig. 5.3--Creep Strain vs Time for Nb + 15% Ti Coated with TRW Coating No. 1 at 1700°F and 5300 psi

REACTOR MATERIALS IRRADIATIONS (TASK 23) (D. E. Johnson, B. Czech, D. Guggisberg, H. Johnson)

Irradiation Programs Sponsored at Other Sites

Three capsules were fabricated by Battelle Memorial Institute under the terms of a previous subcontract. Each capsule contained two specimens of each of the following materials: (1) 20 v/o UO_2 - 80 v/o BeO, (2) 20 v/o UC - 80 v/o graphite, and (3) 20 v/o UC_2 - 80 v/o graphite. In each case, the fuel was in the form of a dispersion of particles with an average diameter of approximately 150 μ. Each specimen consisted of four pellets of one of the above materials combinations clad in stainless steel. The irradiation of the capsules in the MTR began on July 26, 1959. One capsule (MTR-31-3) was discharged from the MTR on May 31, 1960. The estimated peak burnup limits in this capsule at the time of discharge were 1.66×10^{20} to 2.45×10^{20} fissions/cm^3 of fuel pellet (30,400 $\frac{Mwd}{Ton\ U}$ to 44,800 $\frac{Mwd}{Ton\ U}$). The peak surface temperature of the clad specimens during irradiation was approximately 1500°F.

Examination of fuel irradiation capsule number MTR-31-3 in the General Atomic Hot Cell Facility has been partially completed. All of the UO_2 - BeO pellets were removed intact from their respective claddings and no fragmentation or appreciable swelling of the pellets were observed. Dimensional data for these pellets are noted in Table 5.1.

The dimensional data obtained from the BeO - UO_2 pellets were treated statistically and it was found that there was no dimensional change within a 5 per cent significance level.

The individual specimen claddings were punctured and the accumulated fission gases were collected in liquid-nitrogen-cooled activated-charcoal traps. The traps were subsequently analyzed by gamma spectrometry. The results of the analyses are given in Table 5.2.

Table 5.1

DIMENSIONAL DATA FOR THE UO_2-80 v/o BeO FUEL PELLETS FROM IRRADIATION

CAPSULE NUMBER MTR-31-3

Pellet No.	Diameter (in)		Length (in)	
	Pre-irradiation	Post-irradiation	Pre-irradiation	Post-irradiation
4-1	0.2223	0.2225	0.2508	0.2505
4-2	0.222	0.2225	0.2485	0.2505
4-3	0.2226	0.2225	0.2499	0.2510
4-4	0.2218	0.2223	0.2494	0.2515
6-1	0.2227	0.2223	0.2510	0.251
6-2	0.2229	0.222	0.2501	0.2505
6-3	0.2241	0.2221	0.2493	0.2501
6-4	0.222	0.2203	0.2503	0.2503

Table 5.2

FISSION GASES COLLECTED FROM MTR-31-3 CAPSULE SPECIMENS

Fuel Material	Kr-85 Collected (μ c)
UC-graphite	345.
UC-graphite	397.
UC_2-graphite*	240.
UO_2-BeO	2.16
UO_2-BeO	1.82

* The gas sample from one UC_2-graphite specimen was lost. A detailed analysis of the data is in progress and will be reported during the next quarterly period.

The second of the three irradiation capsules was discharged from the MTR on September 12, and is being shipped to the General Atomic Hot Cell Facility for examination. The irradiation of the third capsule is continuing. Data concerning these capsules will be reported in future quarterly progress reports.

Irradiations Programs at General Atomic (D. Johnson, J. M. Tobin, G. Czech, D. Guggisberg, H. Johnson)

The fission gas release capsule (MGCR-5) was returned to General Atomic for modification. The capsule was originally designed to study the diffusion release of fission products from a nickel clad fuel pin; the fuel used was fully enriched UO_2 diluted with 80 v/o alumina. Because of the interest in fuels that are diluted with BeO and clad with Hastelloy-X, the capsule is being modified to permit tests of these materials.

The MGCR-4 fuel irradiation capsule is designed for the irradiation of 3/8-in. diameter fuel pellets composed of 70 v/o BeO-30 v/o UO_2 at surface temperatures of 1500°F to 1700°F. The objective of the test is to provide information on the performance of this fuel composition during high temperature reactor irradiation. The capsule is designed for controlled temperature operation with a variable conductivity gas annulus as the temperature control feature.

The fabrication and assembly of the MGCR-4 fuel irradiation capsule and the associated instrumentation console is approximately 75% complete. Extensive heat transfer tests were performed with an electrically heated mock-up of the capsule. The results of the tests indicate that excellent temperature control can be obtained at the design heat generation rate (250 w/cm) plus or minus forty per cent.

DEVELOP NONFUEL MATERIALS FOR THE REACTOR (TASK 24) (D. Johnson, J. M. Tobin, W. Wyman, B. Czech, D. Guggisberg, H. Johnson)

BeO Irradiations

A BeO moderator irradiation capsule, designated MGCR-1, was installed in a specially constructed irradiation tube in the E-5 position in the GETR core. The irradiation of the capsule began on September 3. The temperatures obtained in the capsule at full reactor power (30 Mev) are given in Fig. 5.4. The peak temperature in the capsule of approximately 1970°F exceeded the expected temperature by 250°F to 300°F.

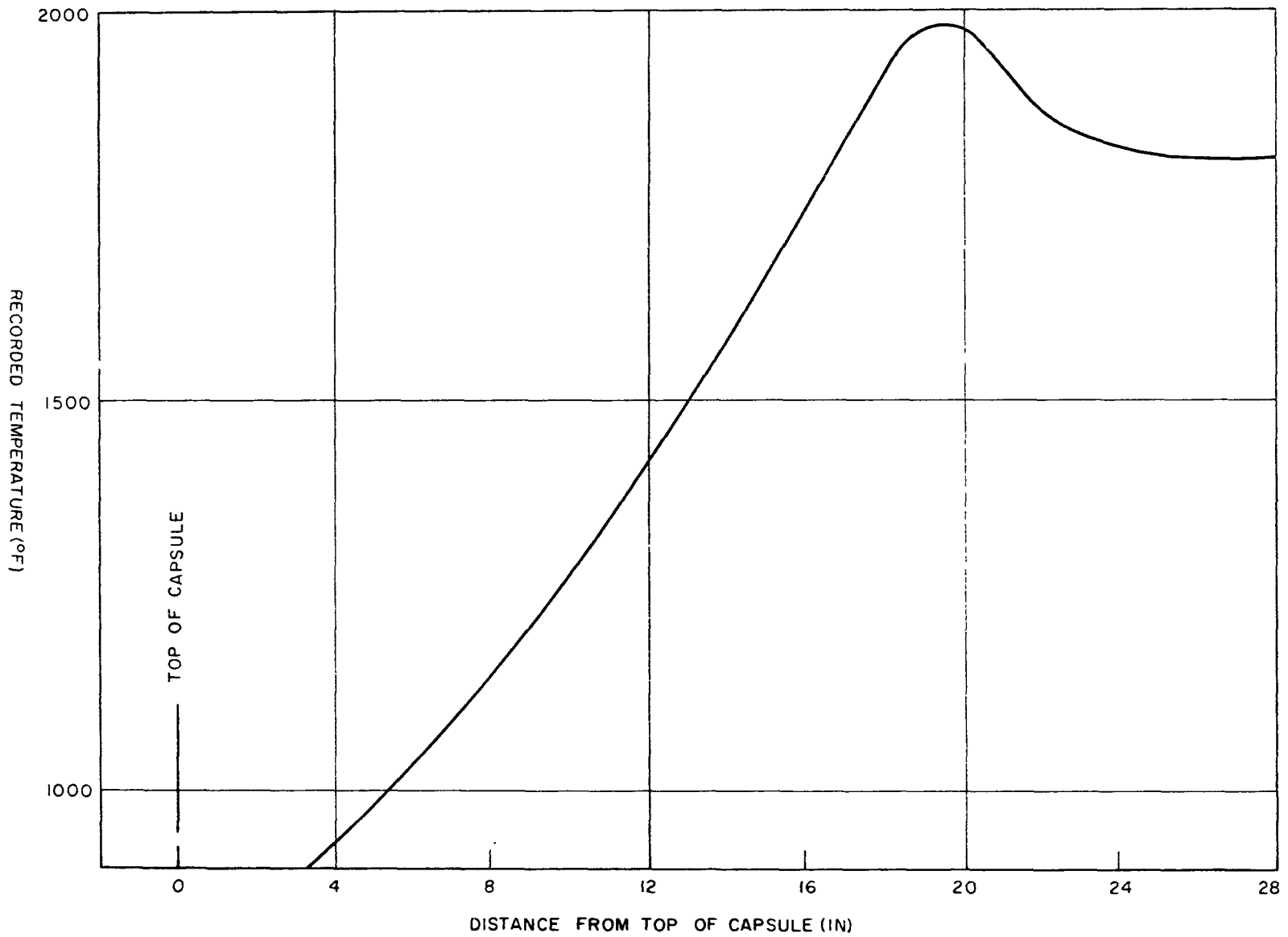

Fig. 5.4--MGCR-1, BeO Irradiation Capsule Temperatures at 30 Mw Reactor Power

On September 4, a sudden severe temperature increase in the capsule was observed. All but two of the ten thermocouples indicated a temperature in excess of 2000°F. This behavior was attributed to leakage of nitrogen from the lead tube into the helium filled irradiation capsule gas annulus. The nitrogen in the lead tube was replaced with helium and the capsule was purged with helium. The recorded temperatures following this operation are presented in Fig. 5.5. It was estimated that a peak temperature of 2500°F may have been reached for a few minutes. Four thermocouples became unreliable during this temperature excursion. The remaining thermocouples indicated that normal operation had been re-established in about 1-1/4 hrs. The irradiation of the capsule following the temperature excursion has been uneventful.

Creep and Stress-rupture Testing of Fuel Element Cladding Materials (A. Weinberg, R. Wallace, R. Coburn)

The short time creep-rupture properties of Hastelloy X are being determined over the range of temperatures shown in Table 5.3. The tests are being performed to provide data for use in the evaluation of the behavior of Hastelloy X clad fuel elements in the event of a loss-of-coolant accident. All tests are being conducted in a pure helium (less than 10 ppm impurities) environment. The results obtained to data are also presented in Table 5.3.

Metallographic examinations have been performed on ruptured specimens. These examinations together with hardness measurements have indicated precipitation hardening during the testing period and the onset of re-crystallization which occurs at approximately 1700°F. The decreased ductility at elevated temperatures appears to be associated with increased inter-crystalline crack formation.

The creep-rupture tests are being continued and will include test temperatures up to at least 2100°F.

ELECTRIC BOAT DIVISION MATERIALS INVESTIGATION AND TESTS (TASK 19) (D. W. Carreau, M. J. Donachie, R. Shepheard, B. Lund)

Self-welding in Helium at Elevated Temperatures

The second series of self-welding tests of metals in helium atmospheres has been completed. As in the first, specimens of different materials were loaded in compression in high temperature, high purity helium. After 1000 hrs. of exposure at 1300°F, the specimens were removed. Those which adhered were pulled apart and the force required to separate them recorded. A summary of results of both tests is given in Tables 5.4 and 5.5.

The third series of self-welding tests has been started.

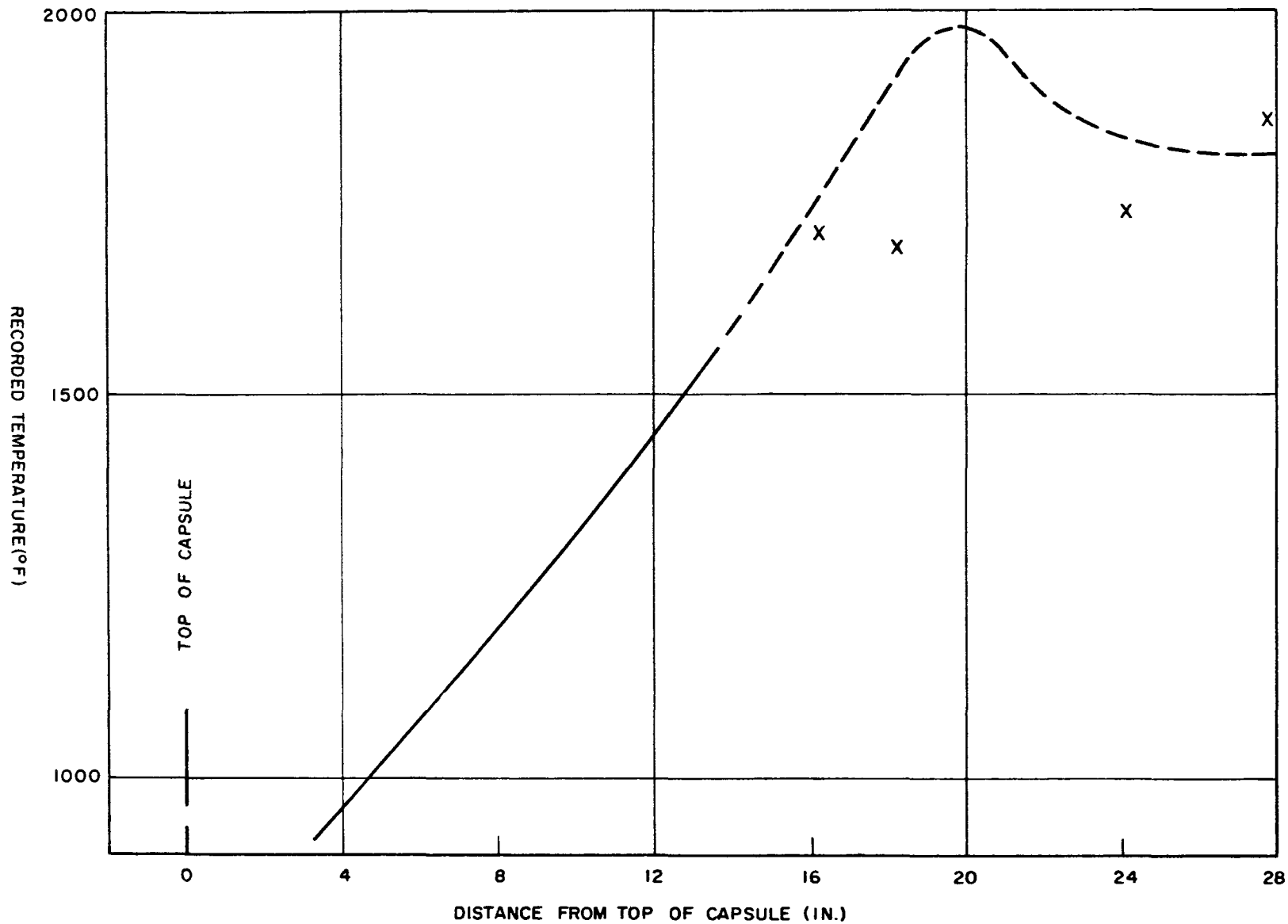

Fig. 5.5--MGCR-1, BeO Irradiation Capsule Temperatures at 30 Mw Reactor Power after the Temperature Excursion

Table 5.3

SHORT TIME STRESS-RUPTURE CHARACTERISTICS
OF HASTELLOY X IN A HELIUM ATMOSPHERE

Specimen	Temperature (°F)	Stress (psi c 10^{-3})	Rupture Life (hrs)	Elongation (%)/2-in.	Reduction of Area (%)	Hardness+ (R_c)
2 - 4	1200	80	0.37	57.5*	37.8	33.1
3 - 1		73	0.55	55*	--	--
1 - 5		63	6.4	57*	42.3	32.2
4 - 5A	1400	43.5	0.74	52.5*	35.5	29.2
4 - 5B		43.5	0.92	50*	47.2	29.2
6 - 4		41	1.2	68	--	--
5 - 4		38	1.68	70*	58.4	28.5
8 - 6	1600	23.5	0.74	46	44.0	25.5
7 - 6		22.5	0.87	36	--	--
9 - 4		21.5	1.0	--	--	22.7
10 - 5	1700	16.5	0.77	50	44.8	20.1
12 - 4		15.5	0.35	38	40.5	18.0
14 - 5		15.25	0.98	42	--	--
13 - 6		14.9	0.50	24	37.1	20.8
18 - 5		14.3	1.07	36	42.3	17.5
16 - 5	1800	9.75	0.45	21	--	--
19 - 6		9.2	0.97	22	23.2	15.6
17 - 6		8.8	2.03	20	19.6	14.9

* Elongation obtained from motion of cross-head. Values for other specimens were obtained from gauge marks.

\+ Hardness of as-received material is R_c 15.3.

Table 5.4

SELF-WELDING TEST NO. 1

Mating Components	Contact Pressure (psi)	Breaking Load (lbs.) Specimen Number 1	2	3	4	5	6
713C to D979	25,000	0	0				
713C to D979	50,000	0	0				
713C to W545	25,000	80	48	0			
713C to W545	50,000	+	+	+			
D979 to W545	25,000	135	+				
D979 to W595	50,000	25	+				
D979 to D979	25,000	0					
D979 to D979	50,000	+					
Stellite No. 1 to 316L	4,000	182	100	>965*	>500	290	310
Stellite No. 6 to 316L	4,000	>500	849	427	>500	550	505
Stellite No. 1 to Stellite No. 6	4,000	0	0	0	0		
304 to 304 SS	4,000	95	143	170			
316L to 316L SS	4,000	170	467	150			
410 to 410 SS	4,000	0	575	0			
Inconel to 316L SS	4,000	410	0				
Inconel to 304 SS	4,000	0	0	0	55		
410 to 316L SS	4,000	+					

Notes: 0 = Not adhered

+ = Separated when clamping for test

* = Not separated owing to grip slippage

Table 5.5

SELF-WELDING TEST NO. 2

Mating Components	Contact Pressure (psi)	Breaking Load (lbs) Specimen Number 1	2	3	4	5	6
Stellite No. 6 (cast) to Stellite No. 12 (cast)	4,000	0	100	+			
Stellite No. 12 (cast) to 1 1/4 Cr-1/2 Mo	4,000	+					
1 1/4 Cr-1/2 Mo to 316	4,000	492	243	0			
1 1/4 Cr-1/2 Mo to Inconel	4,000	0	0				
1 1/4 Cr-1/2 Mo to 410	4,000	0	1005*	0			
410 to 316	4,000	452	1195	980	1080*		
1 1/4 Cr-1/2 Mo to 304	4,000	0	1275*	0			
Inconel X to W545	25,000	0	0	0	0		
Inconel X to 713C	25,000	0					
Inconel X to 713C	50,000	0					
D979 to 713C	25,000	0	0	0			
D979 to 713C	50,000	0	0	0			
D979 to D979	25,000	0					
D979 to D979	50,000	0					
Inconel to Inconel	4,000	0	345				
304 to 316 SS	4,000	1415*	790	1200*			
304 to 410 SS	4,000	0	1205*	0			
Hastelloy X to 410 SS	4,000	0	0	0			
1 1/4 Cr-1/2 Mo to Stellite No. 1 Butter	4,000	0	40	95	0		

Notes: 0 = Not adhered

+ = Separated when clamping for test

* = Not separated owing to grip slippage

Galling Tests

The program of preliminary galling tests on valve materials has been completed by Crane Company.[1] The specimens were loaded at 4000 psi contact pressure at 1300°F in a pure helium atmosphere and were oscillated through an angle of 23° at a rate of 17.25 min. per 1000 cycles. Table 5.6 lists the materials tested and the number of cycles before the test specimens seized.

Table 5.6

Alloy	Cycles to Failure
Stellite No. 1 on Stellite No. 1	89
Stellite No. 12 on Stellite No. 12	79
Stellite No. 6 on Stellite No. 6	32
Colmonoy 70 on Colmonoy 70	23
Coast Metals 7 on Coast Metals 7	2

From these results, it was observed that the cobalt-base alloys performed better than the nickel-base or iron-base alloys. There also appears to be a correlation between the total per cent of hardener atoms to the number of cycles to failure. The life of all specimens tested was far shorter than desired.

Crane Company has submitted recommendations for the composition of, and methods for producing hard facing deposits suitable for unlubricated high temperature operation in pure helium. Therefore, a new series of galling tests are planned which will examine greater number of specimens, including several of those combinations that performed satisfactorily in the self-welding experiments. Electric Boat Division has designed a smaller and simpler machine (Fig. 5.6) in an effort to conduct these environmental galling tests at low cost.

Creep-rupture Testing of Welded Specimens

Seven rupture tests (in air) at 1000°F and four (in air) at 1200°F were performed to evaluate the properties of welded specimens of 1-1/4 Cr-1/2 Mo steel against those of base metal. The results are shown in

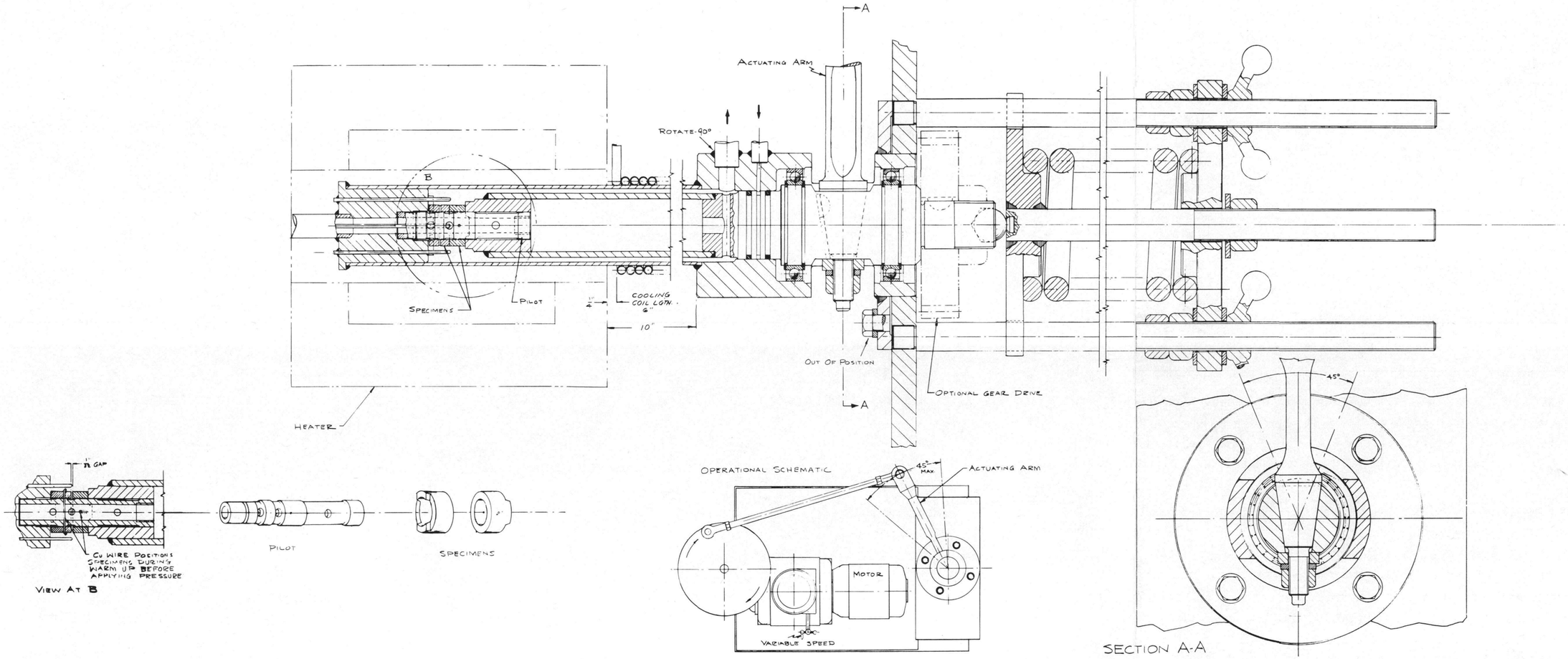

Fig. 5.6-- MGCR-Galling and Wear Test Apparatus Study.

Table 5.7 and Figs. 5.7 and 5.8. As seen in Fig. 5.7, the rupture times were in good agreement with the stress-versus-rupture time curves determined from helium and air tests of nonwelded specimens. However, the fracture locations and per cent elongations in the 2-in. test section were different in the rupture tests of cross-weld specimens. All base metal specimens showed an average ductility, as measured by per cent elongation in two inches, of at least 16% for equivalent rupture times to those of the cross-weld specimens. The ductility of the cross-weld specimens decreased with increasing rupture times. This decreased average ductility may not be significant because the individual regions (base metal, heat affected zone, weld deposit) of a welded specimen probably have sufficient intrinsic ductilities for design purposes.

Table 5.7

Cr-Mo STEEL CROSS-WELD RUPTURE TEST RESULTS

Specimen Type	Nominal Stress (psi)	Rupture Time (hrs)	Elongation in approx. 2-in. (%)	RA (%)	Fracture Location
		1000°F			
WB-1 - Rect. Base-plate	40,000	1103.5	17.0	60.5	Base metal
WB-2 - Rect. Base-plate	50,000	272.0	17.4	57.7	Base metal
WB-3 - Round Base-plate	40,000	1217.2	16.1	59.5	Base metal
WB-4 - Rect. Base-plate	65,000	11.8	20.2	61.8	Base metal
W-1 - Cross-weld	40,000	920.7	3.5	12.5	Fusion line
W-2 - Cross-weld	50,000	456.0	8.1	27.0	Fusion line and Base Metal
W-3 - Cross-weld	65,000	29.7	11.5	60.0	Base metal
		1200°F			
WB-5 - Rect. Base-plate	10,000	123.5	17.4	63.6	Base metal
WB-7 - Rect. Base-plate	20,000	12.5	34.0	81.8	Base metal
W-7 - Cross-weld	10,000	146.7	5.3	33.4	Fusion line
W-4 - Cross-weld	20,000	11.4	30.6	53.0	Fusion line

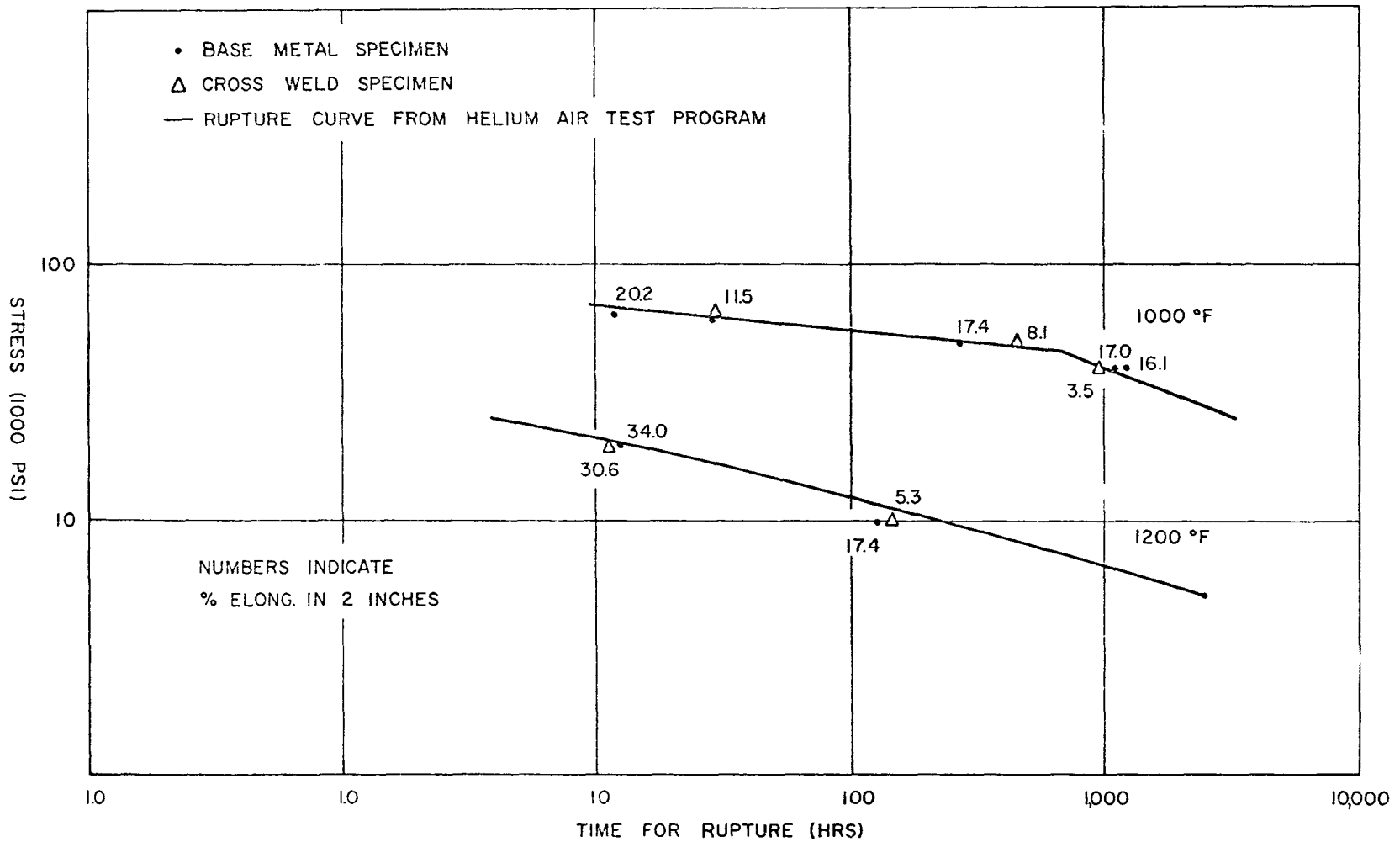

Fig. 5.7--1-1/4 Cr-1/2 Mo Steel, Cross Weld Specimen Creep Rupture Heat Results

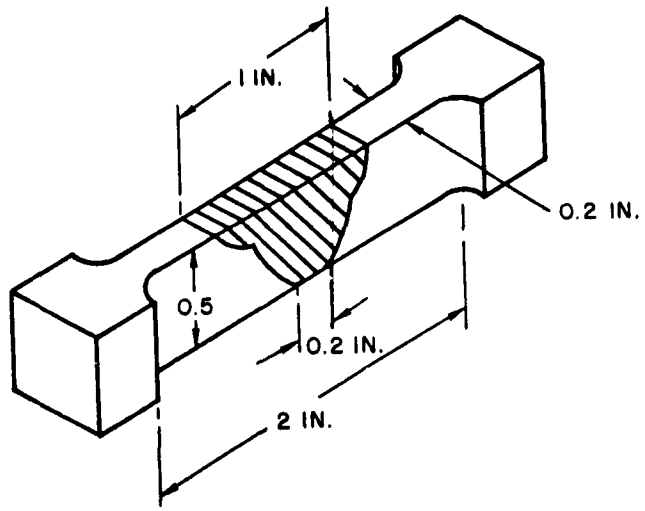

Fig. 5.8--Creep Rupture Test Specimen

Westinghouse Metallurgical Program[2]

Stress-Rupture Tests (Task 5)

Based on the materials required for the high-pressure drive cycle, testing in the past quarter was concentrated on W-545 at 1200°F, Inconel X at 1300°F, and Inco 700 at 1500°F. The maximum stress and temperature levels for 1300°F operation will permit the use of Inconel X for the turbine blades and W-545 for the turbine discs. Re-blading with Inco 700 would permit short-time operation of the turbine at 1500°F and provide sufficient cooling of the turbine discs. The long-time stress-rupture tests on D-979 and Inco 713C are to be continued.

Fatigue Tests

Table 5.8 shows the helium combined load data obtained on D-979 at 1200°F, W-545 at 1200°F, and Inconel X at 1300°F. This data was obtained using smooth bar specimens tested at an alternating to steady stress ratio of 0.25.

Table 5.8

HELIUM FATIGUE DATA - COMBINED STRESS
(AS/SS* = 0.25)

Specimen	Material	Temp. °F	Maximum Stress, Psi	Cycles Millions	
1	W-545	1200	81,000	9.9	
2	W-545	1200	76,700	93.4	No Failure
3	W-545	1200	80,600	95.6	No Failure
4	W-545	1200	84,800	94.0	No Failure
5	D-979	1200	82,300	92.88	No Failure
6	D-979	1200	87,500	50.82	No Failure
7	D-979	1200	99,400	6.00	
8	D-979	1200	94,950	20.86	
9	D-979	1200	98,000	10.56	
10	Inconel X	1300	60,000	100.0	No Failure
11	Inconel X	1300	62,500	89.7	
12	Inconel X	1300	67,600	40.0	

These preliminary results, combined with the pure alternating fatigue and stress-rupture data obtained previously, show an elliptical relationship for the stress-range diagram of each alloy.

*AS = Alternating Stress; SS = Steady Stress

REFERENCES

1. Crane Company Engineering Division, Materials Testing Program for Maritime Gas-Cooled Reactor System Valves, Crane Company File No. EL7622, August 22, 1960.

2. Quarterly Progress Report, July 1 to September 30, 1960, prepared for the Electric Boat Division, General Dynamic Corporation, by Westinghouse Corporation.

VI. SITE DEVELOPMENT

PROTOTYPE SITE DEVELOPMENT (TASK 18) (W. T. Furgerson, H. N. Wellhouser)

Work during this quarter has been concentrated on the development of the site requirements for a 10 MW(t) Beryllium Oxide Reactor Experiment (BORE).

The area required for the BORE site is estimated to be about 350-ft. by 500-ft. or about four acres. The major site installations will be:

1. Reactor Building
2. Pump House
3. Storage Warehouse
4. Water Storage Tank, domestic and fire protection
5. Demineralized Water Storage Tank
6. Fuel Oil Storage Tank
7. Cooling Tower
8. Low Pressure Helium Storage Tank
9. Liquid Waste Leaching Pond
10. Sanitary Waste System Tank and Leaching Pit
11. Electrical Substation

The primary heat dump will be a helium-to-air heat exchanger so arranged that the effluent air is exhausted up a stack. The stack diameter will be about 8-ft.; the height will be determined by the site requirements. The cooling tower, (item 7 above), will have a capacity of about 2×10^6 Btu/hr and will supply cooling water for the primary shields, fission product traps, spent fuel storage and other small heat sources.

The Reactor Building, approximately 75-ft. wide, 120-ft. long, and 34-ft. high, is the main building in the site complex. The reactor will be located below ground to keep the building height to a minimum, take advantage of the earth shielding and to facilitate water flooding of the reactor for fuel handling. A wet fuel handling system is planned for maximum flexibility and low cost, however, a dry fuel handling system is being given some consideration.

In addition to the reactor system, the reactor building will house the control room, office space, personnel change rooms, chemistry laboratory, maintenance shop, new fuel storage as well as support components such as electrical switch gear, heating and ventilation.

About 1.5 Mw of electrical power will be required for the BORE. The largest single load will be the 1000 hp main coolant blower.

Using the helium-to-air heat exchanger to dump the main heat load will keep the total site water requirements minimal. It is estimated that 50 gpm will be adequate for make-up and blow-down for the small cooling tower and at the same time provide sufficient water for domestic and sanitary requirements. Depending on the site requirements, a capability for pumping larger quantities of water may be required for fire protection.

MGCR PROJECT ORGANIZATION

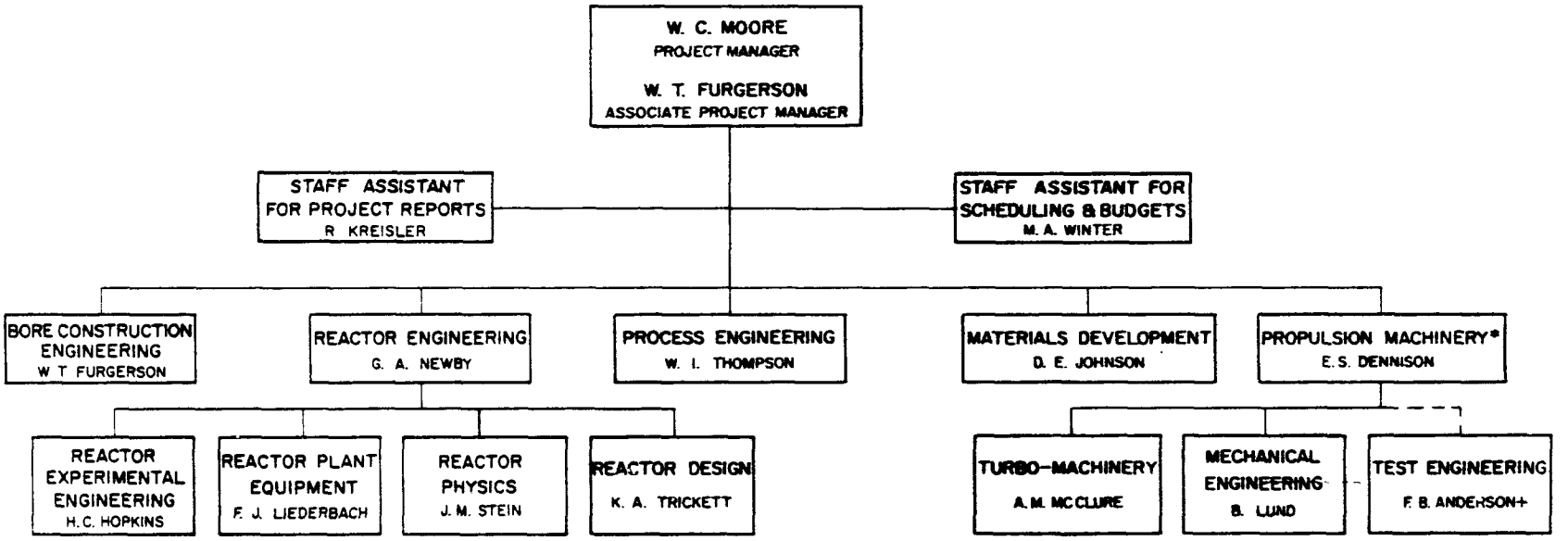

* -ELECTRIC BOAT DIVISION

+ -ON A PART-TIME CONSULTING BASIS